

**EFFICIENCY OF 2-AMINOPYRIDINE AS  
CORROSION INHIBITOR UNDER CHLORIDE AND  
CARBONATED ENVIRONMENT**

*A thesis submitted in the partial fulfilment of the  
requirement for the award of degree of*

**MASTERS OF ENGINEERING**

**IN**

**STRUCTURAL ENGINEERING**

*Submitted By:*

**APURAV BHARTI**

**Roll No. 801524005**



**UNDER THE SUPERVISION OF**

**Dr. Shweta Goyal**

**(Associate Professor)**

**DEPARTMENT OF CIVIL ENGINEERING**

**THAPAR UNIVERSITY, PATIALA-147004, INDIA**

## DECLARATION

I, Apurav Bharti, hereby declare that this thesis entitled “**EFFICIENCY OF 2-AMINOPYRIDINE AS CORROSION INHIBITOR UNDER CHLORIDE AND CARBONATED ENVIRONMENT**” in fulfilment of the requirement for the award of Degree of Master of Engineering in Structural Engineering at Thapar University, Patiala, is an authentic record of my work carried out during a period from January 2017 to July 2017 under the supervision of **Dr. Shweta Goyal, Associate Professor**, Department of Civil Engineering, Thapar University, Patiala.

This matter presented in this thesis has not been submitted by me for the award of any other degree of this or any other University.

Date: 30<sup>th</sup> July, 2017

Apurav

**Apurav Bharti**

**(Roll No.801524005)**

## CERTIFICATE

This is to certify that above statement made by the student concerned is correct and true to the best of my knowledge and belief.



**Dr. Shweta Goyal**

*Associate Professor*

*Department of Civil Engineering*

**Thapar University, Patiala**

## **ABSTRACT**

The durability problems encountered in reinforced concrete structures are of serious concern to the concrete infrastructure across the world. The durability of reinforced concrete structures is dependent on the surrounding environmental and exposure conditions. One of the major factors responsible for the deterioration of reinforced concrete structures is the corrosion of reinforcement inside the concrete. The corrosion of concrete takes place majorly due to CO<sub>2</sub> and chloride present in the environment. Reinforcement corrosion is generally accompanied by the loss of reinforcement cross-section and a build-up of corrosion products. The corrosion products occupy a larger volume than the original steel, this in turn generates tensile stresses causing cracking and spalling of the concrete cover. Thus, decreasing the service life of the Reinforced Concrete structure.

The purpose of this thesis is to study the effectiveness of 2-Aminopyridine as a corrosion inhibitor against the Carbonation as well as Chloride induced corrosion. Firstly, the experiment was conducted on the pore solution simulating concrete and the effectiveness of inhibitor was checked. Then, concrete specimens using OPC and PPC were cast using the inhibitor and checked under carbonation and chloride induced corrosion. Three types of tests, i.e., Linear polarization Method, Half cell potential and Galvanic potential are performed to find out the values of I<sub>corr</sub> and HCP. Cubes were also cast using OPC and PPC to check the carbonation depth in the concrete.

From the results, it was observed that corrosion current i.e. I<sub>corr</sub> values were reduced both in pore solution as well as concrete. The inhibitor takes time in forming the layer around the rebar and reducing the corrosion rate in concrete as well as pore solution. The amine group in the 2-Aminopyridine forms a chelate ring around the steel bar. This makes a passive layer around the steel bar, hence providing resistance to corrosion. The carbonation depth was also controlled by the inhibitor admixed specimens as compared to the non-inhibitor admixed specimen.

## TABLE OF CONTENTS

CONTENT	PAGE NO
DECLARATION	i
CERTIFICATE	i
ACKNOWLEDGEMENT	ii
ABSTRACT	iii
TABLE OF CONTENTS	iv
LIST OF FIGURES	vi
LIST OF TABLES	ix
<b>CHAPTER 1 – INTRODUCTION</b>	<b>1</b>
1.1 GENERAL	1-2
1.2 DEFINATION OF CORROSION	2
1.3 CLASSIFICATION OF CORROSION	2
1.3.1 Uniform or general corrosion	2-3
1.3.2 Galvanic corrosion	3
1.3.3 Localized corrosion	3-4
1.3.4 Microbiologically influenced corrosion (MIC)	5
1.3.5 Erosion corrosion	6
1.4 MECHANISM OF CORROSION	6-8
1.5 FACTORS AFFECTING CORROSION	8-12
1.6 PREVENTIVE MEASURES	12
1.7 OBJECTIVES	13
1.8 FORMAT OF THESIS REPORT	13
<b>CHAPTER 2 – CORROSION INHIBITORS</b>	<b>14</b>
2.1 GENERAL	14
2.2 CORROSION INHIBITORS	14-15
2.3 CLASSIFICATION	15
2.3.1 Based on physical mode of protection	15-16
2.3.2 Based on the mechanism of protection	16-17
2.4 MECHANISM OF SOME COMMONLY	

USED COMMERCIALY AVAILABLE INHIBITORS	17-19
<b>CHAPTER 3 – LITERATURE REVIEW</b>	<b>20-37</b>
<b>CHAPTER 4 – EXPERIMENTAL PROGRAM</b>	<b>38</b>
4.1 GENERAL	38
4.2 TEST PROGRAMME	38
4.3 MATERIALS	38
4.3.1 Cement	39-40
4.3.2 Coarse Aggregates	41-42
4.3.3 Fine Aggregates	42-43
4.3.4 Water	43
4.3.5 Reinforcement	43
4.3.6 Corrosion Inhibitor	44-45
4.4 MIX PROPORTION USED IN STUDY	45
4.5 CASTING OF SPECIMENS	45
4.5.1 Pore solution	45-46
4.5.2 Concrete Specimens	46-48
4.6 TESTS CONDUCTED	48
4.6.1 Tests on Pore Solution	49-50
4.6.2 Tests on Concrete Specimens	51-55
<b>CHAPTER 5 – RESULTS AND DISCUSSION</b>	<b>56</b>
5.1 INTRODUCTION	59
5.2 PORE SOLUTION TEST RESULTS	56
5.2.1 Half Cell Potential Test	56-58
5.2.2 Linear Polarisation Resistance Test	59-60
5.2.3 Chemistry between Corrosion Inhibitor and Steel Surface	61
5.3 EFFECT OF 2-AMINOPYRIDINE ON CONCRETE	62
5.4 CARBONATION DEPTH	62-65
5.5 CONCRETE PRISMS TEST RESULTS	66
5.5.1 Half Cell Potential Test	66-69
5.5.2 Linear Polarisation Resistance Test	69-73
5.5.3 Galvanic Potential	73-75
<b>CHAPTER 6 – CONCLUSIONS</b>	<b>76</b>
<b>REFERENCES</b>	<b>77-82</b>

## LIST OF FIGURES

<b>Fig._No.</b>	<b>Description</b>	<b>Page No.</b>
Fig. 1.1	Uniform corrosion and galvanic corrosion	3
Fig. 1.2	Types of localised corrosion	5
Fig. 1.3	MIC corrosion and Erosion corrosion	6
Fig. 1.9	Corrosion mechanism	7
Fig. 3.1	Variation of the rebar corrosion potential ( $E_{corr}$ ) With time (a) blank specimens (b) treated with inhibitor	21
Fig. 3.2	Variation of the rebar $I_{corr}$ and CR as a function of time (a) Blank specimens. (b) Treated with inhibitor.	21
Fig. 3.3	MFP penetration profiles (determined MFP / total applied MFP in %) in carbonated or not carbonated hardened cement pastes.	22
Fig. 3.4	Evolution of the steel corrosion potential after applying MFP solution or water onto reinforced mortar surface	23
Fig. 3.5	Corrosion potential-time curves for Group 1 specimens	25
Fig. 3.6	$I_{corr}$ -time curves for Group 1 specimens	25
Fig. 3.7	$E_{corr}$ -time curves for Group 2 specimens	26
Fig. 3.8	$I_{corr}$ -time curves for Group 2 specimens	26
Fig. 3.9	Corrosion rates and Half-cell potentials for 10mm cover samples	28
Fig. 3.10	Polarization curves recorded on steel in carbonated chloride solution	29
Fig. 3.11	Corrosion potential-time plots of steel rebar exposed in saturated $Ca(OH)_2$ solution different concentrations of NaCl and DMEA inhibitor.	30

Fig. 3.12	Corrosion potential plots at different molar ratio of $[Cl^- / NO_2^-]$	31
Fig. 3.13	Corrosion potential (versus Ag/AgCl) versus time diagrams	33
Fig. 3.14	Icorr calculated at three different monitoring periods	34
Fig. 3.15	Variations of the Icorr and Ecorr for the specimens in solutions (1–3) with the concentrations of chloride ions.	35
Fig. 3.16	Variations of the Ecorr and Icorr for the specimens in solutions (4–6) with the concentrations of chloride ions.	36
Fig. 4.1	Molecular Structure of 2-Aminopyridine	44
Fig. 4.2	Actual Photograph of 2-Aminopyridine	44
Fig. 4.3	Prepared prism specimen	48
Fig. 4.4	ACM Setup used for testing	49
Fig. 4.5	Input readings for HCP test for solution and concrete	50
Fig. 4.6	Test Setup for LPR and Half-cell potential	50
Fig. 4.7	Input readings for Half-Cell Potential test for solution and concrete	52
Fig. 4.8	Half cell potential test arrangement	53
Fig. 4.9	Input readings for LPR Sweep for concrete specimens	53
Fig. 4.10	LPR Sweep test arrangement for concrete	54
Fig. 4.11	Diagram showing connection of resistor for Galvanic Potential	54
Fig. 4.12	(a) Prepared Concrete cube for Carbonation Depth (b) Splitting Concrete Cube into two halves	55

Fig. 5.1	Variation of Half-cell potential of solution specimens with time	58
Fig. 5.2	Corrosion current density of specimens at different time in solution	60
Fig. 5.3	Condition of steel rebars after the test at different time	60
Fig. 5.4	(a) Chelate ring formed by 2-Aminopyridine around steel bar (b) Molecular Structure of 2-Aminopyridine	61
Fig. 5.5	Carbonation depth specimen showing carbonated and non-carbonated part	62
Fig. 5.6	Carbonation depth with time for various OPC cubes	64
Fig. 5.7	Carbonation depth with time for various PPC cubes	65
Fig. 5.8	Variation of Half Cell potential with time for OPC prisms	68
Fig. 5.9	Variation of Half Cell potential with time for PPC prisms	69
Fig. 5.10	Variation of corrosion current with time for different OPC prisms	71
Fig. 5.11	Variation of corrosion current with time for different PPC prisms	71
Fig. 5.12	Comparison of corrosion current with time for OPC and PPC prisms	72
Fig. 5.13	Variation of Galvanic Potential with time for different OPC prisms	74
Fig. 5.14	Variation of Galvanic Potential with time for different PPC prisms	74

## LIST OF TABLES

<b>Table No.</b>	<b>Description</b>	<b>Page No.</b>
Table 3.1	Composition and pH of the simulated concrete pore solutions	35
Table 4.1	Physical Properties of OPC Cement	39
Table 4.1	Physical Properties of PPC Cement	40
Table 4.3	Chemical Composition of Cement	40
Table 4.4	Sieve analysis of coarse aggregates	41
Table 4.5	Physical Properties of coarse aggregates	42
Table 4.6	Physical Properties of Fine aggregates	42
Table 4.7	Sieve Analysis of Fine Aggregates	43
Table 4.8	Mechanical Properties of Reinforcement Used	43
Table 4.9	Properties of 2-Aminopyridine	45
Table 4.10	Mix Design	45
Table 4.11	Corrosion condition corresponding to HCP values.	51
Table 5.1	Nomenclature of Solutions	56
Table 5.2	Values of Half-cell potential and corrosion current for solutions	57
Table 5.3	Nomenclature of Concrete specimens	63
Table 5.4	Carbonation depth values of cubes	63
Table 5.5	Values of Half-cell potential in mV for different prisms	66
Table 5.6	Corrosion condition corresponding to Half-Cell Potential Readings	67
Table 5.7	Values of I <sub>corr</sub> for different type of prisms	70
Table 5.8	Values of Galvanic potential in mV for different prisms	73

## **CHAPTER 1 – INTRODUCTION**

### **1.1 GENERAL**

Metals and alloys are used extensively in industry. The expansions of many innovative technologies make use of some rare and costly metals. In addition, the escalating pollution of the surroundings produces a more corrosive medium. So the corrosion protection techniques are required more than ever. Corrosion results in a great economic loss both directly and indirectly. For instance, there is additional cost in using safety methods, replacing of corroded tools, using other additional costly resistant metals, as well as production and efficiency loss and industrial accidents due to corrosion. Study is needed to better be aware of the thorough mechanisms of corrosion also as a result discover additional efficient methods of corrosion control.

The problems related to durability faced in R.C. structures are of severe alarm to the concrete infrastructure all over the world. The durability of R.C. structures is reliant on nearby exposure conditions and environment. One of the key reason accountable for the weakening of R.C. structures is the reinforcement corrosion. Corrosion of reinforcement normally goes along with the loss of reinforcement cross-section and a build-up of corrosion products. The products of corrosion take a bigger volume than the original bars from which they were formed; this leads to tensile stresses in concrete which leads to cracking and spalling of the concrete cover. Also the corrosion in reinforcement leads to the loss of interfacial bond connecting concrete and reinforcement and decrease in cross-sectional area of the rebar, thus decreasing the load carrying ability of R.C. structures.

Material when comes in contact with the surroundings leads to brutal attack of corrosion. The grave penalty of the corrosion process has become a setback of global importance. In addition to our day by day encounter with this form of deprivation, corrosion leads to plant shutdown, waste of expensive resources, loss or contamination of manufactured goods, decrease in efficiency, expensive maintenance and costly overdesign. It also put at risk safety and inhibits technical progress. The multidisciplinary feature of corrosion problems shared with the distributed responsibilities linked with such nuisance only add to the difficulty of the subject. Corrosion control is attained by understanding corrosion mechanisms by using corrosion-resistant materials. Mild steel is extensively used in a lot of industries because of cost-

effective and simple fabrication, but it is prone to take on corrosion in violent environmental conditions. The surroundings may be a liquid, gas or combination of solid and liquid.

## **1.2 DEFINATION OF CORROSION**

Corrosion is an expensive and severe material science crisis. Corrosion of metals is defined as the spontaneous damage of metals in the course of their chemical, electrochemical and biochemical exchanges with the surroundings. Thus, it is precisely the opposite of extraction of metals from ores. In the majority of environments the metals are not inherently stable, and most likely to revert to compounds which are more stable, a course of action which is called corrosion. Corrosion is also defined as worsening of intrinsic properties in a material due to its reactions with environment. It is the oxidation of metals reacting with water or oxygen. Corrosion is derived from the Latin word “Corrosus” meaning “gnawed away”.

When a metal is subjected to corrosion, its properties are altered due to the non deliberate but destructive reaction with the exposed surroundings. The corrosion process is ongoing and permanent. Generally it consists of a set of electrochemical redox reactions. Thus the metal is oxidized to a corrosion product at anodic sites (e.g.  $M = M^{2+} + 2e^-$ ) and some species are reduced at cathodic sites (e.g.  $2H^+ + 2e^- = H_2$ ). Because of the electrochemical nature of almost all corrosion processes, electrochemical methods are helpful equipment for learning corrosion. More explicitly, electrochemical techniques can be used to calculate the kinetics of electrochemical processes (e.g., corrosion rates) in particular environment and also calculate or control the oxidizing power (i.e., potential) of the surroundings.

## **1.3 CLASSIFICATION OF CORROSION**

There is no universally accepted categorization for corrosion, but the following classification is adapted:

### **1.3.1 Uniform or general corrosion**

Uniform or general corrosion, as the name imply, results in a fairly uniform penetration over the complete exposed metal surface. The general attack results from local corrosion cell action, that is, multiple anodes and cathodes are operating on the metal surface at any given time. The place of the anodic and cathodic areas continues to move about on the surface, ensuing uniform corrosion. In this case the exposed metal surface area is completely corroded in an environment such as a liquid electrolyte (chemical solution, liquid -metal), gaseous

electrolyte (air, CO<sub>2</sub>, SO<sub>2</sub> etc.,) or a hybrid electrolyte (solid, water, biological organisms, etc.). Fig 1.1 (a) shows a steel storage tank corroded uniformly over the whole outer surface.

### 1.3.2 Galvanic corrosion

Galvanic corrosion is an electrochemical action of two different metals in the company of an electrolyte and an electron conductive path. It take place when different metals are electrically coupled in a common solution, the more negative (more active) metal will be the anode of the galvanic corrosion cell and its corrosion rate will increase. The more positive (more noble) metal will be the cathode and its corrosion rate will decrease and it is detectable by the presence of a build-up of corrosion at the joint between the dissimilar metals. For example when aluminium alloys or magnesium alloys are in contact with steel (carbon steel or stainless steel), galvanic corrosion can occur and accelerate the corrosion of the aluminium or magnesium. Fig 1.1 (b) shows an example of galvanic corrosion.

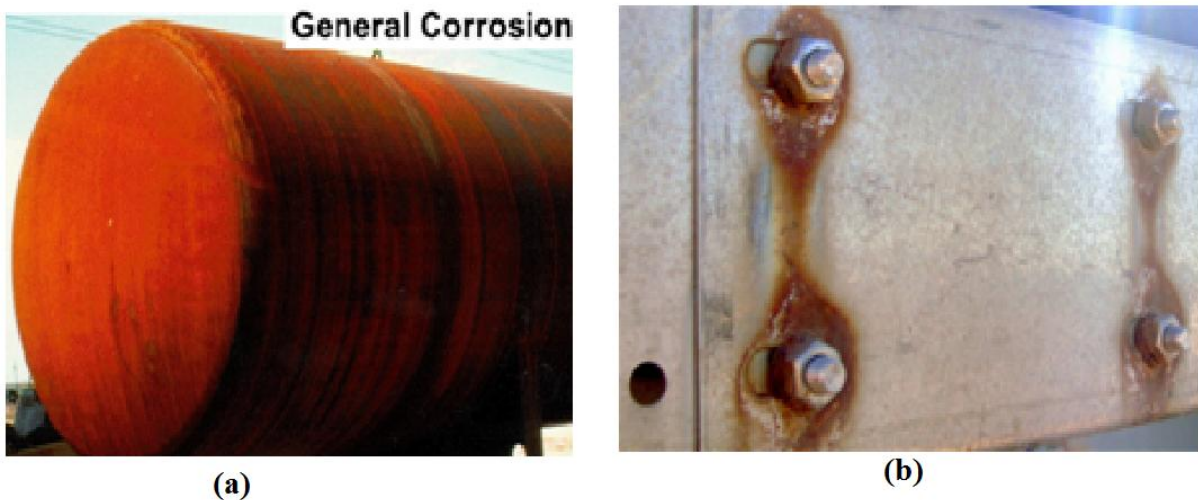


**Fig 1.1:** (a) Uniform corrosion on a storage tank (<http://chemblinks.blogspot.in>)  
(b) Galvanic corrosion (<http://www.tecnoconverting.com>)

### 1.3.3 Localized corrosion

This term implies that, specific parts of an exposed surface area corrode in a suitable electrolyte. This form of corrosion is more difficult to manage than the general corrosion. Localized corrosion can be classified as

**a) Crevice corrosion:** This form of corrosion starts due to changes in local chemistry such as reduction of oxygen in the crevice, increase in pH with increasing hydrogen ion concentration and boost of chloride ions. Crevice corrosion may take place on any metal and in any

corrosive environment. The material responsible for forming the crevice corrosion need not be metallic. Wood, plastic, rubber, glass, concrete, asbestos, wax and living organisms have been reported to cause crevice corrosion. It is frequently more intense in chloride environments. The mechanism of crevice corrosion is electrochemical in nature. It requires a prolong time to start the metal oxidation process, but it may get accelerated afterwards. Fig. 1.2 (a) shows Crevice corrosion on a stainless steel flange exposed to a chloride-rich medium.

**b) Filiform corrosion:** It is basically a special type of crevice corrosion, sometimes termed as “under film” corrosion. This sort of corrosion takes place under painted or plated surfaces as can be seen in Fig. 1.2 (b), when moisture penetrates the coating. Lacquers and "quick-dry" paints are most susceptible to the problem. Their use should be avoided except absence of an adverse effect has been established by field experience.

**c) Pitting corrosion:** Pitting Corrosion is "self-nucleating" crevice corrosion, starting at occluded cells. Corrosion products frequently cover the pits, and might form "chimneys". Pitting is considered to be more risky than uniform corrosion damage because it is more complex to detect, predict and prevent. A small, narrow pit with negligible overall metal loss can escort to the failure of a complete engineering system. Once they start, both crevice and pitting corrosion can be explained with the help of differential concentration cells, cathodic reactions, i.e., oxygen reduction or hydrogen evolution may start in the crevice or the pits. Huge surface areas will turn out to be cathodic and pits or crevices will turn into anodic and corrode. Metal dissolution will thus be concentrated in tiny areas and will continue at much higher rates than with uniform corrosion. Fig 1.2 (c) shows Pitting corrosion on sink surface.

**d) Intergranular corrosion:** Intergranular corrosion is a local type of corrosion. It is a preferential attack on the grain boundary phases or the zones straight adjacent to them. Little attack is experienced on the main body. This results in loss of strength and ductility. The attack is often quick, penetrating severely into the metal and leading to failure. Fig 1.2 (d) shows Intergranular corrosion of stainless steel.

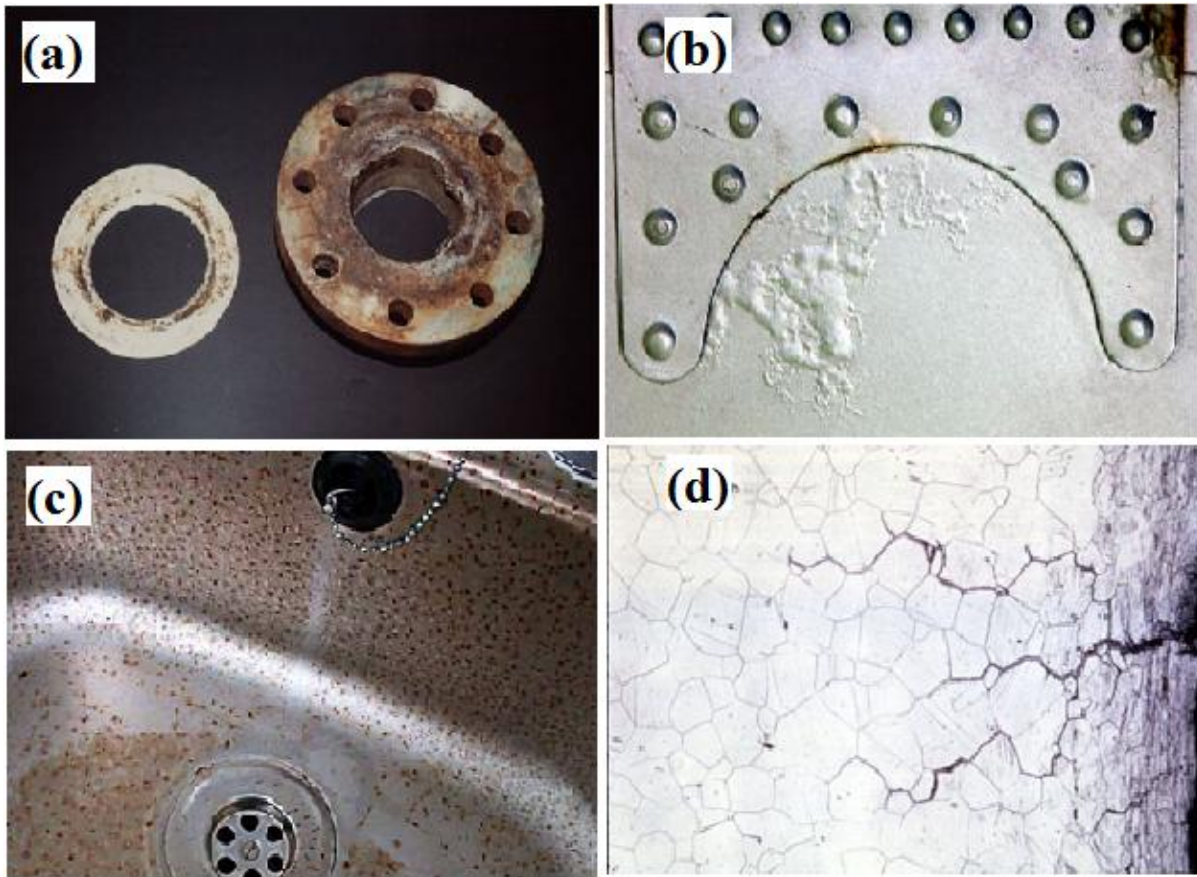


**Fig 1.2: (a) Crevice corrosion on a stainless steel flange exposed to a chloride-rich medium. (b) Filiform corrosion spreading beneath painted surface (c) Pitting corrosion on sink surface (d) Intergranular corrosion of stainless steel**

*(<https://www.gewater.com/handbook/>)*

#### **1.3.4 Microbiologically influenced corrosion (MIC)**

MIC refers to corrosion that is affected by the existence and activities of microorganisms (bacteria, fungi etc.) and their metabolites. An aerobic bacterium produces highly corrosive type as part of their metabolism. Most resources, including metals, polymers, glass and ceramics can be degraded in this manner. The production of corrosive species such as minerals, organic acids, ammonia, sulphide and a variety of types of microbes tend to act synergistically in the corrosion of materials with their interactions characteristically being of a complex nature. Fig. 1.3 (a) shows MIC corrosion inside fire sprinkler systems.

### 1.3.5 Erosion corrosion

The term “erosion” applies to deterioration due to mechanical power. When the factors contributing to erosion hasten the rate of corrosion of a metal, the attack is called “erosion corrosion”. It is the effect of a combination of an aggressive chemical environment and elevated fluid surface velocities. This can be the effect of fast fluid flow past a stationary object, such as the case with the oilfield check valve, or it can be the outcome from the quick motion of an object in a stationary fluid, such as when a ship's propeller churns the ocean. Surfaces which have undergone erosion corrosion are usually fairly clean, unlike the surfaces from a lot of other forms of corrosion.

The red arrow points to pin holes in the pipe wall. Notice the crushed pipe wall which is much thinner than normal (blue arrow). Fig. 1.3 (b) is a view of a section of the failed pipe showing the interior surfaces. The blue arrow in Figure points to the normal wall thickness of the copper tubing, while the red arrow points to an excessively thin wall area where pin hole leaks had occurred. This thinning of the copper pipe wall in new installations is characteristic of the phenomenon called erosion-corrosion.



**Fig 1.3 (a) MIC corrosion inside a fire sprinkler systems.**

**(b) Erosion corrosion inside a pipe (<http://www.croberts.com/erosion-corrosion.htm>)**

### 1.4 MECHANISM OF CORROSION

The corrosion process that takes place inside the concrete is electrochemical in nature. Corrosion results in the flow of electrons between anodic and cathodic sites on the steel bar. Concrete, when exposed to wet and dry cycles, has adequate conductivity to serve as an electrolyte.

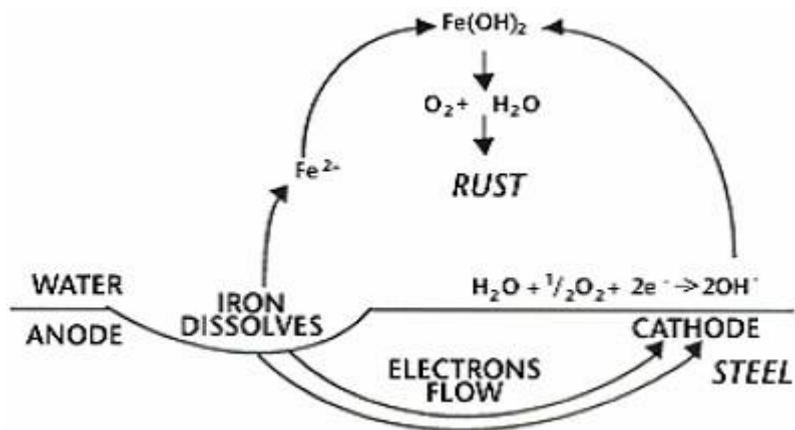
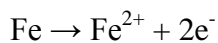


**Fig 1.4 Corrosion mechanism** (<http://www.multibriefs.com>)

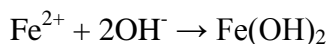
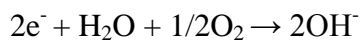
The corrosion of steel in concrete in the occurrence of oxygen but without chlorides takes place in several steps:

**a) Corrosion in absence of chlorides**

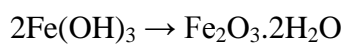
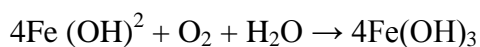
At the anode, iron is oxidized to the ferrous state and releases electrons.



These electrons migrate to the cathode where they combine with water and oxygen to form hydroxyl ions.

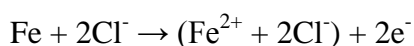


In the presence of water and oxygen, the ferrous hydroxide is further oxidized to form Fe<sub>2</sub>O<sub>3</sub>

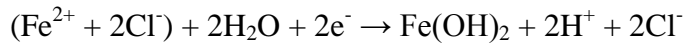


**b) Corrosion in presence of Chloride**

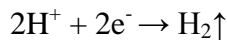
At anode, formation of intermediate soluble iron chloride complex takes place as iron reacts with chloride ions.



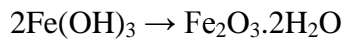
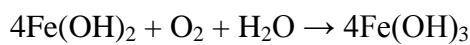
When the iron–chloride composite diffuse from the bar to an area with greater Ph and amount of oxygen, it react with hydroxyl ions to form Fe(OH)<sub>2</sub>. This complex reacts with water to make ferrous hydroxide.



The hydrogen ions then combine with electrons to form hydrogen gas.

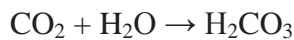
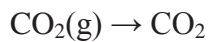


As in the case of corrosion of steel without chlorides, the ferrous hydroxide, in the presence of water and oxygen, is further oxidized to form Fe<sub>2</sub>O<sub>3</sub>

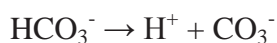


### c) Corrosion in presence of CO<sub>2</sub>

The corrosion mechanism of CO<sub>2</sub> and its effect on mild steel under changing condition of pressure, temperature and pH. Carbon dioxide gas gets dissolved in water and form a “weak” carbonic acid through hydration by water.



The carbonic acid (H<sub>2</sub>CO<sub>3</sub>) then partially dissociates to form the bicarbonate ion, which can additionally dissociate to yield the carbonate ion:



It is extensively known that solutions that contain H<sub>2</sub>CO<sub>3</sub> are more corrosive to mild steel than solutions of strong acids.

## 1.5 FACTORS AFFECTING CORROSION

### a) Nature of the metal

The tendency of the metal to go through corrosion is mainly dependent on the nature of the metal. In general more reactive metal have low electrode potential and is more susceptible for corrosion and metal with high electrode potential is less reactive and less susceptible for corrosion. For example, metals like K, Na, Mg, Zn etc., undergo corrosion very easily due to

their low electrode potential where as noble metals like Ag, Au, and Pt have higher electrode potential, their corrosion rates are negligible. But there are few exceptions as some metals show the property of passivity like Al, Cr, Ti, Ta, etc., According to electrochemical series, metal with more positive potential are stable then those with more negative potential. If we know the electrode potentials of metals in some electrolyte, we can predict if the metal would corrode or not. The electromotive force, E is the difference between electric potentials of cathodic and anodic reactions,

$$E = E_{\text{cathodic}} - E_{\text{anodic}}$$

This value is related to Gibbs free energy which is represented by the equation,

$$\Delta G = -nFE \text{ where,}$$

$\Delta G$  is the change of Gibbs free energy of corrosion reaction, n is the number of electrons taking part in the corrosion reaction and F is Faraday's constant.

In corrosion processes where hydrogen evolution is the cathodic reaction, hydrogen over potential (resistance to hydrogen evolution) is another important factor effecting the corrosion. Each metal in a given environment has characteristic hydrogen over potential. Thus a metal with low hydrogen over potential in a given environment undergoes fast corrosion. In the case of alloys, other entities when added in micro-quantities can alter the hydrogen over potential which can affect the corrosion process.

### **b) Surface state of the metal**

The corrosion product is usually the oxide of the metal, and the nature of the product determines the rate of corrosion process. If the oxide layer formed on the surface is exceedingly insoluble and non-porous in nature with low ionic and electronic conductivity, then that type of layer efficiently prevents further corrosion which acts as a protective film. For example, Al, Cr and Ti develop such a layer on their surface and become passive to corrosion, and some metals like Ta, Zn and Mo not only form such protective layers but are capable of self repairing oxide films when it is damaged. Hence these are extremely passive metals. If the oxide layer formed on the metal surface is soluble, unstable and porous in nature and has an appreciable conductivity, it cannot control corrosion on metal surface. Extremely polished and smooth surface resists corrosion while an uneven surface containing various types of imperfections such as clearance steps, dislocations, point defects etc., is liable to severe attack.

### **c) Protective film**

Some metals like Al have an affinity to form a protective film on the surface which acts as physical barrier (passivation) among the metal and the medium, thereby curtailing the corrosion.

### **d) pH of the medium**

In general, corrosion rate is higher in acid pH rather than in neutral and alkaline pH. In case of iron, at higher pH, protective coating of iron oxide is formed which is also known as the passive layer which prevents corrosion where as at lower pH severe corrosion takes place. But for metals like Al, rate of corrosion is high even at high pH. For metals like zinc, iron, magnesium etc., hydrogen evolution is thermodynamically favoured cathodic reaction. Corrosion of every metal in acidic medium is consequently highly pH dependent. Reduction in pH helps the rate of hydrogen evolution and hence increases the corrosion rate of metals. In case where a protective film is shaped on the metal surface, change in solution pH may influence the solubility of the film and therefore influence the corrosion process. Thus under changing pH conditions of the medium, a corroding surface may display activity, immunity or passivity.

### **e) Temperature of the medium**

Corrosion is an activation-controlled chemical reaction, the pace of which is to a huge extent affected by temperature. Usually, corrosion rate increases considerably as temperature increases. A thumb rule is that, when corrosion is controlled by diffusion of oxygen, the rate of corrosion at given oxygen concentration roughly doubles for every 10 °C rise in temperature. In an open vessel, allowing dissolved oxygen to get away, corrosion rate increases with increasing temperature to about 80 °C and then falls to an extremely low value at the boiling point. The lower corrosion rate above 80 °C is connected to a marked decrease of oxygen solubility in water as the temperature is increased and this effect eventually overshadows the accelerating result of temperature alone. In a closed system, on the other hand, oxygen is not allowed to escape, and the corrosion rate continues to rise with temperature until all of the oxygen is consumed. When corrosion is supported by hydrogen evolution, the corrosion rate is more than twice for every 10 °C rise in temperature. In general, as the temperature rises the diffusion rate increases, and both viscosity and over-voltage decrease causing depolarization by hydrogen evolution. Increased diffusion leads to more dissolved oxygen to react with cathodic surface, therefore depolarizing the corrosion

cell. A decrease in viscosity helps depolarization mechanism, and it favours the solution having atmospheric oxygen and increases hydrogen evolution. In a domestic water system, an increase in temperature from 25 °C to 75 °C may increase the corrosion to an extent of 400 percent. An increase in temperature is usually expected to speed up a chemical reaction according to thermodynamic considerations.

#### **f) Effect of dissolved oxygen**

Dissolved oxygen plays an extremely important role in the corrosion of metals. Oxygen takes part in cathodic process on the surface of metal in neutral, alkaline, and acidic media. If dissolved oxygen is absent in water, and then corrosion diminishes near to zero in neutral and alkaline solutions. If the amount of dissolved oxygen increases, corrosion accelerates as a result of oxygen involvement in the cathodic processes. In the presence of oxygen, depolarization of the cathodic products takes place. In most situations, depolarization by oxygen tends to control the rate at which the iron corrodes. However, is generally so rapid that oxygen concentration at the cathodic surface approaches zero. Therefore, rate of oxygen depolarization depends on the rate of diffusion of oxygen through the resistant film at the surface of the metal. Ferrous ion is transformed to the ferric state by further oxidation and the maximum of common rust comprises of hydrated ferric oxide. Often, a black layer of magnetic hydrous ferrous ferrite ( $\text{Fe}_3\text{O}_4 \cdot n\text{H}_2\text{O}$ ) forms between  $\text{Fe}_2\text{O}_3$  and  $\text{FeO}$ . Thus, the rust film usually consists of three layers of iron oxide in variant states of oxidation. Even though increase in oxygen concentration at first accelerates the corrosion of iron, but, beyond a decisive concentration, the corrosion rate drops down once more to a low value.

#### **g) Corrosion due to Carbonation**

The Carbon dioxide gas from the atmosphere reacts with hydrated concrete (alkaline hydroxides) and partly neutralizes the alkaline nature of concrete. This course of action is known as carbonation. Carbonation lowers down the pH value of concrete from over 12-13 to less than 9. When depth of carbonation reaches the reinforcement, it breaks down passive film around the steel and makes the steel embedded in the concrete more active. The higher carbonation rates are obtained by using higher  $\text{CO}_2$  concentration and controlled environment (i.e., temperature, RH). It is observed that a RH within the range of 50–70% is commonly used in the experiments. This is because the carbonation reaction rate of concrete is highest within this RH range.

## **h) Corrosion due to Chlorides**

Chloride ions present in concrete around the reinforcement when comes in contact with alkaline solution at anode to form hydrochloric acid which wipes out the passive protective layer on the reinforcement steel. The surface of steel then gets available locally to form the anode, with the passive surface forming the cathode, setting the electrolytic process. Occurrence of free  $\text{Cl}^-$  ions in concrete depends upon total chloride content of concrete. Chlorides are present in concrete due to the materials, mixing water and calcium chloride used as accelerating admixtures etc. Chlorides also go into concrete due to salt water in sea shore or through atmosphere.

### **1.6 PREVENTIVE MEASURES**

Some of the methods that can be used to prevent corrosion or limit the damage of corrosion are discussed on the following section.

1. Adequate thickness of concrete cover to cut off reinforcing steel from ingress of harmful chemicals.
2. Use of concrete that is effectively impermeable and long-lasting to maintain the chemical blockade.
3. Preventing chloride-containing admixtures in materials, admixtures or mixing water.
4. Improvement of chemical barrier through use of protecting overlays, waterproof membranes or polymer penetration on the outer surface of concrete.
5. Use of corrosion inhibitors to protect passivity of reinforcing steel if damaging chemicals somehow penetrate.
6. Use of non-corrosive materials for reinforcement such as stainless steel or epoxy coating on the surface of reinforcing steel.
7. Use of cathodic protection to prevent steel from corrosion.
8. Monitoring of corrosion conditions can be performed using delaminating monitors, half-cell potential measurements, chloride analysis, corrosion rate probes or electrical resistivity measurements.

## **1.7 OBJECTIVES**

There are various methods to prevent corrosion but one of the most effective methods is the use of Corrosion Inhibitors. Commercially available corrosion inhibitors are quite effective in preventing corrosion. The migratory inhibitors can also be applied, once the corrosion has already started in order to protect the passivity of reinforcing steel. Still, there is a huge scope of study in this field to identify more economical and efficient corrosion inhibitors. The past studies show that the Amine group corrosion inhibitors have performed well. So, in this thesis the efficiency of chemical, 2-Aminopyridine as corrosion inhibitor is checked.

## **1.8 FORMAT OF THESIS REPORT**

The thesis presentation has been organized in five chapters.

1. In the first chapter, Mechanism and Causes of Rebar Corrosion are presented.
2. Second chapter deals with the Corrosion inhibitors, classification of corrosion inhibitor and some commonly used corrosion inhibitors
3. Third chapter deals with the Literature Review justifying the objectives of the research work which is presented.
4. In fourth chapter, the experimental investigation carried out for measurement of half-cell potential, Linear Polarization resistance on prism and pore solution specimens subjected to chloride and carbonated induced corrosion to establish the suitability of 2-aminopyridine as a stable corrosion inhibitor.
5. Chapter five deals with the results and discussions of the experiment.
6. In Chapter six, conclusions are presented.

## **CHAPTER 2 - CORROSION INHIBITORS**

### **2.1 GENERAL**

Corrosion has made a place in our lives. The damage it makes is pretty much clear. The economic costs of corrosion are clearly huge. Like other natural hazards such as earthquakes and harsh weather turbulence, corrosion can cause dangerous and costly damages to infrastructure, waterways, ports, railroads, hazardous materials storage, drinking water, sewer systems, electrical utilities, telecommunications, automobiles, ships, aircrafts, mining, petroleum refining, chemical, petrochemical and pharmaceutical production, pulp and paper, agricultural production, food processing, electronics, defence, home appliances, gas transmission pipelines and highway bridges. Losses continued by corrosion amounts to many billions of dollars yearly. The financial factor is the main object for much of the current study in corrosion. Additional aspect is the safety of functioning equipments such as pressure vessels, boilers, material containers for toxic materials and may be the most significant of all is the equipment for nuclear power plants and disposal of nuclear wastes.

### **2.2 CORROSION INHIBITORS**

The use of chemical inhibitors to reduce the rate of corrosion processes is quite diverse. In the oil extraction and processing industries, inhibitors have always been considered to be the first line of defence against corrosion. A great number of scientific studies have been dedicated to the topic of corrosion inhibitors. Although, for the most part is known has been grown from trial and error experiments, both in the laboratories and in the field. Rules, equations, and theories to guide inhibitor growth or use are very restricted by definition, a corrosion inhibitor is a chemical substance that, when added in small concentration to an environment, efficiently decreases the corrosion rate. The competence of an inhibitor can be articulated by a measure of this improvement:

$$\text{Inhibitor efficiency (\%)} = 100 \frac{[\text{CR}(\text{uninhibited}) - \text{CR}(\text{inhibited})]}{\text{CR}(\text{uninhibited})}$$

Where, CR(uninhibited)=corrosion rate of the uninhibited system,

CR(inhibited)=corrosion rate of the inhibited system.

The scientific corrosion literature has descriptions and listing of plentiful chemical compounds that show inhibitive properties. Out of these, only the minority are actually used in practice. This is partly because the desirable properties of an inhibitor usually extend beyond those simply related to metal protection. Considerations of cost, toxicity, availability, and environmental easiness are of substantial significance.

## 2.3 CLASSIFICATION

### 2.3.1 Based on physical mode of protection:

**a) Admixed inhibitors:** Those compounds which are added to the fresh concrete at the time of mixing for new structures are known as admixed inhibitors (*Jamil et al. (2005)*). Admixed inhibitors are commercially available since 1960's (*Soylev et al. (2008)*). These compounds are added immediately after the addition of water to cement. Admixed inhibitor influence initial set, later strength gain or other properties i.e. hydration processes of cement. To overcome this, retarder was added to concrete mix which balances the acceleration of the inhibitors and provided a little more retardation.

The inorganic compounds which are based upon calcium nitrite (*Berke et al. (2004)*), sodium nitrite, sodium benzoate and sodium chromate are used as admixed inhibitors. Organic compounds based upon mixtures of alkanolamines, amines or amino-acids, or based on an emulsion of unsaturated fatty acid ester of an aliphatic carboxylic acid and a saturated fatty acid also proposed as admixed inhibitors.

**b) Migrating inhibitors:** These are the chemical which are applied on the hardened concrete surface and are able to diffuse through concrete to the underlying rebar where they act to suppress both the anodic and cathodic corrosion reactions by forming a monolayer film at the steel-concrete interface (*Soylev et al. (2008)*). According to physical mode of application these types of inhibitors are also known as Surface applied corrosion inhibitors or Penetrating corrosion inhibitors. Use of migrating corrosion inhibitors are proposed in the last 15-20 years and are generally proposed for the repair works.

These inhibitors are typically based either on mixtures of alkanolamines and amines or on inorganic compounds based upon Monofluoro-phosphate [MEP] (*Ormellase et al.(2006)*). In addition, nitrite ions can penetrate into concrete by absorption and diffusion if applied to the surface by spraying or ponding with aqueous solutions. Alkanolamines and amines have relatively high vapour pressure under atmospheric conditions, assisting diffusion and

migration into concrete. Amino alcohols, such as ethanolamine and dimethylethanolamine, can act at the cathode and prevent oxygen reduction to hydroxyl ion by a blocking mechanism, following adsorption on the steel surface (*Gaidis (2004)*).

### **2.3.2 Based upon the mechanisms of protection:**

#### **a) Anodic inhibitors**

Anodic inhibitors form a protective oxide film on the surface of the metal leading to a large anodic shift of the corrosion potential. This leads to the shift of metallic surface into the passivation region. They are also called as passivators from time to time. Chromates, nitrates and tungstate are some basic instances of anodic inhibitors.

#### **b) Cathodic Inhibitors**

Cathodic inhibitors either slow down the cathodic reaction itself or selectively precipitating on cathodic areas to bound the diffusion of reducing species to the surface. Cathodic poisons can also be used to reduce the rate of cathodic reactions. However, cathodic poisons can also raise the vulnerability of a metal to hydrogen induced cracking as hydrogen can also be absorbed by the metal through aqueous corrosion or cathodic charging. Reduction in corrosion rate can also be done by the use of oxygen scavengers that react with dissolved oxygen. Sulfite and bisulfite ions are some examples of oxygen scavengers that can combine with oxygen to form sulfate.

#### **c) Mixed Inhibitors**

Mixed inhibitors work by reduction in both the cathodic and anodic reactions. The formation of precipitates takes place on surface blocking both anodic and cathodic sites indirectly as they are usually the film forming compounds. Hard water that is high in calcium and magnesium is less corrosive than soft water because of the tendency of the salts in the hard water to precipitate on the surface of the metal thus forming a protective film. The most common inhibitors of this sort are silicates and phosphates. Sodium silicate, for instance, is used in many household water softeners to avoid the occurrence of corrosive water. In aerated hot water systems, sodium silicate protects steel, copper and brass. However, protection is not at all times reliable and depends a great deal on pH. Phosphates also need oxygen for efficient inhibition. Silicates and phosphates do not afford the degree of protection

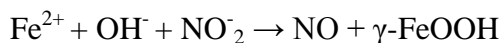
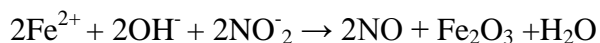
provided by chromates and nitrites; however, they are very useful in situations where non-toxic additives are required.

#### **d) Volatile inhibitors**

Volatile corrosion inhibitors (VCIs) are also known as vapour phase inhibitors (VPIs). They are compounds which are moved to a closed environment to the place of corrosion by volatilization from a source. Morpholine is one of the volatile basic compounds which when transported with steam to stop corrosion in condenser tubes in boilers by counterbalancing the acidic carbon dioxide or by shifting the surface pH towards less acidic. If the corrosion product is volatile, it volatilizes as soon as it is created, thereby leaving the underlying metal surface uncovered for further attack. This causes fast and continuous corrosion leading to too much corrosion. For example, molybdenum oxide, the oxidation corrosion product of molybdenum is volatile. In closed vapor process (shipping containers), volatile solids such as salts of dicyclohexylamine, cyclohexylamine and hexamethylene amine are used as volatile corrosion inhibitors.

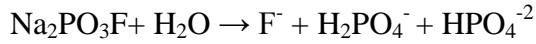
### **2.4 MECHANISM OF SOME COMMONLY USED COMMERCIALY AVAILABLE INHIBITORS:**

**a) Calcium nitrites:** Nitrites (calcium or sodium salt) are recognized as an anodic inhibitors since they compete with chloride ions for the ferrous ions at the anode to form a film of ferric oxide,  $\text{Fe}_2\text{O}_3$  as indicated in the equations below (*Gaidis J.M (2004)*):



These reactions are a lot quicker than the transfer of ferrous ions via chloride ion complex formation. Thus nitrite ions aid the creation of a stable passive layer even in the company of chloride ions (with  $\gamma$  FeOOH being the most stable oxide in company of chlorides). However, full protection depends to a great extent on the concentration of aggressive ions such as the chloride ion, and severe pitting may occur when inadequate quantity of inhibitor is used compared to the level of chloride in the concrete.

**b) Monofluorophosphate (MFP):** The inhibition mechanism of the MFP ( $\text{Na}_2\text{PO}_3\text{F}$ ) is not clear; it may be anodic, cathodic or mixed (*Alonso et al. (2000)*).  $\text{Na}_2\text{PO}_3\text{F}$  hydrolyses in aqueous and neutral media to form orthophosphate and fluoride through a process like that indicated in the following equation:



The inhibiting action of  $\text{Na}_2\text{PO}_3\text{F}$  may be attributed to the formation of phosphates, and so the anodic formation of a passive layer of  $\text{Fe}_3\text{O}_4$ ,  $\gamma\text{-Fe}_2\text{O}_3$  and  $\text{FePO}_4 \cdot \text{H}_2\text{O}$ . However, as  $\text{PO}_3\text{F}^{2-}$ ,  $\text{PO}_4^{3-}$  and  $\text{OH}^-$  are all potential corrosion inhibitors, it is difficult to say which, if any, of these ions may be responsible for corrosion inhibition effects induced by  $\text{Na}_2\text{PO}_3\text{F}$ . The finding of various research studies confirms this dual effect of the phosphates. *Soylev et al. (2008)* confirm that at low values of inhibitor to chloride ion ratio, phosphate (sodium phosphate) acts as a cathodic inhibitor, whereas at higher ratios, it becomes a mixed inhibitor.

**c) Amino alcohol based (AMA) inhibitor:** In AMA-based organic inhibitor the main component is aminoalcohol, which is the volatile component and aminoalcohol is transported mainly by gas diffusion. The second component is in general an acid component. This acid component is reported to react with hydration products (*Tritthart J. (2003)*). The reaction with calcium hydroxide results in a gel formation that blocks the pores of the concrete (*Soylev et al. (2007)*).

**d) Amine ester based:** Amine- and ester-based inhibitors contain twin actions in concrete as the amine compound acts as an inhibitor whereas the carboxylate ester compound has pore-blocking effect, which blocks the ingress of the chlorides (*Gaidis (2004)*). For Surface applied type amino carboxylates-based inhibitors the pore-blocking effect as a secondary protection mechanism against reinforcement corrosion (*Soylev et al. (2007)*). The esters become hydrolysed by the alkaline mix water to form the carboxylic acid and its corresponding alcohol. The reaction proceeds as shown, where R and R` represent different hydrocarbon molecules:



The carboxylic anion is quickly converted in concrete to the insoluble calcium salt of the fatty acid. The created fatty acids and their calcium salts provide a hydrophobic coating within the pores (*Nmai (2004)*).

**e) Mixed inhibitor:** An organic corrosion inhibitor comprising an aqueous emulsion of ester and amino alcohol is a mixed inhibitor, affecting corrosion through a combination of active and passive mechanisms (*Wombacher et al. (2004)*). A study extending over a decade investigated the active part, a layer-forming amino alcohol which is generally taken to be a cathodic inhibitor.

The passive part of the inhibitor mechanism reduces permeability by hydrolysis of an organic ester and deposition of insoluble calcium salts of fatty acid which hydrophobe the concrete pores to reduce ingress of chloride ions.

### CHAPTER 3 – LITERATURE REVIEW

The solution of corrosion in concrete has not been found despite the extensive research conducted over the last 20 years. The abundant factors involved in the corrosion process instigate a number of studies to help understand the phenomenon and bring about its prevention.

**Morris et al. (2002)** studied a migrating corrosion inhibitor in concrete containing with different chloride content. The performance of a surface-applied migrating corrosion inhibitor based on an alkyl-aminoalcohol on concrete specimens with rebar segment was investigated. Two blank specimens (with no inhibitor) and two treated with the inhibitor were exposed to a so-called “marine” environment. These specimens were placed in a metallic cage located at the top terrace of a forty-floor building. Fig. 3.1 shows the variation of the rebar corrosion potential in time for the specimens (blank and treated with inhibitor) exposed to the marine environment. The blank and the treated specimens showed no significant difference between the rebar corrosion potential trends obtained on each of the three mixes containing admixed chlorides (A, B and C). The difference in the rebar corrosion potential trend of mix D (w/c = 0.6 and no admixed chlorides) became evident after approximately 400 days of exposure. After this period, the  $E_{corr}$  values of the blank specimens start shifting towards more negative potentials. While, the rebar corrosion potential values of the treated specimens demonstrate an increasing trend in time, attaining values characteristic of passive steel. Therefore, even when blank and treated specimens present similar chloride concentrations at the rebar surface, the presence of the inhibitor in mix DI seems to maintain the passive state of steel.

Fig. 3.2 present the rebar CR evolution in time for the blank and treated specimens expose to marine environment. No significant difference was observed between the CR values measured on blank and treated specimens prepared with admixed chlorides (A, B and C). As could be expected, the rebar CR of both blank and treated specimens increased as the initial chloride content in these mixes increased. In the case of mix D (no admixtures chlorides, w/c = 0.6), the treated specimens presented CR values that were almost one order of magnitude lower than the values measured on the blank specimens.

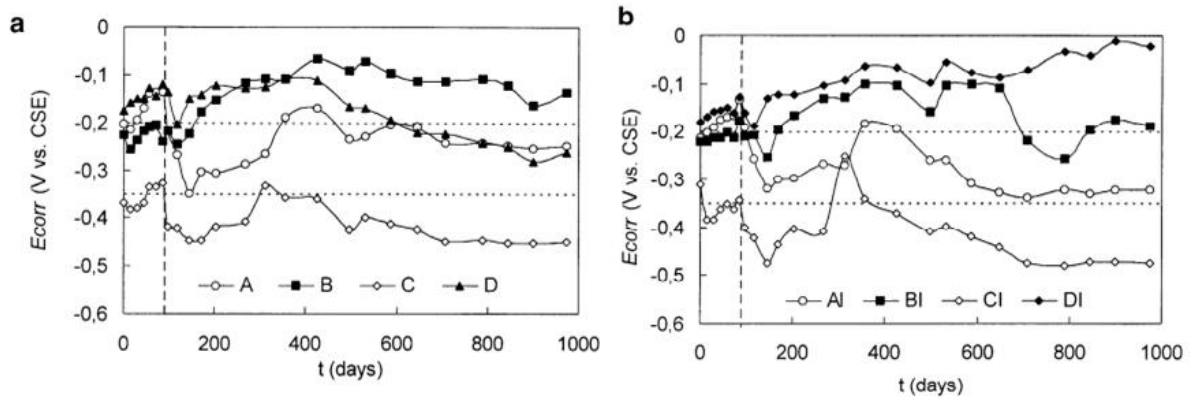


**Fig. 3.1: Variation of the rebar corrosion potential ( $E_{corr}$ ) with time (a) Blank specimens. (b) Treated with inhibitor (Morris et al., 2002)**

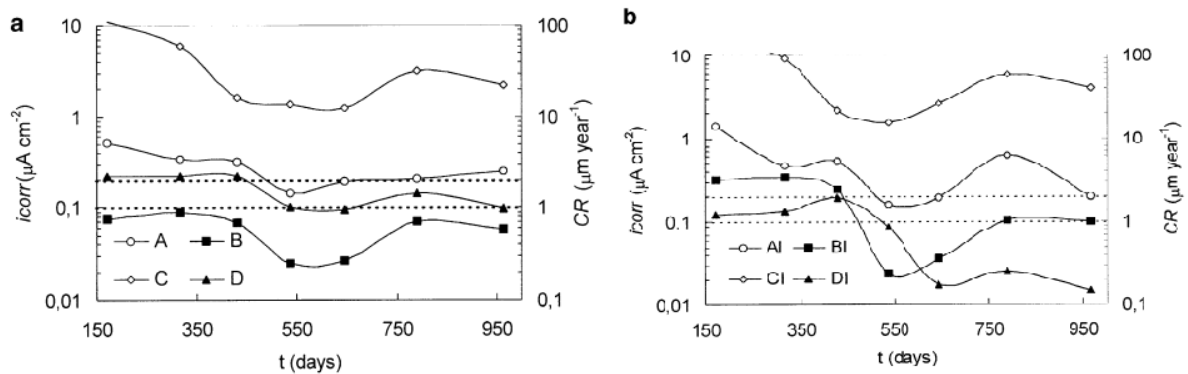


**Fig. 3.2: Variation of the rebar  $I_{corr}$  and corrosion rate (CR) as a function of time (a) Blank specimens. (b) Treated with inhibitor. (Morris et al., 2002)**

The efficiency of the inhibitor strongly depends on the initial chloride ions concentration in concrete. The inhibitor was able to reduce the CR of steel in concrete only when the initial chloride concentration was approximately 0.2 wt. % referred to the content of cement in concrete. In this case, the inhibitor was applied to concrete having no admixed chlorides and even when samples had  $w/c = 0.6$  and were exposed to a marine condition for 1000 days, the CR decreased almost one order of magnitude to values typical steel in passive state ( $CR < 1 \text{ mm year}^{-1}$ ). After this period of exposure, the concentrating of total chlorides raised upto a approximately 1% at the rebar surface due to the incorporation of chlorides coming from the environment.

**Chaussadent et al. (2005)** studied effectiveness of sodium monofluorophosphate as a corrosion inhibitor for concrete reinforcements and focuses on the understanding of MFP, in particular in terms of its potential penetration into concrete materials. Cylindrical mortar

specimens with 35 mm diameter and 40 mm long, containing a centred mild steel of 6 mm diameter, were cast with ordinary Portland cement and a water-cement ratio of 0.5. All specimens were wrapped in an adhesive aluminium sheet, in order to reduce moisture loss, and then preserved for one year at 20°C before the experimental campaign.

Monofluorophosphate penetration profiles in carbonated or non-carbonated hardened cement pastes were calculated. These profiles were obtained at 7 and 28 days, after the application of MFP aqueous solution on the outside of cement paste specimens. A 5-mL volume of an aqueous MFP solution (20% by mass) was applied to one of the surfaces perpendicular to the axis of cylindrical cement paste specimens. (3cm diameter, 6cm high), either carbonated or not.

The MFP penetration profiles in hardened cement pastes, both carbonated and not, as shown in Fig. 3.3. In the non-carbonated cement pastes, the MFP remains mainly within the first centimetre from the surface of application. It was observed that MFP penetration has been slowed due to the fact that this compound reacted with portlandite to form fluoroapatite. However, MFP at low contents level (only 0% to 10% of MFP applied) was found at greater depths as a result of initial capillary penetration. In carbonated cement pastes, MFP was scattered uniformly throughout the depth. The presence of  $\text{CaCO}_3$  (instead of  $\text{Ca(OH)}_2$ ) has made it possible for MFP to penetrate, with no interaction being observed between calcite and MFP.

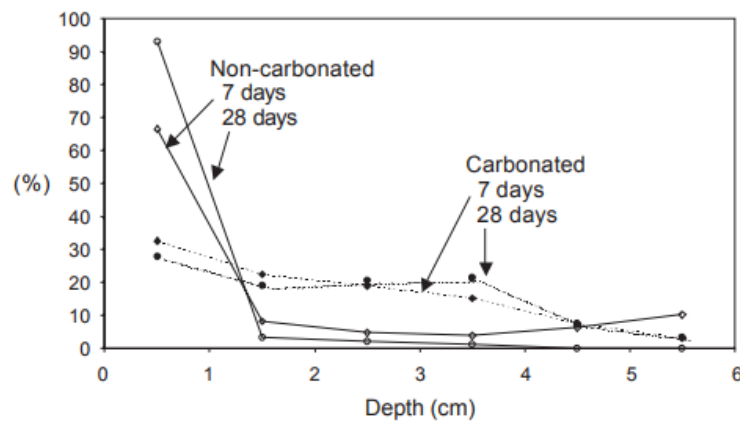


**Fig 3.3 MFP penetration profiles (determined MFP / total applied MFP in %) in carbonated or not carbonated hardened cement pastes. (Chaussadent et al., 2005)**

The monitoring of steel corrosion potential in the mortar specimens were performed upon application of MFP solution for a period of 48 hr. Fig. 3.4 showed that potential was constant

over a certain time and then a rapid decrease (100 to 150 mV SCE) appeared. At the end of this decrease, the potential once again remained constant. No effect ascribable to the action of MFP was observed on the steel corrosion, although the inhibitor was found quite near to the steel surface (2% to 9% of the applied MFP was identified after total dissolution of the mortar in nitric acid). This finding was simply due to the absence of free MFP ions, resulting from their reactivity with portlandite in a non-carbonated mortar.

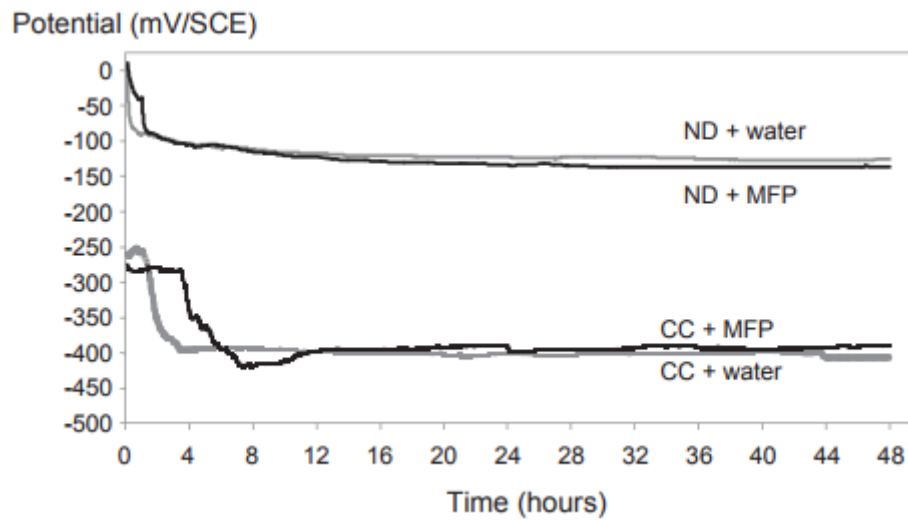


**Fig 3.4 Evolution of the steel corrosion potential after applying MFP solution or water onto reinforced mortar surface (non-carbonated mortars) (ND: nondegraded – CC: chloride contaminated). (Chaussadent et al., 2005)**

Soylev et al. (2007) studied the outcome of two amino alcohol based surface applied corrosion inhibitor (SACI) on the different stages of corrosion in chloride environment. Concrete prisms of size 280x280x75 mm were taken, which were reinforced by two horizontally placed reinforcing bars were used for corrosion testing. The concrete cover was 18 mm. The cement used was Irish Portland cement. The inhibitors used for experiment were two new-generation amino alcohol-based organic SACI. For Group 1 specimens, chloride cycles involve four-day ponding with 70g/l NaCl solution followed by three-day air drying in the laboratory environment. Both of the inhibitors were applied in a similar way, on the ponding-surface by a brush as suggested by the manufacturer and at the recommended dosage of 500 g/m<sup>2</sup>. The inhibitors were applied before chloride application and after first chloride cycle and their effect on corrosion were compared to control samples. The specimens are named accordingly as ORG1a, ORG1b, ORG2a and ORG2b. Group 2 specimens consist of control, ORG1 and ORG2 specimens exposed only to one ponding cycle but with higher

concentration of 5MNaCl solution. For this group of prisms, the inhibitor application took place after the chloride ponding and the results were compared with control specimens until the end of the testing duration without adding any more chloride. The specimens were wetted before corrosion measurement to obtain lower resistivity for concrete during the testing.

After the chloride application, there was a sharp drop in  $E_{corr}$  values for all specimens, varying between approx. -350 and -395 mV. The  $E_{corr}$  value of the control specimens decreased gradually with increasing chloride ponding cycles from -393 mV up to -522 mV, and fluctuated between approx. -500 mV and -420 mV. The higher  $E_{corr}$  value was seen for ORG2b specimens, remaining more or less stable at first cycles and then escalating despite increasing chloride ponding cycles. ORG1(a,b) specimens displayed lower (more negative)  $E_{corr}$ , the drop for ORG1b being slightly lower. However, there is no significant difference between ORG1(a,b) and control specimens.  $I_{corr}$  of control continued a sharp increase from 1.14 to 2.69  $\mu\text{A}/\text{cm}^2$  and fluctuated between approx. -500 mV and -420 mV. The higher  $E_{corr}$  was measured for ORG2b specimens, remaining almost stable at first cycles and then increasing despite increasing chloride ponding cycles. ORG1(a,b) specimens displayed lower (more negative)  $E_{corr}$ , the drop for ORG1b being slightly lower. However, there is no significant difference between ORG1(a,b) and control specimens.  $I_{corr}$  of control continued a sharp increase from 1.14 to 2.69  $\mu\text{A}/\text{cm}^2$  and fluctuated between 2.69  $\mu\text{A}/\text{cm}^2$  and 1.59  $\mu\text{A}/\text{cm}^2$ . ORG2(a,b) specimens, which had the highest  $E_{corr}$  (less negative) had the lowest  $I_{corr}$  values.  $I_{corr}$  of ORG2a decreased from 1.17 to 0.90  $\mu\text{A}/\text{cm}^2$  after the first sharp increase and remained stable around this value. ORG2b had very similar behaviour and the values are very close to those of ORG2a. The  $I_{corr}$  values for ORG1(a,b) are not very different from the control as in the case of  $E_{corr}$ . Fig. 3.5 and Fig. 3.6 show the results of  $E_{corr}$  and  $I_{corr}$  for Group 1 specimens and Fig. 3.7 and Fig. 3.8 for group 2 specimens.

It was established that the new-generation amino alcohol-based inhibitor was efficient against corrosion when it was applied before the chloride application or immediately after the first chloride ponding cycle. It kept the  $I_{corr}$  at 1  $\mu\text{A}/\text{cm}^2$  which can be accepted as a threshold value for corrosion initiation, despite high chloride content at the level of the embedded steel. It was also found that once concrete is contaminated with chloride and when the inhibitor was applied after a high corrosion rate (2  $\mu\text{A}/\text{cm}^2$ ) both of the inhibitors are ineffective. The new-generation amino alcohol-based inhibitor appeared to be a good repair strategy when it is applied before the initiation of corrosion or the corrosion rate is relatively low.

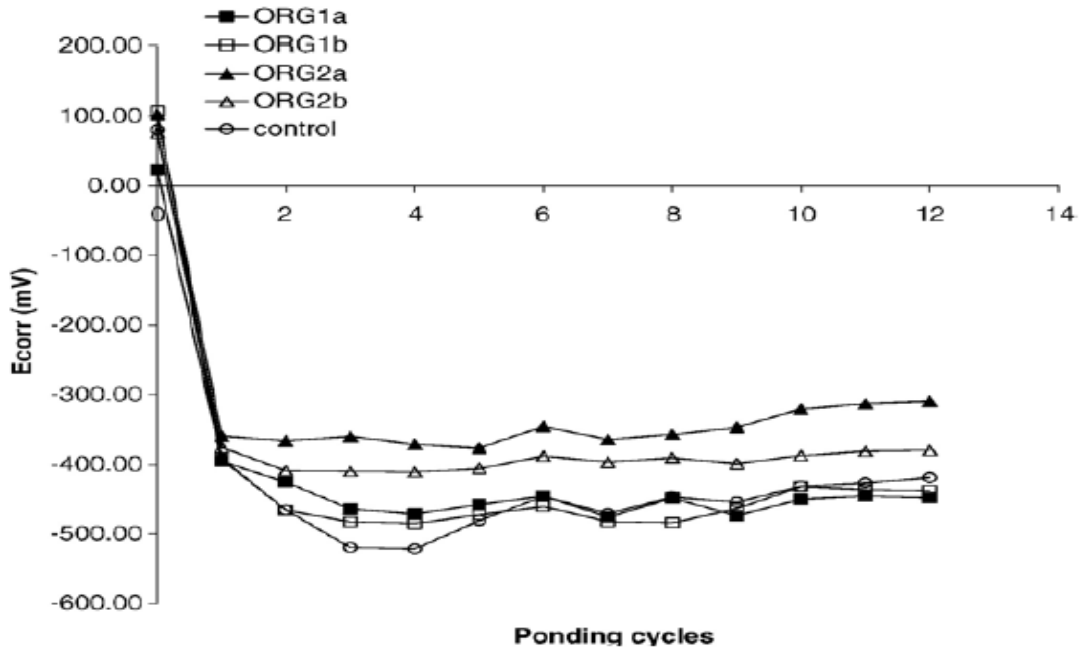


Fig. 3.5: Corrosion potential-time curves for Group 1 specimens (Soylev et al., 2007)

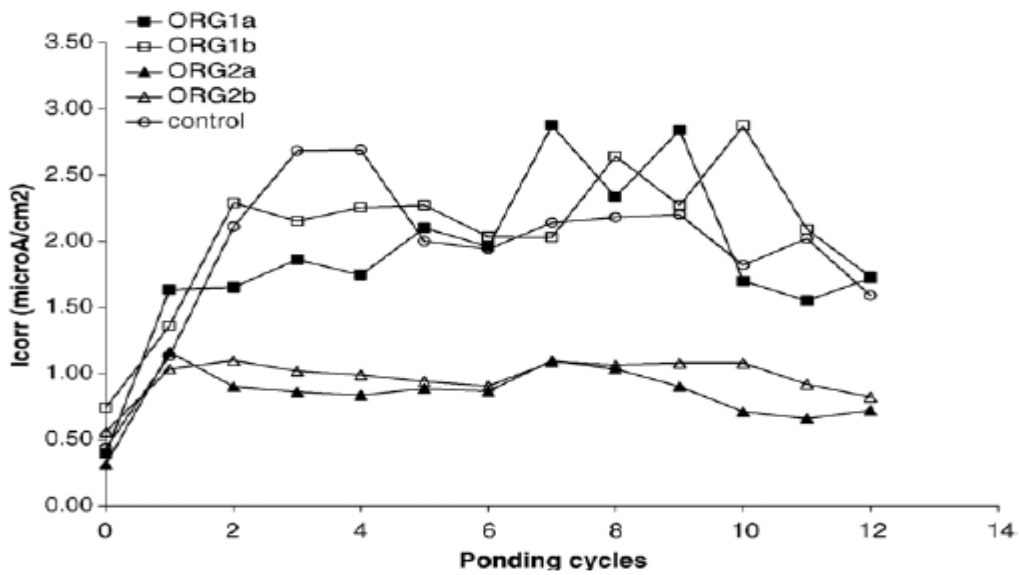


Fig. 3.6: I<sub>corr</sub> -time curves for Group 1 specimens (Soylev et al., 2007)

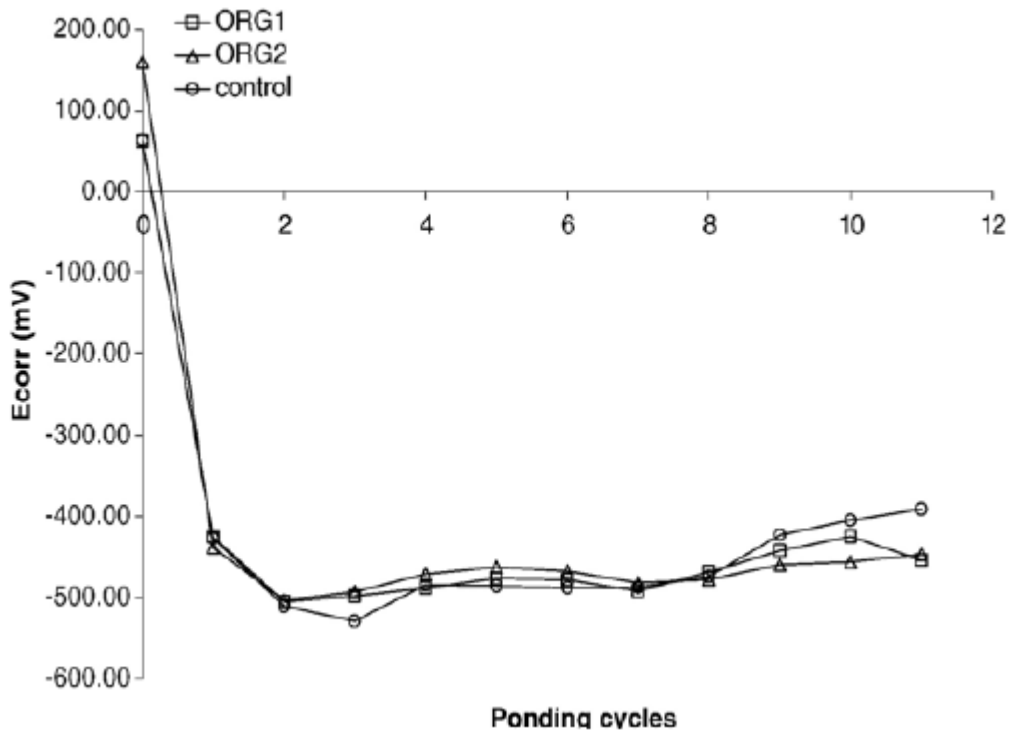


Fig. 3.7:  $E_{corr}$ -time curves for Group 2 specimens (Soylev et al., 2007)

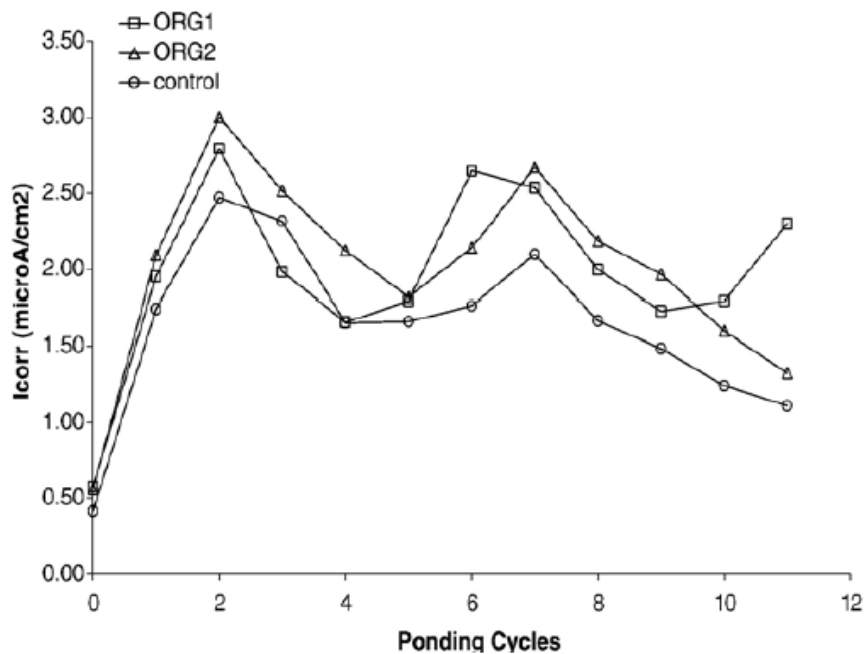


Fig. 3.8:  $I_{corr}$  -time curves for Group 2 specimens (Soylev et al., 2007)

Heiyantuduwa et al. (2006) studied the performance of an organic, penetrating corrosion inhibitor in reducing the rate of corrosion and delaying the onset of corrosion in carbonated concrete. The objective was to improve understanding of the use of such materials, as well as

limitations in this approach. The 30 MPa concrete mix was selected for corrosion test specimens, since it was most typical of structural concrete and was well penetrated by the corrosion inhibitor. Concrete test specimens were blocks of size 120mmx120mmx380mm, with each specimen containing a 16mm high tensile ribbed steel reinforcing bar longitudinally at the centre, at nominal covers of 10 or 20mm. Twelve concrete blocks were cast using the grade 30 CEM 1 mix, six blocks for each reinforcement cover depth(i.e., 10 Or 20 mm cover). Each group of six had 2 control specimens, 2 specimens that were treated with the penetrating inhibitor before the carbonation process (BC), and two specimens that were treated with the penetrating inhibitor after the carbonation process (AC).

The corrosion inhibitor was applied to BC and AC specimens by brush at a rate of 0.1 L/m<sup>2</sup> on each of the test specimens over there consecutive days, to give a total of 0.3 L/m<sup>2</sup>. The inhibitor taken for experiment was a mixed water-based impregnation for R.C, also with an organic film-forming amino compound (amino alcohol) and an inorganic component (Burge 1997). Each coat of the penetrating inhibitor was allowed to dry for 24 hr before application of the next coat. Twenty-four hours after the application of the final coat the concrete surface was wetted with tap water, this procedure being repeated for two consecutive days. The application of water saturated the surface layer of the concrete, thereby aiding the penetration of the inhibitor through diffusion and preventing evaporation of the inhibitor from the surface.

For AC specimens accelerated carbonation was done using a chamber maintained at 10% carbon dioxide, 30°C, and a relative humidity of 85 ± 5%. Twelve corrosion test specimens and concrete cubes were placed in the carbonation chamber for accelerated carbonation 6 days after casting (28 days after treatment for BC specimens). Specimens were kept in the carbonation chamber until sufficient carbonation had taken place to activate corrosion, roughly two or four months for 10 and 20 mm cover, respectively.

In the 10mm cover specimens, control with no inhibitor maintained at highest corrosion rates (and the most negative potentials). Average measured corrosion rates in this case ranged from about 0.1 to 0.9  $\mu\text{A}/\text{cm}^2$  corresponding to active corrosion. Average corrosion rates of the blocks where the inhibitor was applied before the carbonation process and after the carbonation process, showed much lower values in comparison with the concrete control samples: the ranges were between 0.05 and 0.4  $\mu\text{A}/\text{cm}^2$ , and 0.07 and 0.40.4  $\mu\text{A}/\text{cm}^2$ , respectively. Trends similar to those in the 10mm cover specimens were also displayed in the

20mm cover specimens. Average corrosion rates for these specimens ranged from about 0.1-0.5  $\mu\text{A}/\text{cm}^2$ . Corrosion rates of the samples that were treated with the inhibitor before carbonation and after carbonation showed much lower corrosion rates of between 0.09 and 0.02  $\mu\text{A}/\text{cm}^2$  and 0.1 and 0.22  $\mu\text{A}/\text{cm}^2$  for BC and AC, respectively. Fig. 3.9 indicate that penetrating corrosion inhibitors can be effective, when applied to the surface of existing or new structures, in extending the useful life of reinforced concrete exposed to carbonation.

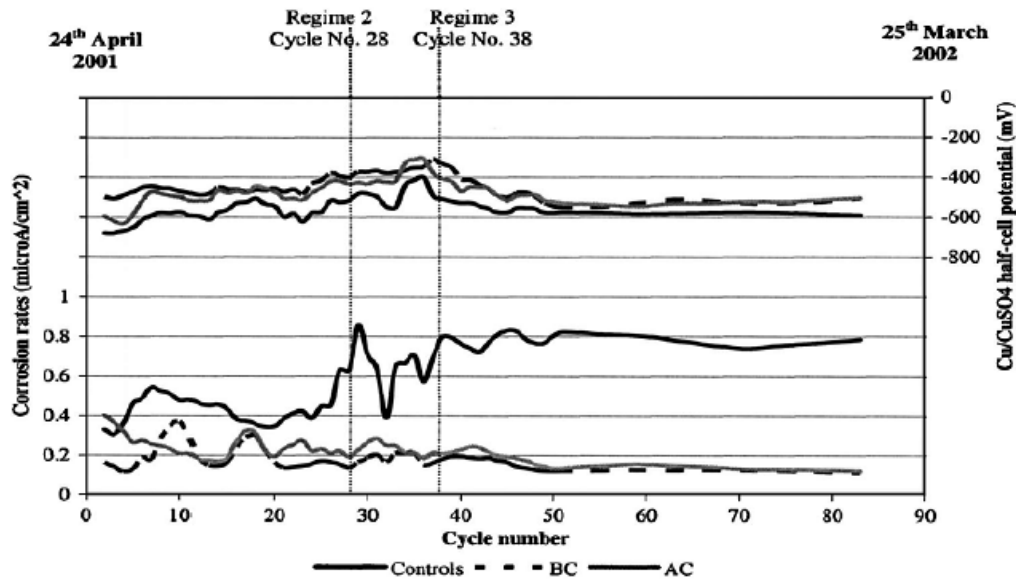


**Fig. 3.9: Corrosion rates and Half-cell potentials for 10mm cover samples.**  
(Heiyantuduwa et al., 2006)

Monticelli et al. (2011) have studied about two corrosion inhibitors, that is sodium 2-amino-benzoate (2AMB) and sodium glycerophosphate (GPH), in a synthetic solution simulating the composition of the pore solution in a carbonated concrete, containing chlorides. Tests have been performed to verify if the simultaneous use of the two substances is compatible and if their addition can efficiently hinder the corrosion attack in the presence of both chlorides and carbonation. The artificial solution was made by bubbling carbon dioxide through a saturated and filtered solution of  $\text{Ca}(\text{OH})_2$ , containing 0.1M NaCl, in order to reach pH 7. He prepared ribbed AISI 1033 type of steel bars of 10mm diameter, commercialized as concrete reinforcement (composition: C=0.31%; Mn=0.94%; Cr=0.26%; Ni=0.19%; Cu=0.50%; Si=0.14%; Co=0.02%; Al=0.04%; S=0.03%; remaining iron) with exposed surface area of 4.5  $\text{cm}^2$ . These electrodes are exposed to the test solutions after grinding by emery papers up to grade 600, washing with double distilled water and degreasing with acetone.

From this experiment he conclude that in carbonated chloride-containing solution (from here on the blank solution) no significant variation of steel corrosion behaviour is achieved by prolonging the immersion period from 45 min up to 72 h. This suggests that the corrosion product film growing on the metal surface is not protective. At the end of the immersion period,  $I_{CORR}$  is close to  $1.2 \times 10^{-5} \text{ A/cm}^2$ , as estimated by the Tafel method by extrapolation of the cathodic polarization curve. The addition of 0.05M 2AMB to the blank solution affords no inhibiting effect on the corrosion process after 45 min of immersion. However, after 24 h of immersion  $E_{COR}$  is ennobled up to  $-0.58 \text{ VSCE}$ , owing to the increase in the slope of the anodic polarization curve, likely due to the formation of a surface film. The protectiveness of this film is scarce (as suggested by the measured  $I_{CORR}$  values which are only slightly lower than those measured in the blank solution) and diminishes with time, as the anodic curve shifts again towards higher current densities, at the end of 72 h immersion. Fig. 3.10 shows Polarization curves recorded on steel in carbonated chloride solution, both in the absence and in the presence of 0.05M 2AMB.

Polarization curve recording and EIS technique have shown that the mixture inhibiting action develops slowly within 24 h, during which a surface porous film forms with a higher pore resistance and particularly a higher mass transport resistance with respect to those evaluated in the blank solution. The polarization curve analysis suggests that diffusion of  $\text{Fe}^{2+}$  cations from the metal surface to the aggressive solution may be the mass transport process controlling the steel corrosion rate in inhibited solutions.

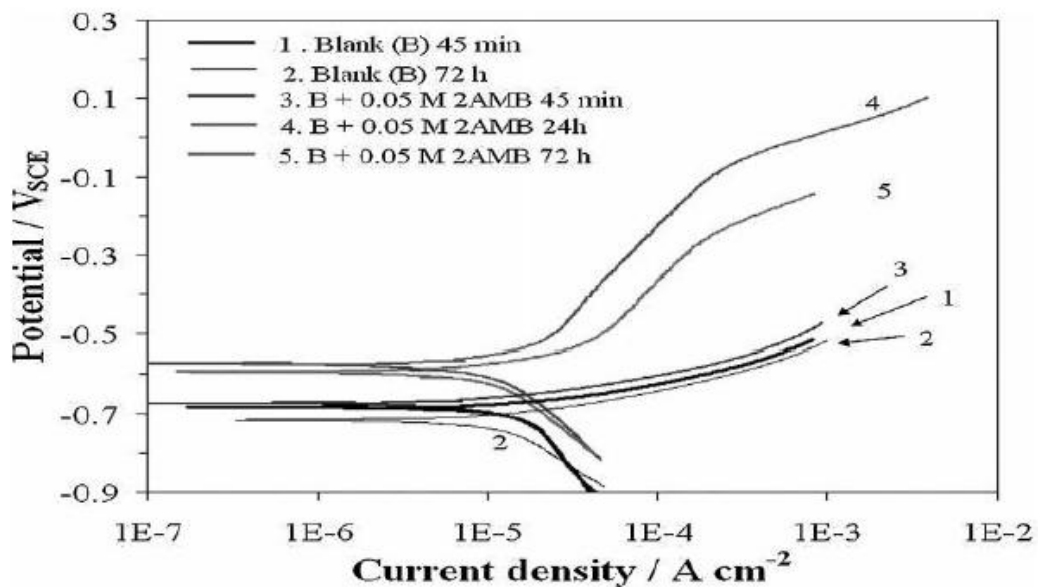


**Fig. 3.10: Polarization curves recorded on steel in carbonated chloride solution, both in the absence and in the presence of 0.05M 2AMB. (Monticelli et al., 2011)**

**Ryu et al. (2016)** used commercially available N, N'-Dimethyl ethanol amine (DMEA) inhibitor and studied in different concentrations of NaCl in saturated Ca(OH)<sub>2</sub> solution. The performance of inhibitor was evaluated by potential time, electrochemical impedance spectroscopy and potentiodynamic techniques. This inhibitor was mixed in saturated Ca(OH)<sub>2</sub> solution and it was made in double distilled water by proper mixing. The pH of saturated Ca(OH)<sub>2</sub> solution was 12.60 at room temperature (25 °C ± 1 °C). Different concentrations of NaCl were mixed in saturated Ca(OH)<sub>2</sub> solution with different content of inhibitor. The mild steel rebars with 16 mm diameter were cut and mounted in acid/alkali resistance thermosetting resin. The mounted samples were polished with emery paper started from 180 to 1200 μ. Thereafter, cloth polished of steel rebar was carried out and degrease with acetone prior to start the electrochemical experiments.

Prior to start the experiments, steel rebars were exposed in solution and the potential was stabilized with potentiostat. These electrochemical studies were performed by three electrode systems where steel rebar work as working electrode (WE), platinum wire as a counter electrode (CE) and silver-silver chloride as a reference electrode (RE). The area of working electrode was 0.78 cm<sup>2</sup> and it was fixed for every samples.

The corrosion potential time studies were performed on steel rebars in saturated Ca(OH)<sub>2</sub> solution with different concentrations of NaCl and DMEA inhibitor. The corrosion potential time plots are shown in Fig. 3.11.

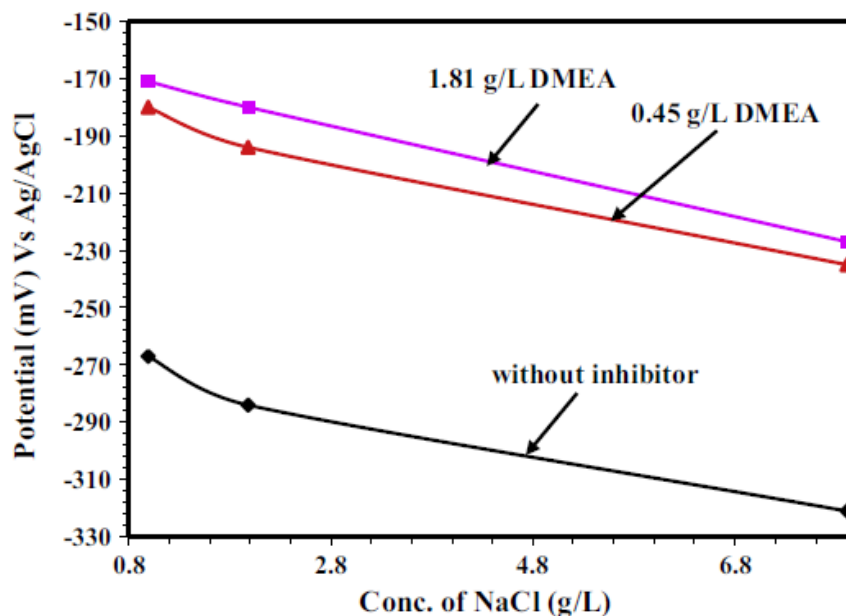


**Fig. 3.11: Corrosion potential-time plots of steel rebar exposed in saturated Ca(OH)<sub>2</sub> solution different concentrations of NaCl and DMEA inhibitor. (Ryu et al., 2016)**

Ryu et al. (2017) studied the effect of  $\text{LiNO}_2$  was evaluated by electrochemical impedance spectroscopy (EIS) and potentiodynamic studies.  $\text{LiNO}_2$  works as mixed type corrosion inhibitor by stabilizing the iron oxides/hydroxides in their stable form and stifle the corrosion of steel rebar. Different concentrations of dissolved  $\text{LiNO}_2$  inhibitor solution was added in saturated  $\text{Ca(OH)}_2$  with different content of  $\text{NaCl}$ . The solution was made in double distilled water by mixing them vigorously. The pH of this solution was 12.5 ( $\pm 0.1$ ) at 25 °C ( $\pm 1$  °C). In this study different molar ratio of  $[\text{Cl}^-/\text{NO}_2^-]$  i.e. 0 (without inhibitor), 0.3 and 0.6 were taken to study the effect of  $\text{LiNO}_2$  inhibitor with 0.99, 3.96 and 7.91 g/L  $\text{NaCl}$ .

The black milled scale of 16 mm steel rebar was descaled by using 10 v/v% of  $\text{HCl}$ , ringed with distilled water and dried. After descaling of milled scale from steel rebar surface, it was cut and mounted in acid/alkali resistance thermosetting resin. The mounted steel rebar was abraded with emery paper started from 180 to 1200  $\mu\text{m}$ . Thereafter, cloth polished of steel rebar was carried out and degreased with acetone prior to start the electrochemical experiments.

Prior to start the experiments, the steel rebars were exposed in inhibitor and without inhibitor containing saturated  $\text{Ca(OH)}_2$  solutions to stabilize the potential with potentiostat.

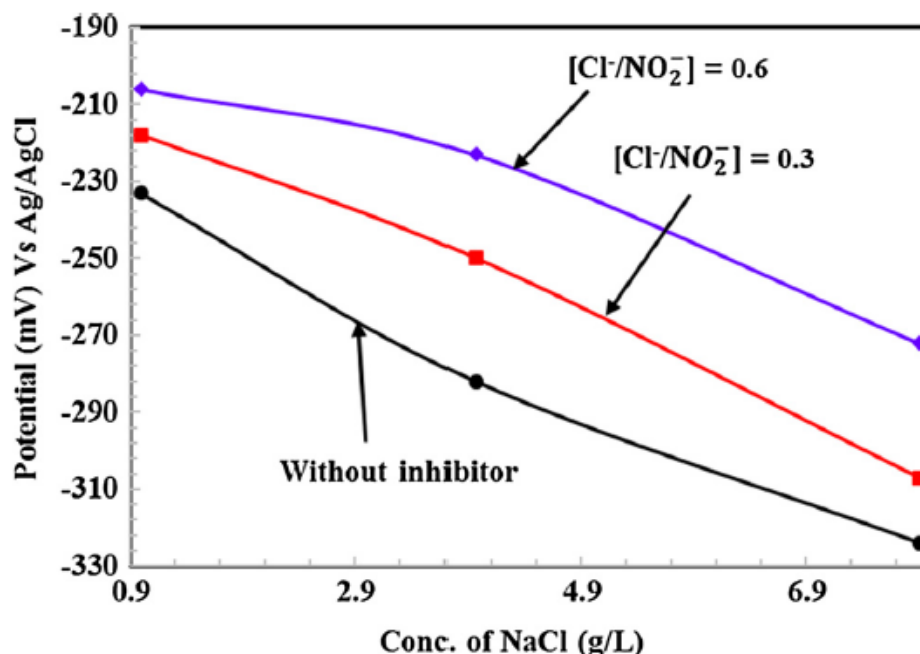


**Fig. 3.12: Corrosion potential plots at different molar ratio of  $[\text{Cl}^-/\text{NO}_2^-]$ . (Ryu et al., 2017)**

Electrochemical studies were performed by three electrode systems where steel rebar work as working electrode (WE), platinum wire as a counter electrode (CE) and silver-silver chloride

as a reference electrode (RE). The WE and RE were fixed in such a manner that both are close to each other, since there will be less solution resistance caused. The area of working electrode was 0.78 cm<sup>2</sup> and it was fixed for every sample.

The corrosion potential of steel rebars were measured in saturated Ca(OH)<sub>2</sub> with different content of NaCl at different molar ratio of [Cl<sup>-</sup> /NO<sub>2</sub><sup>-</sup> ] and it is shown in Fig. 3.12.

**Fedrizzi et al. (2005)** studied the use of migrating corrosion inhibitors to restore motorways concrete structures infected by chlorides. The efficiency of the repair mortars barrier effect and MCI has been tested using corrosion potential (E<sub>corr</sub>) versus time measurements, electrochemical impedance spectroscopy (EIS) and, at the end of the monitoring period (from 220 to 420 days), chloride penetration analysis. The concrete specimens were cast in parallelepiped blocks (30×30×9 cm<sup>3</sup>) using an ordinary Portland cement. Six steel rods without any rust of dia 10 mm and 400 mm length were embedded into the concrete and used as rebars. At the end of the curing period which was at least 28 days, the superior surface of each specimen was coated with one of three different types of mortar of 1 cm thickness, with or without the addition of an MCI at the interface between the concrete substrate and the coating. 60 to 70g of inhibitor per specimen of the was applied by brush on the outside of the concrete before applying the repair mortars.

Corrosion potentials of the six rebars of each specimen have been measured during the exposure time. An average between the three upper bars and the three lower bars has been made to obtain a statistical value of the potential versus time trend. The figure 3.13 also show the effect of inhibitor treatment on the potential of the reinforcing bars of the specimens, which were subjected to ponding by a sodium chloride solution besides the already present amount of chlorides added in the concrete mix. The mean potential values of the upper and lower steel bars show that the repair mortars A and B offer a better barrier effect compared to the Standard Mortar of reference (Fig. 3.13 a and c). With control specimen, covered with Standard Mortar and free from inhibitor, the potential was very high and permanently negative, especially for the upper rebars (Fig. 3.13 a). It is interesting to note that the samples with the alkanol-amine-based inhibitor applied at the concrete–mortar interface have corrosion potential values (Fig. 3.13 b and d) less negative or similar to those of control specimens, covered with the different coatings but without the MCI (Fig. 3.13 a and c).

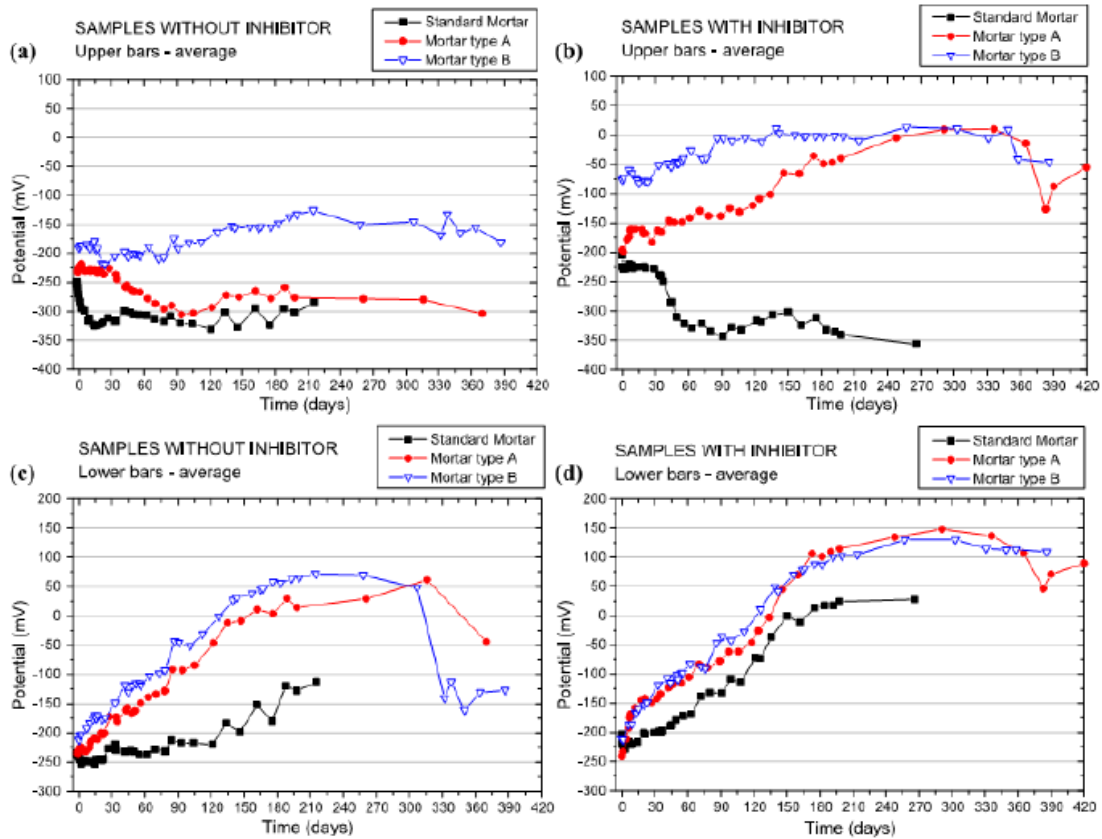


**Fig. 3.13: Corrosion potential (versus Ag/AgCl) versus time diagrams. (Fedrizzi et al.,2005)**

The comparison amongst the corrosion rates of the upper bars (Fig. 3.14 a) shows that the Standard Mortar on itself cannot offer a adequate barrier action against rebar corrosion in these severe conditions. Icorr increases with the exposure time for the upper rebars of the reference specimen, which means high corrosion levels reached, while its average value is low for the deeper reinforcements (Fig. 3.14 c) and has the tendency to decrease with time. A similar trend in upper rebars corrosion rates (Fig. 3.14 a) is evident for Mortar type A, with increasing values of Icorr versus time, but delayed 20 days and always at lower values than Standard Mortar. Very different is the behaviour of Mortar type B, whose average upper rebars Icorr remains stable and low during the first 200 days. The migrating inhibitor when added shows its effect on standard mortar sample in the first days of the monitoring period, delaying the start of the severe corrosion on the upper rebars (Fig. 3.14 b). There is no significant variation between the lower rebars with or without inhibitor addition (Fig. 3.14 d versus 3.14 c); in both conditions, the tendency is to diminish the corrosion rate. The comparison between the upper bars (Fig. 3.14 b versus 3.14 a) shows the long-term efficacy of the MCI when associated to repair mortars, such as Mortar type A and Mortar type B.

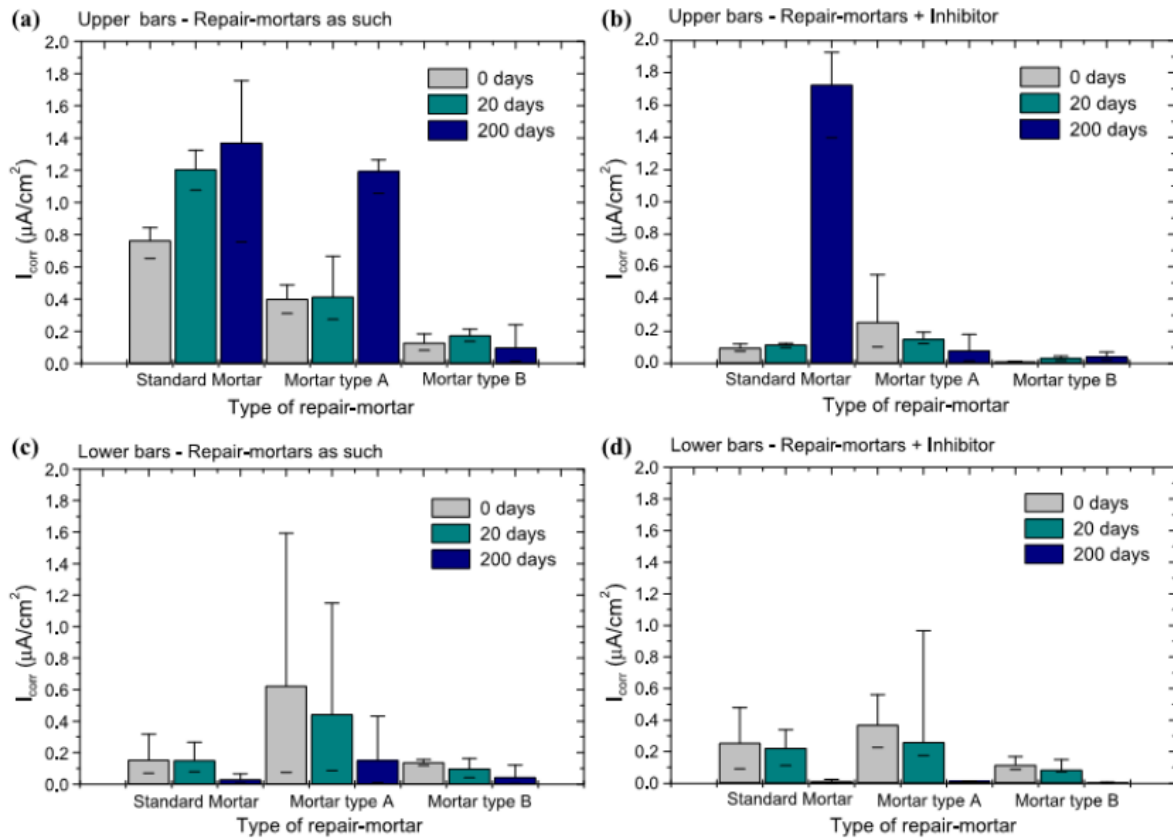


**Fig. 3.14:  $I_{corr}$  calculated at three different monitoring periods (Fedrizzi et al., 2005)**

Liu et al. (2014) study included two different kinds of simulated concrete pore solutions: the  $Ca(OH)_2 + KOH + NaOH$  solution and the cement extract. Compared with the familiar  $Ca(OH)_2 + KOH + NaOH$  solution, the cement extract represents the real environment of the concrete pore solution due to the hydration action of the cement. This study was conducted to examine the effect of the carbonation on chloride-induced reinforcement corrosion in the simulated concrete pore solutions. The corrosion monitoring of the steel was based on the open-circuit potential ( $E_{corr}$ ) and the corrosion current density ( $I_{corr}$ ), which was calculated by electrochemical impedance spectroscopy (EIS).

A cylindrical steel specimen with a diameter of 1 cm and length of 3 cm was used. A copper wire was welded to one end surface of the steel specimen and the other end surface was used to test in the electrochemical methods. The flank and the end surface with a thick copper wire were sealed with the help of epoxy resin. The tested surface was polished with SiC water polishing papers. The cement extract was made by dissolving 20 g cement powder in 2 L distilled water. The cement used in this study was No. 42.5 ordinary Portland cement made in China. Varying concentrations of sodium bicarbonate were added to the exposure solutions to produce different levels of carbonation, which systematically assess the effect of carbonation

on chloride-induced reinforcement corrosion. The aggressive chloride ions were supplied by sodium chloride and added 0.01 mol/L every 2 days. All chemical reagents used in this work were of analytical grade reagents and experimental water was deionized water.

A classical 3-electrode device system was employed: the steel bar was a working electrode, while a saturated calomel electrode and a platinum electrode were joined to work as a reference and auxiliary electrode, respectively.

**Table 3.1 Composition and pH of the simulated concrete pore solutions. Liu et al. (2014)**

SOLUTION	COMPOSITION	pH
1	Ca(OH) <sub>2</sub> + KOH + NaOH	13.12
2	Ca(OH) <sub>2</sub> + KOH + NaOH + 0.02M NaHCO <sub>3</sub>	12.71
3	Ca(OH) <sub>2</sub> + KOH + NaOH + 0.2M NaHCO <sub>3</sub>	9.46
4	Cement extract (w/c = 10:1)	12.95
5	Cement extract (w/c = 10:1) + 0.02M NaHCO <sub>3</sub>	12.59
6	Cement extract (w/c = 10:1) + 0.2M NaHCO <sub>3</sub>	9.43

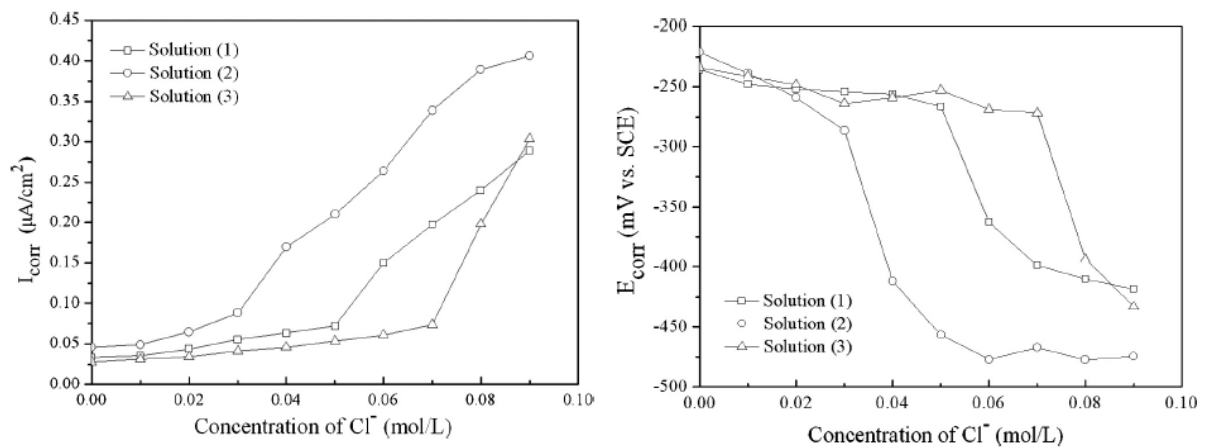


**Fig. 3.15: Variations of the  $I_{corr}$  and  $E_{corr}$  for the specimens in solutions (1–3) with the concentrations of chloride ions. (Liu et al., 2014)**

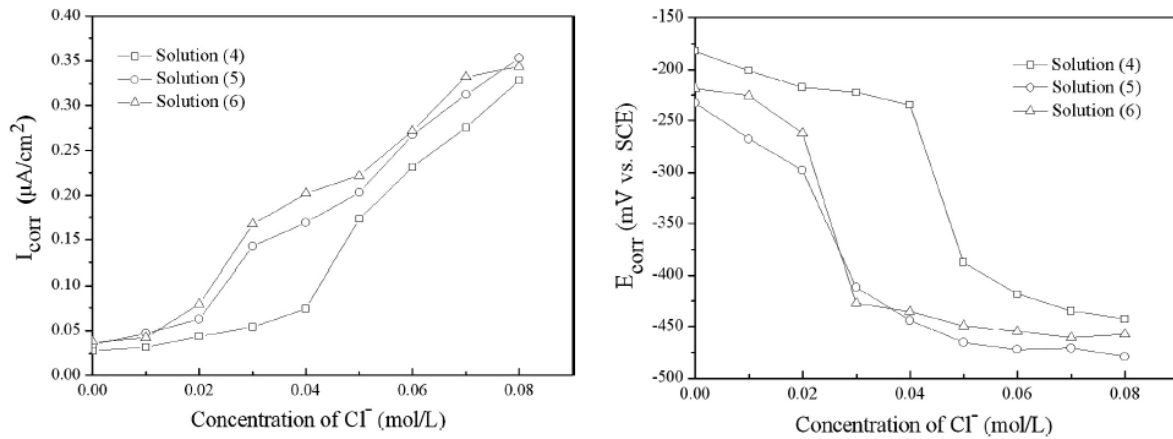


**Fig. 3.16: Variations of the  $E_{corr}$  and  $I_{corr}$  for the specimens in solutions (4–6) with the concentrations of chloride ions. (Liu et al., 2014)**

Fig. 3.15 results shows that the corrosion resistance to chloride ion of the steel in concrete is affected by the degree of carbonation: high concentrations of bicarbonate lower the danger of chloride-induced corrosion of the steel, but quite on the contrary, the steels under the condition of low  $\text{HCO}_3^-$  concentrations are more likely to corrosion.

Fig. 3.16 give the evolutions of the  $E_{corr}$  and  $I_{corr}$  for the specimens immersed in solutions (4–6) with the concentrations of chloride ions, respectively. The initial  $E_{corr}$  for the steel specimens in a passive state are relatively higher (less negative), and the corresponding  $I_{corr}$  are quite low. With the more level of chloride ions, the  $E_{corr}$  reduce and  $I_{corr}$  increase by degrees. Then, when a certain concentration of chloride ions is added, a sudden shift of  $E_{corr}$  and  $I_{corr}$  appear: the value of  $E_{corr}$  decreases to more negative and the value of  $I_{corr}$  increases to much higher. The fact is related to the rupture of the passive film caused by the aggressive chloride ions.

The addition of bicarbonate ions decreases the chloride level needed for the active corrosion and increases the corrosion susceptibility of the steel specimens, which is disagree with the results obtained from the  $\text{Ca}(\text{OH})_2 + \text{KOH} + \text{NaOH}$  solution. The reason for the different results is mainly own to the difference between the two kinds of simulated solutions. The hydration products of OPC such as C–S–H gel and CH can interact with the bicarbonate and chloride ions. The chloride ions can be physical absorbed to the C–S–H gel and react with the unhydrated  $\text{C}_3\text{A}$  to form the Friedel's salt. Meanwhile, the bicarbonate ions will react with CH and the C–S–H gel to form solid products and the concentrations of the soluble bicarbonate ions are very low Hence, the solution (6) shortens the time needed for the onset of pitting corrosion because of the low soluble bicarbonate ions, although the initial addition of bicarbonate ions in solution (6) is very high. In the  $\text{Ca}(\text{OH})_2 + \text{KOH} + \text{NaOH}$  solution, the

effect of bicarbonate ions on the corrosion behavior of the steel specimens depends on the concentration of bicarbonate ions. A high  $\text{HCO}_3^-$  concentration will enhance the stability of the passive film and the corrosion resistance of the steel specimen, while the low concentration of  $\text{HCO}_3^-$  ions accelerates the corrosion. However, no agreement on the effect of  $\text{HCO}_3^-$  ions has been obtained in the cement extract. The added  $\text{HCO}_3^-$  ions in the cement extract plays a role in promoting the corrosion initiation because of the low concentration of the soluble  $\text{HCO}_3^-$  ions.

## **CHAPTER 4 - EXPERIMENTAL PROGRAM**

### **4.1 GENERAL**

In this chapter, the experimental setup is presented to evaluate the performance of reinforced concrete under chloride and carbonation induced corrosion. Various corrosion monitoring devices used are Half-Cell Potential, Long term LPR sweep test and Galvanic Potential test. The experimental setup and the corrosion monitoring devices are discussed in the following sections.

### **4.2 TEST PROGRAMME**

The objective of test programme is to study the effectiveness of corrosion inhibitor under chloride and carbonation induced corrosion in pore solution and concrete. Reinforced concrete prisms and cubes using different cement type were cast to study the effect of corrosion inhibitor. The test programme involved:

1. Preparation of pore solution and solution with admixture under chloride and carbonation, to check the efficiency of inhibitor.
2. Determination of basic properties of constituent materials namely cement, fine aggregates, coarse aggregates and steel bars as per relevant Indian standard specifications.
3. Casting of prisms of size 300 x 300 x 150 mm<sup>3</sup> with 12 mm diameter TMT steel bar. One rebar was placed at top with a clear cover of 5mm and two rebars were embedded at the bottom with cover of 25 mm. Casting of 100 mm cubes for determination of the carbonation depth.
4. Admixing of corrosion inhibitor and NaCl into the concrete specimens at the time of casting.
5. The prisms and cubes were subjected to carbonation in a chamber with temperature controlled at 28-32° and RH 50-70% with the rate of CO<sub>2</sub> concentration maintained at 5%.

### **4.3 MATERIALS**

Materials used were Cement, Coarse Aggregates, Fine Aggregates, TMT bars, NaCl, Corrosion inhibitors and Water. The main aim for studying properties of materials used is to

verify the acceptance of material as per codes. The description materials and their calculated properties used in this work are discussed in following sections:

#### 4.3.1 Cement

Cement is a material that binds fine aggregates with coarse aggregates and is responsible for holding together of concrete. It is a fine powder which mainly controls strength and hardness properties in concrete. The Cement used in this work is Ordinary Portland Cement of Grade 43 and Pozzolonic Portland Cement of brand Ultratech Cement. The cement complies with the requirements of IS: 269-2015 for OPC and IS: 1489-1991 for PPC. The Physical properties of OPC and PPC are given in table 4.1 and 4.2 respectively. The chemical composition of cement is shown in table 4.3.

**Table 4.1: Physical properties of OPC cement**

<b>CHARACTERISTICS</b>	<b>RESULTS OBTAINED</b>	<b>RECOMMENDED VALUES AS PER IS 8112:1989 (BIS 1989)</b>
Grade of cement	OPC 43	-
Specific gravity	3.15	-
Standard consistency of cement (%)	26	30
Setting Time		
i. Initial setting time (Min.)	160 min	30 min (Min.)
ii. Final setting time (Max.)	225 min	600 min (Max.)
Compressive Strength		
i. 3 days strength of cement (N/mm <sup>2</sup> )	32.5	23 (Min.)
ii. 7 days strength of cement (N/mm <sup>2</sup> )	42.9	33 (Min.)
iii. 28 days strength of cement (N/mm <sup>2</sup> )	57.5	43 (Min.)
Soundness		
Le-Chat Expansion (mm)	0.5	10 (Max.)
Fineness of cement (m <sup>2</sup> /kg)	254	225 (Min.)

**Table 4.2: Physical properties of PPC cement**

<b>CHARACTERISTICS</b>	<b>RESULTS OBTAINED</b>	<b>RECOMMENDED VALUES AS PER IS 1489:1991</b>
Specific gravity	2.9	-
Standard consistency of cement (%)	33.5	-
Setting Time		
iii. Initial setting time (Min.)	150 min	30 min (Min.)
iv. Final setting time (Max.)	225 min	600 min (Max.)
Compressive Strength		
iv. 3 days strength of cement (N/mm <sup>2</sup> )	28.6	16 (Min.)
v. 7 days strength of cement (N/mm <sup>2</sup> )	38.6	22 (Min.)
vi. 28 days strength of cement (N/mm <sup>2</sup> )	58	33 (Min.)
Soundness		
Le-Chat Expansion (mm)	0.5	10 (Max.)
Fineness of cement (m <sup>2</sup> /kg)	390	300 (Min.)
% of Fly ash addition	25	15-35

**Table 4.3: Chemical composition of Cement**

<b>Compound</b>	<b>OPC</b>	<b>PPC</b>
SiO <sub>2</sub>	20.68	26.73
Al <sub>2</sub> O <sub>3</sub>	4.87	9.01
Fe <sub>2</sub> O <sub>3</sub>	3.35	4.83
CaO	62.13	49.72
MgO	1.73	0.97
SO <sub>3</sub>	2.43	2.34
Na <sub>2</sub> O	0.21	0.17
K <sub>2</sub> O	0.69	1.23
LOI	2.04	1.73

### 4.3.2 Coarse Aggregates

Aggregates which are retained over IS sieve of 4.75 mm size are called coarse aggregates. In concrete mix, 60% to 80% is occupied by aggregates. High content of aggregates affects properties in both fresh and hard concrete. Main role of aggregates is to provide a solid hardened mass of concrete. These aggregates act as a filler material in concrete. Also, aggregates helps in reducing cost of concrete by replacing cement which is a costly ingredient.

The coarse aggregates used in this work are obtained from local supplier in Patiala. In this work, 10 mm and 20mm aggregates were used.

Sieve analysis of coarse aggregate with 5 Kg of total aggregates is shown in Table 4.4. The physical properties of 20mm and 10 mm coarse aggregates investigated in laboratory are given in Table 4.5

**Table 4.4: Sieve analysis of coarse aggregates**

Sieve Size	Weight retained (g)	% Weight retained	Cumulative % retained
40 mm	0	0	0
20 mm	26	0.52	0.52
10 mm	2650	53	53.52
4.75 mm	2045	40.90	94.42
2.36 mm	218	4.36	98.78
1.18mm	0	0	100
600	0	0	100
300	0	0	100
150	0	0	100
pan	50	1	-
Total	4989		647.24

**Table 4.5: Physical properties of coarse aggregates**

Sr. No.	Characteristics	Value
1.	Type	Crushed
2.	Fineness Modulus	6.47
3.	Specific Gravity 20mm Aggregate	2.69
	10mm Aggregate	2.66
4.	Water absorption 20mm Aggregate	0.55%
	10mm Aggregate	0.64%

### **4.3.3 Fine Aggregates**

Fine aggregates are usually less than 4.75 mm in size. Sand is mostly used as fine aggregate which mainly contains small rounded and angular particles of silica. Fine aggregates mainly act as filler in voids of coarse aggregates and reduce the chances of concrete to shrink or crack.

In this work, fine aggregates were procured from local supplier in Patiala which confirms to Grading zone II confirming to IS 383: 1970. Physical properties of Fine aggregates are shown in Table 4.6. Results of Sieve analysis of fine aggregates performed in laboratory is shown in Table 4.7

**Table 4.6: Physical Properties of Fine aggregates**

Sr.No.	Characteristics	Value
1.	Grading	Grade II
2.	Fineness Modulus	3.93
3.	Specific Gravity	2.64
4.	Water absorption	1.21%

**Table 4.7: Sieve Analysis of Fine Aggregates**

S.No.	IS-Sieve(mm)	Wt. Retained(g)	%age Retained	%age Passing	Cumulative % Retained
1.	4.75	40	4	96	4
2.	2.36	397	39.7	56.3	43.7
3.	1.18	277	27.7	28.6	71.4
4.	600 $\mu$	124	12.4	16.2	83.8
5.	300 $\mu$	95	9.5	6.7	93.3
6.	150 $\mu$	40	4	2.7	97.3
7.	Pan	22	2.2		
	Total	1000		Sum	393.5
				FM	3.93

**4.3.4 Water**

Quantity of water in concrete controls many properties like workability, permeability, compressive strength, shrinkage and cracking. Fresh and clean tap water is used for casting the specimens. The water was relatively free from organic matter, silt, chloride, and acidic material as per Indian standard.

**4.3.5 Reinforcement**

HYSD steel of grade Fe 500 TATA Tiscon steel bars of 12 mm diameter were used. The mechanical properties of Reinforcement used is given in Table 4.8.

**Table 4.8: Mechanical Properties of Reinforcement Used**

Mechanical Property	Min. Req. as per IS: 1786 (Fe 500)	TATA TISCON Fe 500
Yield Strength(YS)( N/mm <sup>2</sup> )	500	520
Ultimate Tensile Strength(UTS)(N/mm <sup>2</sup> )	545	601.1
Ratio of UTS to YS	1.08	1.1

#### 4.3.6 Corrosion Inhibitor

Chemical corrosion Inhibitor was used to prevent the corrosion. The inhibitor used was 2-aminopyridine which is an amino based corrosion inhibitor. The IUPAC name for this inhibitor is Pyridine-2-amine. In the past studies Amine group has shown great resistance to corrosion. So, 2-Aminopyridine was selected to check its efficiency as a corrosion inhibitor under carbonation as well as chloride attack.

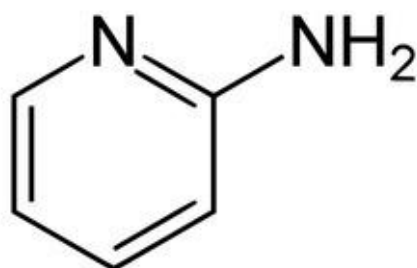


**Fig. 4.1: Molecular Structure of 2-Aminopyridine**



**Fig. 4.2: Actual Photograph of 2-Aminopyridine**

**Table 4.9: Properties of 2-Aminopyridine**

Chemical formula	C <sub>5</sub> H <sub>6</sub> N <sub>2</sub>
Molar mass (g/mol)	94.12
Appearance	Colourless solid
Density (g/cm <sup>3</sup> )	100%
Melting point (°C)	210

#### 4.4 MIX PROPORTION USED IN STUDY

In this study Concrete was made with two different types of cement. The Concrete mix was prepared using OPC 43 grade and PPC cement, fine aggregate, and coarse aggregates. A mix design was prepared as per IS guidelines. The ratio of cement: sand: aggregate was taken as 1:1.39:2.91. The water cement ratio was taken as 0.44. The mix design is given in Table 4.10.

**Table 4.10 Mix Design**

Cement (kg/m <sup>3</sup> )	410
Water (kg/m <sup>3</sup> )	180
Fine aggregates (kg/m <sup>3</sup> )	572.4
Coarse aggregates 20mm (kg/m <sup>3</sup> )	836.34
Coarse aggregates 10mm (kg/m <sup>3</sup> )	360.4
Admixture (% weight of cement)	3.5

#### 4.5 CASTING AND PREPARATION OF SPECIMENS

The preparation of steel bars was done in various steps for pore solution as well as concrete. This chapter deals with preparation of pore solution, preparation of steel bars and casting of concrete specimens for testing.

##### 4.5.1 Pore solution

Pore solution was prepared to check whether the 2-Aminopyridine can be used as corrosion inhibitor in concrete specimens. Two solutions were prepared and were compared to check the efficiency of 2-Aminopyridine in pore solution. The preparation of steel bar and solution is discussed here.

## **1. Preparation of Specimens:**

Steel bars for pore solution were firstly cut into required lengths of 60mm. Then steel bars were threaded at one end according to the requirement of testing procedure. Each piece of steel bar of was then rubbed by wire brush and sand paper to remove any rust present on the surface. They were then further cleaned by soaking in analytical reagent grade hexane and allowed to air dry. After air drying the specimens for 24 hours they were coated with one layer of epoxy which is followed by another layer of epoxy having a time difference of minimum 1 hour between these two layers. The resulting specimens after epoxy coating are kept for 24 hours. After that a nut with two bolts on it were screwed into the hole that was prepared and a copper wire was tightened between the bolts so as to ensure proper electrical conductivity.

## **2. Preparation of Pore solution:**

To make a solution which resembles to concrete which is under carbonation and chloride attack is to decrease the pH value of the saturated calcium hydroxide solution from 12 to around value of 7.4. To prepare the carbonated solution, Standard CO<sub>2</sub> of 99% purity was bubbled through the pore solution. Bubbling of CO<sub>2</sub> gas was done to achieve the carbonation condition in pore solution. Purpose of this process was to simulate corrosion prone carbonation state in the pore solution. The pH value of solution was reduced from 12 to 7.4 due to carbonation of calcium hydroxide. By reducing the pH value of solution to 7.4, a state of extreme carbonation in pore solution was achieved. CO<sub>2</sub> reacts with calcium hydroxide present in lime water to produce calcium carbonate precipitates. This process is being monitored properly as the process converting calcium hydroxide into calcium carbonate while CO<sub>2</sub> bubbling is very fast, an eye should be kept on the pH throughout the process.

Pure NaCl was added into the resultant solution, at a quantity of 3.5% w/w. The resultant solution then was filtered by filter paper.

### **4.5.2 Concrete Specimens**

The concrete samples were made using 2 cement types, OPC and PPC. The comparison was made on the basis of cement type. Duplicate samples were made and average values of samples were taken. The preparation of specimens is discussed in this section.

### **1. Preparation of steel bars:**

Steel bars used for concrete specimens were cut to required length of 360mm and were threaded from one side to make a hole for the nut. Each bar was properly cleaned with hexane and allowed to air dry. Both sides of steel bar were coated with epoxy up to 55mm. The 250 mm middle portion was left exposed for the corrosion process. Stainless steel screw and nut were inserted into the hole and a wire was connected to the nut.

### **2. Preparation of prism specimen:**

The prisms were cast in a mould of size 300 x 300 x 150. A total of 12 prisms were cast. Two types of cement were used i.e. OPC and PPC to evaluate the effect of inhibitor on both the cement types. Therefore, equal number of prisms was cast for both the cement type. Duplicate prisms were cast for each specimen and average values were taken. Firstly, the interior of prisms were oiled, so that prisms can be easily removed while demoulding. The bars were positioned in the centre so that 30 mm bar stays outside from both sides. After this, the concrete mix was poured and vibration was done so that there are no voids left. After demoulding the prisms were water cured for 7 days using gunny bags. Then the prisms were kept in controlled environment with RH 50-70 % and temperature 28-32 °C. The prepared specimen is shown in Fig. 4.3.

### **3. Preparation of concrete cubes:**

For the testing of carbonation depth, cubes of size 100mm were also cast. The cubes were cast for the same concrete used in prisms. Same procedure was adopted for curing and controlled environment. A total of 24 cubes were cast using OPC and PPC cement to evaluate the depth of carbonation in concrete at an interval of 15 days.



**Fig. 4.3: Prepared prism specimen**

#### **4.6 TESTS CONDUCTED**

Corrosion of steel embedded in concrete is not visually evident until the damage reaches to the external signs of deterioration as rust spots, cracks or spalling. In order to predict the corrosion service life of reinforced concrete structures and to determine the need to repair or rehabilitation, it is necessary to use non-destructive techniques for assessing the corrosion activity and measuring the corrosion rate of the reinforcements. In the present study, the corrosion rate of rebar is monitored by electrochemical attacks. The electrochemical measurements are carried out using a versatile instrument, namely ACM model: serial no. 1463 field machine, which is capable of performing various electrochemical tests such as potential measurement, AC impedance technique, potentiostatic cyclic sweep test, LPR (Longterm Potential Resistance) measurements etc. Fig 4.4 shows ACM setup used for electrochemical monitoring. The instrument is capable of processing the data and plotting the outputs automatically. The half cell potential measurements gives only an indication of the corrosion risk of the steel and is linked by empirical comparisons to the probability of corrosion. Therefore along with half cell, linear polarisation (corrosion rate) measurement are taken which provides a valuable insight into the instantaneous corrosion rate of the steel reinforcement, giving more detailed information than a simple potential survey. The LPR

data enables a more detailed assessment of the structural condition and is a major tool in deciding upon the optimum remedial strategy to be adopted.

Hence the two important electrochemical techniques that are used for the studying of corrosion activity are corrosion potential ( $E_{corr}$ ) and corrosion current/current density ( $I_{corr}$ ). These determining parameters indicate the corrosion initiation.



**Fig. 4.4: ACM Setup used for testing**

#### **4.6.1 Tests on Pore Solution**

For bare steel, potentiostatic linear sweep test was carried out on specimens using the ACM Field Machine. The electrochemical cell consists of a cylindrical jar with a wooden lid. It is provided with fittings for connecting the auxiliary electrode, reference electrode and the specimen. Throughout the test, the reference electrode used was saturated calomel electrode (SCE). The test set-up is shown in Fig 4.6. For testing, the bare steel specimen screwed to the working electrode, the reference electrode and auxiliary electrode were attached to the electrochemical cell. The potentiostatic linear sweep test was carried out from -300 mV to 1500 mV with offset from corrosion potential at a sweep rate of 32 mV per minute. The input readings for LPR sweep test is shown in Fig. 4.5

Half cell potential measurements were taken from the current voltage test. Fig. 4.7 shows the input readings for this test. The test setup for the Half-Cell Potential measurements is same as that of LPR measurements.

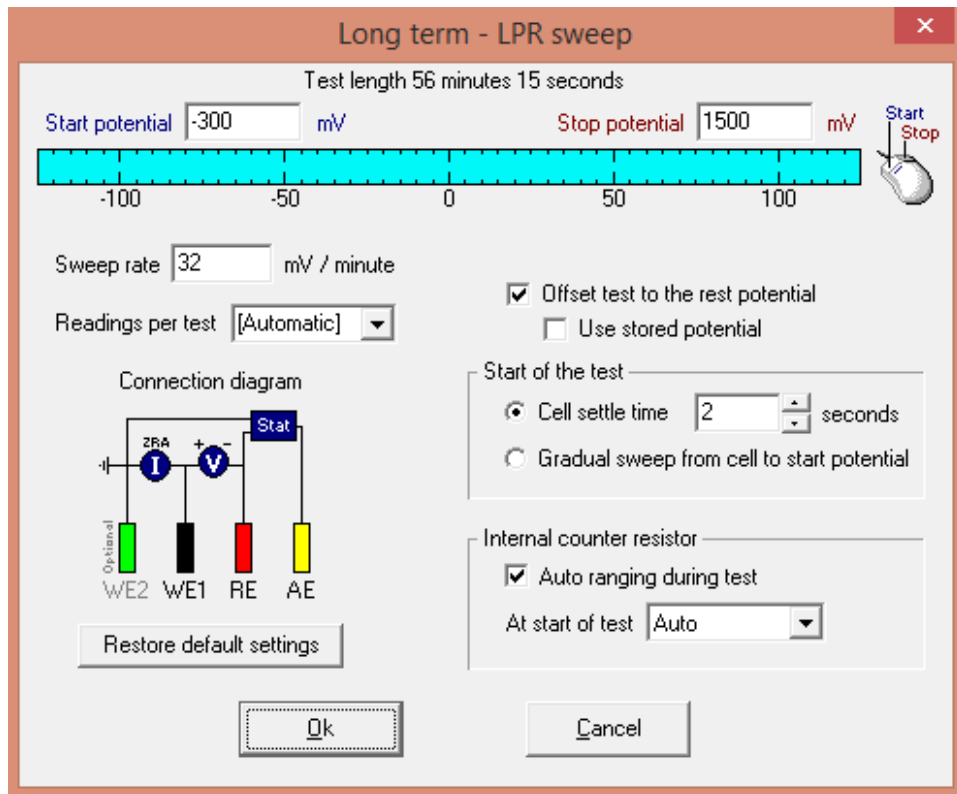


**Fig. 4.5: Input readings for LPR Sweep test for solution**

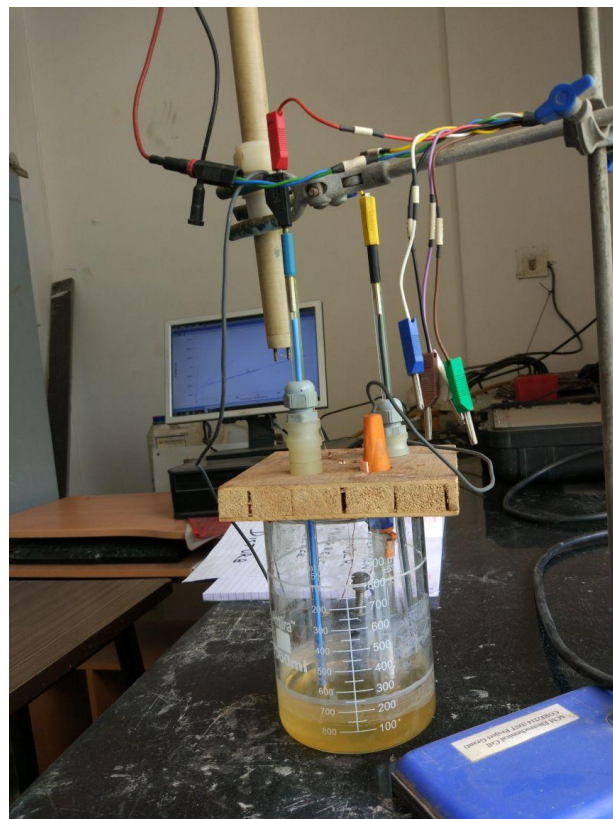


**Fig. 4.6: Test Setup for LPR and Half-Cell Potential**

## 4.6.2 Tests on Concrete Specimens

### 1. Concrete Prisms:

In this study, all the specimens were monitored after every 15 days by half cell potential, Galvanic potential and LPR readings using a saturated calomel reference electrode by placing the electrode on the top surface of the concrete. The procedure followed in ASTM standard C 876. The power supply was switched off one hour before taking the readings in order to completely depolarize it.

Half-cell potential was calculated at four different points on the surface of concrete along the rebar. The half cell potential was calculated using the saturated calomel electrode. The input readings for Half-Cell Potential measurement are shown in Fig. 4.6. The test setup for Half-Cell Potential measurements are shown in Fig. 4.8.

If the corrosion potential reading is more positive than -200mv, probability is that no reinforcing steel corrosion is occurring in the area at the time of measurement and if reading is more negative than -426 mv, probability is that the reinforcing steel corrosion is occurring. The ASTM interpretation of half cell potential (SCE) is summarised in Table 4.11

**Table 4.11: Corrosion condition corresponding to Half-Cell Potential values (ASTM C876)**

Half-cell potential values	Corrosion condition
< -426 mV	Severe corrosion, corrosion induced cracking may occur
< -276 mV	High risk, 90% probability of corrosion
-126 to -275 mV	Intermediate risk, corrosion activity in reduction
0 to -125 mV	Low risk, 10% probability of corrosion

Electrochemical LPR technique is especially good at measuring the localized corrosion. LPR measurements on concrete surfaces are performed using guard ring that is supplied with the field machine for precise location of rebar areas. The guard ring simply connects to the front panel via the supplied cables. Incorporated into the Guard ring is a Cu/CuSO<sub>4</sub> reference electrode. Before performing the test, conducting sponge is wetted with soap solution and

placed on the surface of the prism specimen to have proper electrical contact with the guard ring. Guard ring assembly is then placed above the wetted sponge. The electrical connections are made to the steel rebar. For linear polarization resistance measurement, the working electrode i.e. the steel rebar is polarized to  $\pm 50$  mV from the equilibrium potential. The experimental arrangement for LPR measurement with guard ring arrangement is shown in Fig. 4.10. The polarized surface area of the steel rebar is taken to be that lying under a circle intersecting the midpoint between the two sensor electrodes and only the top half surface area of the steel reinforcement is assumed to be polarized. The input readings are shown in Fig. 4.9.

For calculation of the corrosion current density  $I_{corr}$ , Stern-Geary equation is used:

$$I_{corr} = \frac{B}{R_p}$$

Where B is the Stern-Geary constant and is given by  $B = \frac{(\beta_a \times \beta_c)}{2.3 (\beta_a + \beta_c)}$

$\beta_a$  and  $\beta_c$  are anodic and cathodic tafel constants respectively. The value of B is taken as 26mV considering steel in active condition.  $R_p$  is the polarization resistance.

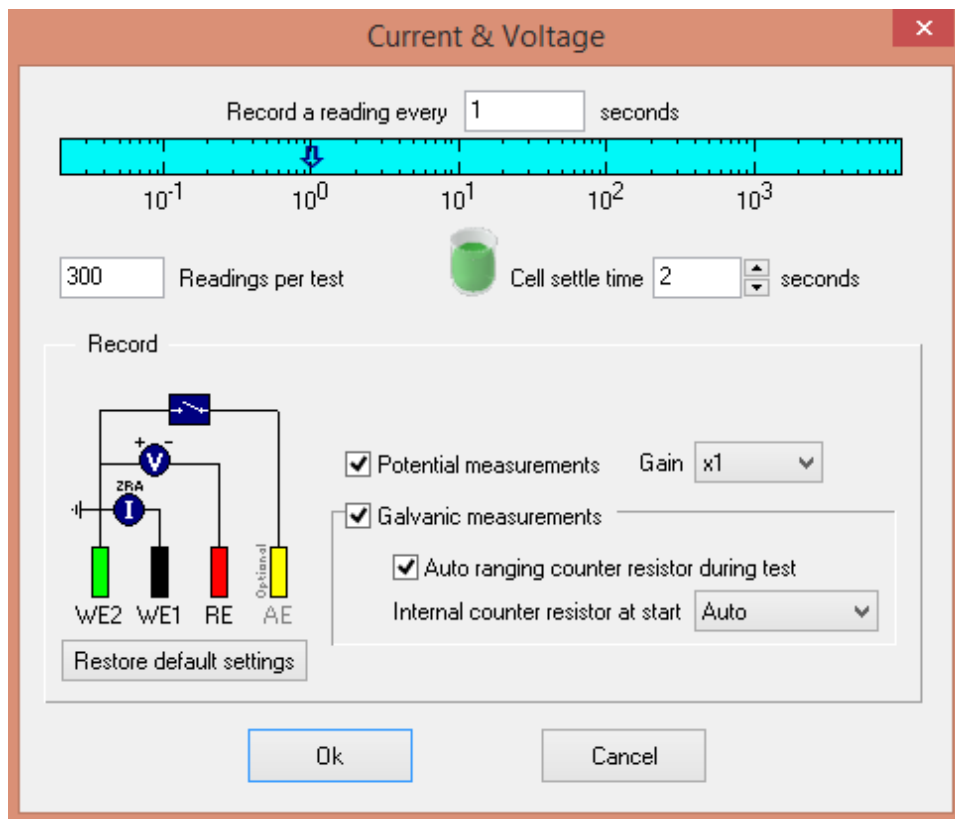


**Fig. 4.7: Input readings for Half-Cell Potential test for solution and concrete**

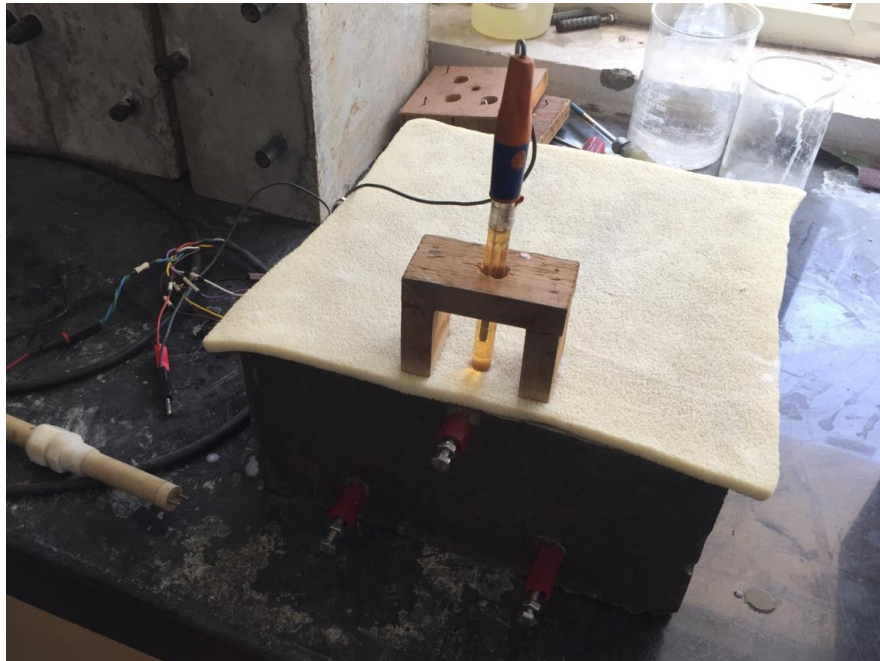


**Fig. 4.8: Half-cell potential test arrangement**

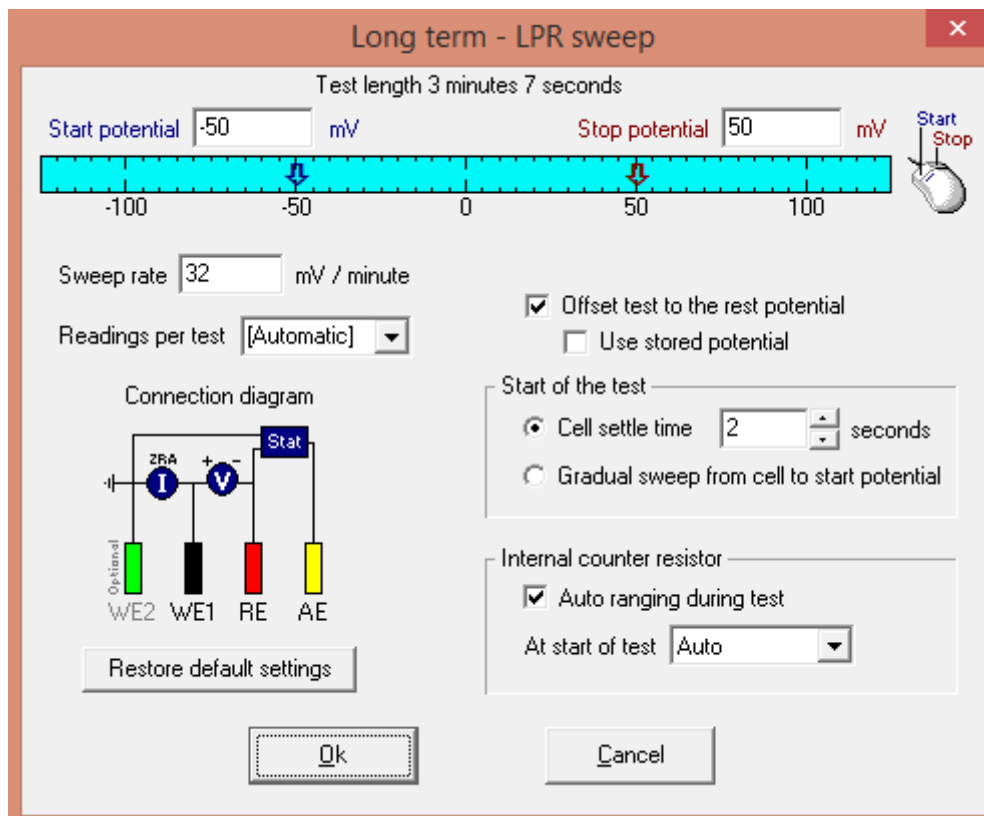


**Fig. 4.9: Input readings for LPR Sweep for concrete specimens**

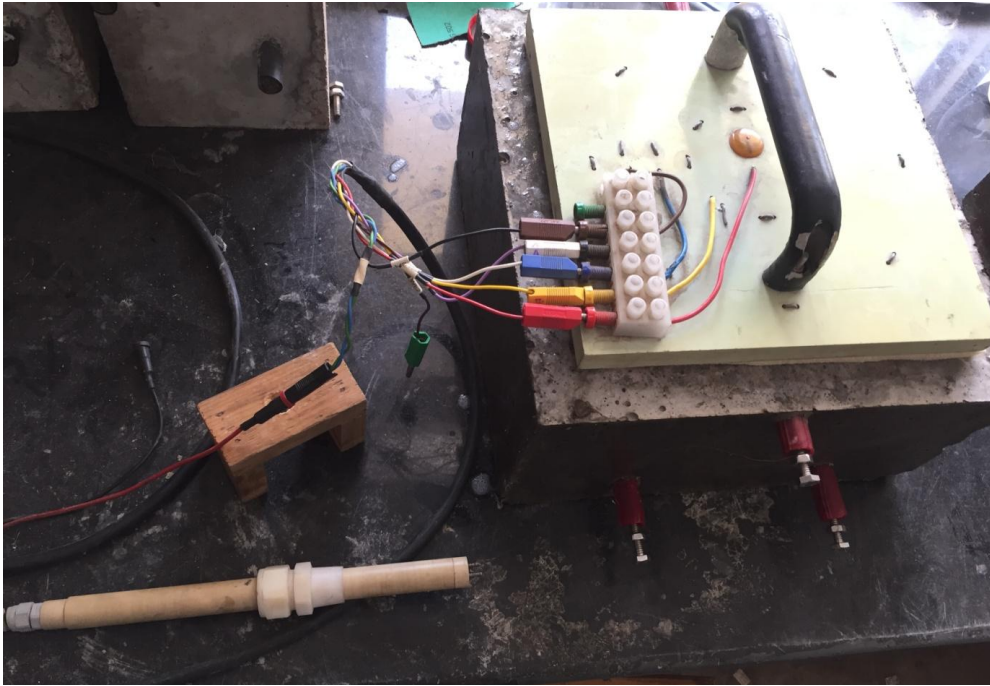


**Fig. 4.10: LPR Sweep test arrangement for concrete**

Galvanic potential gives an idea of Macrocell corrosion. The change in sign of potential difference indicates a reversal in direction of the current between the top steel bar and bottom steel bars and the top steel bar has become anodic. For the Galvanic Potential, the potential difference between the top steel bar and common terminal of bottom steel bars (i.e. potential of top rebar with respect to bottom common terminal) was measured across the 100 Ohm resistor connected between them. For the purpose of potential measurement the corrosion monitoring equipment as stated earlier was used. The potential was measured with the help of Saturated Calomel electrode. The Fig. 4.11 shows the connection of resistor between the top and bottom steel bars.

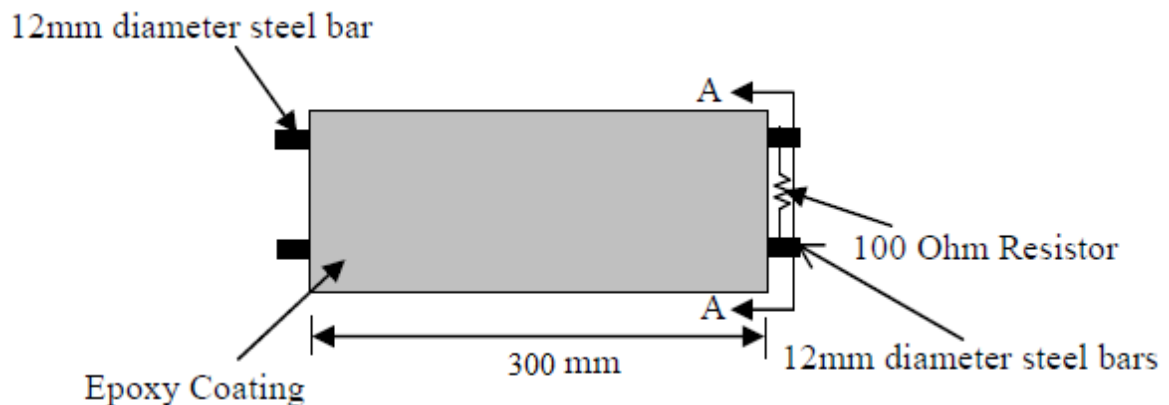


**Fig. 4.11: Diagram showing connection of resistor for Galvanic Potential**

## 2. Concrete Cubes:

For calculation of carbonation depth on cubes of size 100mm. The cubes were split into two halves as shown in Fig. 4.13 and immediately after splitting the exposed surface was cleaned and sprayed with the solution. A solution was prepared using phenolphthalein and ethanol. A 100 ml solution was prepared consisting of 1g phenolphthalein and 90 ml 95.0 V/V% ethanol diluted in water to 100ml. Phenolphthalein indicator gives purple red colour for uncarbonated part and no colour for the carbonated part of the cube. The carbonation depth was measured after every 15 days. The cubes were kept in carbonation chamber throughout the testing period. The carbonation depth was measured using a vernier calliper of least count 0.01mm. A prepared cube specimen is shown in Fig. 4.12.



**Fig 4.12: (a) Prepared Concrete cube for Carbonation Depth (b) Splitting Concrete Cube into two halves**

## **CHAPTER 5 - RESULTS AND DISCUSSION**

### **5.1 INTRODUCTION**

This chapter deals with the use of corrosion inhibitor in chloride and carbonated rich environment. The effect of OPC and PPC was studied. The effect of corrosion inhibitor was monitored in terms of half cell potential measurements, linear polarization resistance, carbonation depth and galvanic potential. Efficiency of corrosion inhibitor was studied at 2 levels. Firstly, pore solution tests were conducted to study the layer forming ability of Corrosion Inhibitor and secondly, tests on concrete samples were conducted. The test results are discussed in the following sections.

### **5.2 PORE SOLUTION TEST RESULTS**

The effect of using Corrosion Inhibitor on the resultant corrosion of steel bar kept in simulated pore solution was studied. Synthetic Pore solution was prepared resembling concrete which consists of saturated calcium hydroxide solution. The base sample of Carbonated and chloride environment was created by adding 3.5% of pure NaCl and CO<sub>2</sub> bubbling of 99% purity to the saturated calcium hydroxide solution. 1 % of corrosion inhibitor w/w was added in sample 2 to check the efficiency of 2-Aminopyridine as a corrosion inhibitor. The nomenclature of the pore solutions prepared for testing of steel bar is given in Table 5.1. The results of half cell potential measurements and linear polarization resistance are discussed.

**Table 5.1 Nomenclature of Solutions**

<b>Sr. No.</b>	<b>Designation</b>	<b>Details of Solution</b>
1	Sample 1	Saturated Calcium Hydroxide Solution + 3.5% NaCl + CO <sub>2</sub> (pH=7.4)
2	Sample 2	Solution 1 + 2-Aminopyridine 1% w/w

#### **5.2.1 Half Cell Potential Test**

Half-cell potentials readings were taken on the steel bars partially immersed in pore solution. Half cell potential readings were taken with respect to Saturated Calomel electrode as reference electrode. The value of half cell potential acquired gives an indication of

depassivation of steel and thus the possibility of corrosion. ASTM C876 suggests that the corrosion possibility of steel bar immersed in concrete is higher than 90% when the open circuit potential is lower than -270 mV (SCE). Also, the corrosion possibility is lower than 10% when the open circuit potential is higher than -120 mV (SCE). It is to mention here that the values of Half-Cell Potential provided in ASTM C876 are for concrete and no values are provided for the solution tests.

The Half-Cell Potential readings were taken at 1 h, 24 h, 48 h, 120 h, 240 h and 480 h to check the efficiency of inhibitor. The Half-Cell Potential gives an idea about the probability of corrosion on the steel bars. Results for Half-cell potential for both samples are given in Table 5.2.

**Table 5.2: Values of Half-cell potential and corrosion current for solutions**

Time	Tests	Sample 1	Sample 2
1 hour	HCP (mV)	-661.2	-545.31
	Icorr (mA/cm <sup>2</sup> )	1.175	1.315
24 hours	HCP (mV)	-711.1	-660.1
	Icorr (mA/cm <sup>2</sup> )	1.275	1.118
48 hours	HCP (mV)	-732.2	-639.1
	Icorr (mA/cm <sup>2</sup> )	2.551	1.84
120 hours	HCP (mV)	-746.2	-653.78
	Icorr (mA/cm <sup>2</sup> )	2.355	1.283
240 hours	HCP (mV)	-738.08	-496.8
	Icorr (mA/cm <sup>2</sup> )	2.276	0.765
480 hours	HCP (mV)	-739.2	-400.5
	Icorr (mA/cm <sup>2</sup> )	2.03	0.017

As can be seen from the Table the values of Half-Cell Potential at all time intervals for both samples are on the higher negative side. From the reading of both the samples it can be seen that the values of Half-Cell Potential are very high irrespective of whether Corrosion Inhibitor is added or not. The Half-Cell Potential value in the pore solutions does not indicate the passive or active state of corrosion and can be used for comparative purpose only. Tests on pore solution are performed in order to compare the Half-Cell Potential readings of

solution with inhibitor and reference solution. *Ormellese (2006), Tommaselli et al. (2009)*, and other researchers also found higher values of Half-Cell Potential for pore solutions in contaminated environment.

The reference Sample 1 showed higher negative values of Half-Cell Potential at all stages of testing i.e. above -650mV. The Half-Cell Potential values gets stabilised at the end of testing period for solution 1 at higher negative side. This shows that there is probability of severe corrosion in the reference sample (Sample 1). The bar chart in Fig. 5.1 shows the variation of both samples at different immersion time.

The sample 2 with 1% 2-aminopyridine showed a decreasing trend of Half-Cell Potential after 24 hours. The corrosion potential for sample 2 shifted towards the passive side with increase in the difference between the Half-Cell Potential readings of sample 1 and 2. The Half-Cell Potential readings for the sample with corrosion inhibitor decreased down to as low as -400.5mV. The probability of corrosion lowered from severe corrosion to high corrosion. The Half-Cell Potential of sample 2 decreases with immersion time and reached to almost half of sample 1 after 480 hours. It clearly indicates that 2-Aminopyridine has the ability to reduce the corrosion probability. Also, the effect of corrosion inhibitor increases with time.

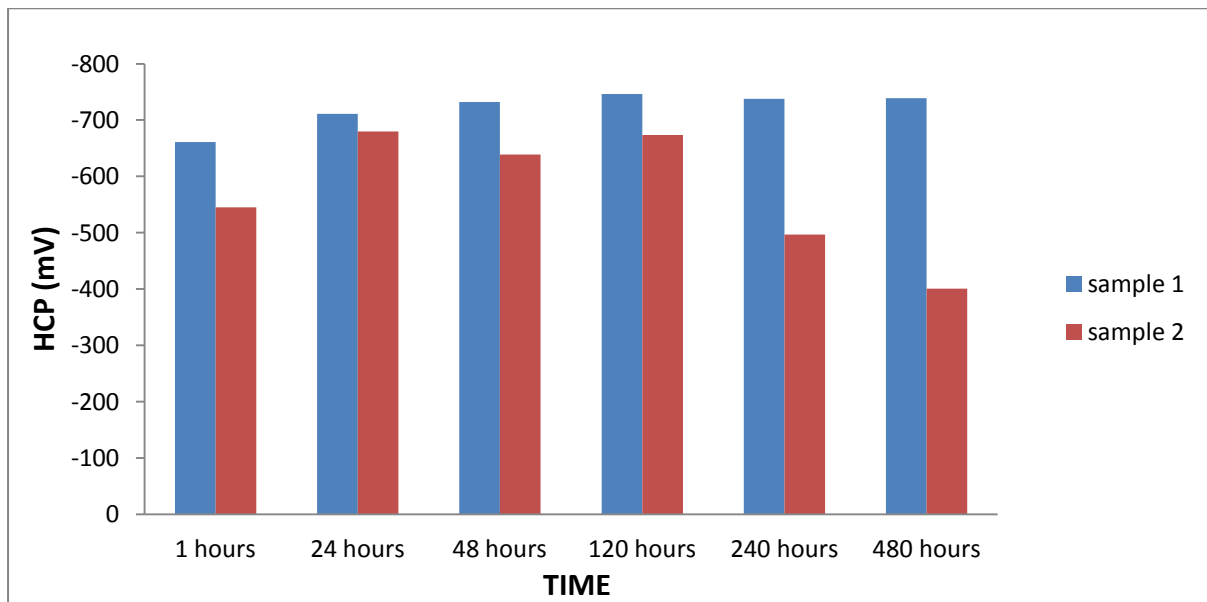


**Fig. 5.1: Variation of Half-cell potential of solution specimens with time**

### 5.2.2 Linear Polarisation Resistance Test (LPR)

Corrosion initiation described as the process by which chloride ions accumulate around the steel bar, thereby breaking down passivity of the reinforcing steel and allowing corrosion to initiate. Corrosion propagation is described as the process by which the rate of corrosion is accelerated by the electric current at a constant voltage. Half cell potential is effective only in monitoring the corrosion initiation. Therefore, LPR measurements are necessary as the values obtained from corrosion current density indicate the progression of corrosion in the propagation phase.

The  $I_{corr}$  values of solution 1 and 2 at different immersion time are shown in Table 5.2 and are further presented in Fig 5.2. The  $I_{corr}$  values give a better explanation of corrosion as compared to the Half-Cell Potential readings which shows the depassivation of steel. From graph it can be seen that the  $I_{corr}$  values of sample 1 are higher than the corresponding values of sample 2 at almost all stages of testing. There is a rise in values of  $I_{corr}$  up to 48 hours as the solution takes time to stabilise. The reference sample i.e. sample 1 reached its peak value at 48 and 120 hours of immersion time. The corrosion products on the steel bar justify the highest  $I_{corr}$  values at these testing periods. After 120 hours, the value of  $I_{corr}$  for sample 1 gets stabilised at the higher side due to the attack of chloride and  $CO_2$  on the steel bar. The values of  $I_{corr}$  for sample 1 lies in the active region throughout the testing period.

On comparing the performance of Sample 2 with sample 1 it can be seen that sample 2 initially behaved almost similar to the sample 1 in terms of  $I_{corr}$  value. The sample 2 shows a decreasing trend in  $I_{corr}$  values after 48 hours of immersion. The  $I_{corr}$  value decreased to almost half after 240 hours of immersion. It can be seen that after 120 hours the sample 2 performed considerably well as compared to the sample 1. The  $I_{corr}$  values shifted to the passive side once the inhibitor started forming passive film around the steel bar. At 480 hours, the  $I_{corr}$  value of sample 2 was close to zero showing the efficiency of 2-Aminopyridine as a corrosion inhibitor.

Condition of steel bar in both test solution at various exposure duration was visually examined and are shown in Fig. 5.3. The corrosion can be seen with the naked eye. Visually, condition of rebar at 48 and 120 hours also depicts the higher corrosion at that time. Formation of corrosion products led to the increase in volume which in turn, led to breakage

of the epoxy layer as can be seen in reference sample at 48 hours. The reference samples are more corroded than the samples with inhibitor.

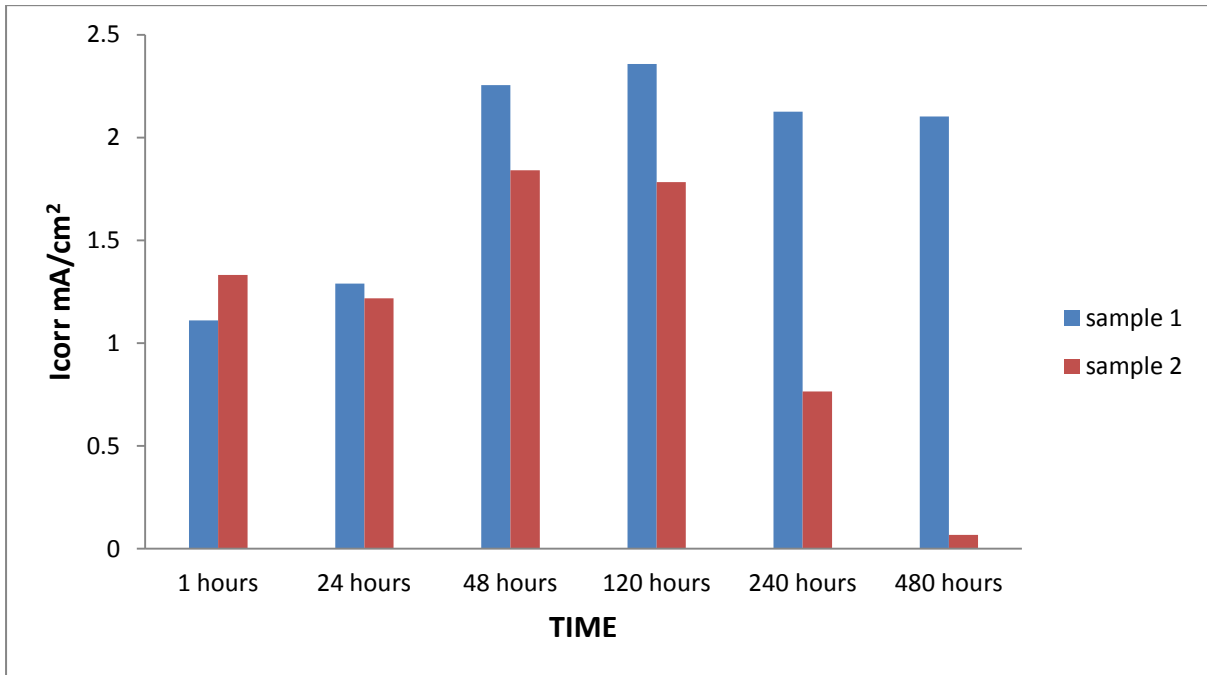


**Fig. 5.2: Corrosion current density of specimens at different time in solution**

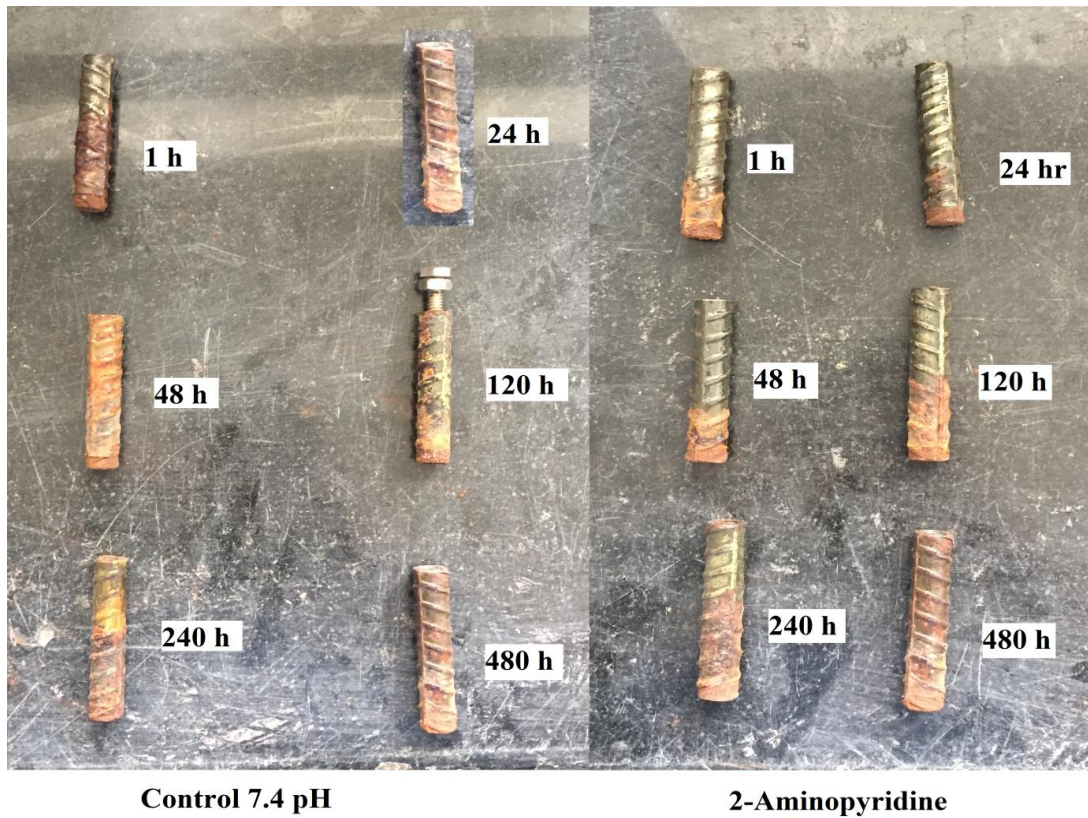


**Fig. 5.3: Condition of steel rebars after the test at different time**

### 5.2.3 Chemistry between Corrosion Inhibitor and Steel Surface

The reason for the chemicals acted as a barrier for corrosion can be explained considering the chemistry between corrosion inhibitor and concrete. Amine based corrosion inhibitor is said to be chelating agent, which can form five or six membered chelate rings. Figure 5.4 shows the way through which the 2-Aminopyridine has formed chelate ring around the steel bar.

These rings are formed as a result of bonding between two or more functional groups from the inhibitor and the cation metal. Due to the presence of rings, Amine organic inhibitors have film-forming effects. The film-forming component is an amine group (NH<sub>2</sub>). They get adsorbed on metals and oxides because of an unshared electron pair of the nitrogen atom. *Welle et al. (1997)* and *Nmai (2004)* report that amines and the associated radicals form a layer on the steel surface which completely cover all the anodic and cathodic sites. The film forming effect therefore depends on the property of corrosion inhibitor and does not depend upon the quality of concrete.

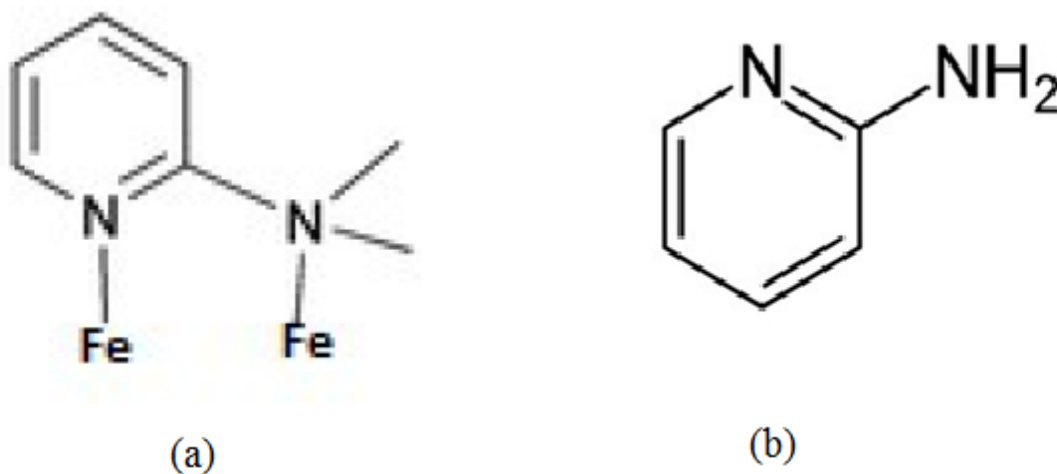


**Fig.5.4: (a) Chelate ring formed by 2-Aminopyridine around steel bar (b) Molecular Structure of 2-Aminopyridine**

Both the nitrogen Atoms of 2-Aminopyridine makes a bond with the steel surface thus making a passive layer around the steel bar which completely covers all the anodic and cathodic sites. The chemistry of action of 2-Aminopyridine on steel surface indicate that it has capacity of layer formation around the steel bar. The pore solution results further confirmed the decrease in I<sub>corr</sub> values by using 2-Aminopyridine as corrosion inhibitor in the pore solution.

### 5.3 EFFECT OF 2-AMINOPYRIDINE ON CONCRETE

To check the effectiveness of 2-Aminopyridine as corrosion inhibitor in concrete, prisms and cubes were cast. For comparison on the basis of cement type, OPC and PPC cements were used for casting of concrete specimens. These specimens were kept under controlled environment throughout the testing period of 60 days. The following sections discuss the results of carbonation depth measured on concrete cubes and electrochemical tests conducted on concrete prisms.

### 5.4 CARBONATION DEPTH

Carbonation depth was measured on cubes of 100 mm. These cubes were placed under carbonation at 5% of CO<sub>2</sub> throughout the testing period of 60 days. The temperature of the carbonation chamber was set to 28-32°C and RH to 50-70%. The carbonation depth values were calculated for concrete cubes made with OPC and PPC cement. The readings of carbonation depth were taken after every 15 days. The carbonation depth was calculated using the phenolphthalein indicator which distinguishes the carbonated and uncarbonated part. Finally the readings were measured using a vernier calliper Fig. 5.5 shows the carbonated and non-carbonated part. The colourless portion represents the carbonated part whereas the portion with purple red colour shows the uncarbonated part. This procedure is used by various researchers to measure the carbonation depth, (*Kulwinder et al., 2016, Fukushima et al., 1998*). The nomenclature of the concrete specimens cast is given in Table 5.3. The final readings of the carbonation depth for various OPC and PPC specimens are shown in Table 5.4.



**Fig. 5.5: Carbonation depth specimen showing carbonated and non-carbonated part**

**Table 5.3: Nomenclature for Concrete specimens**

DESIGNATION	DESCRIPTION
O1	Control OPC specimen
O2	3.5 % Chloride admixed OPC specimen
O3	3.5 % Chloride + 1.5 % 2-Aminopyridine admixed OPC specimen
P1	Control PPC specimen
P2	3.5 % Chloride admixed PPC specimen
P3	3.5 % Chloride + 1.5 % 2-Aminopyridine admixed PPC specimen

**Table 5.4: Carbonation depth values of cubes**

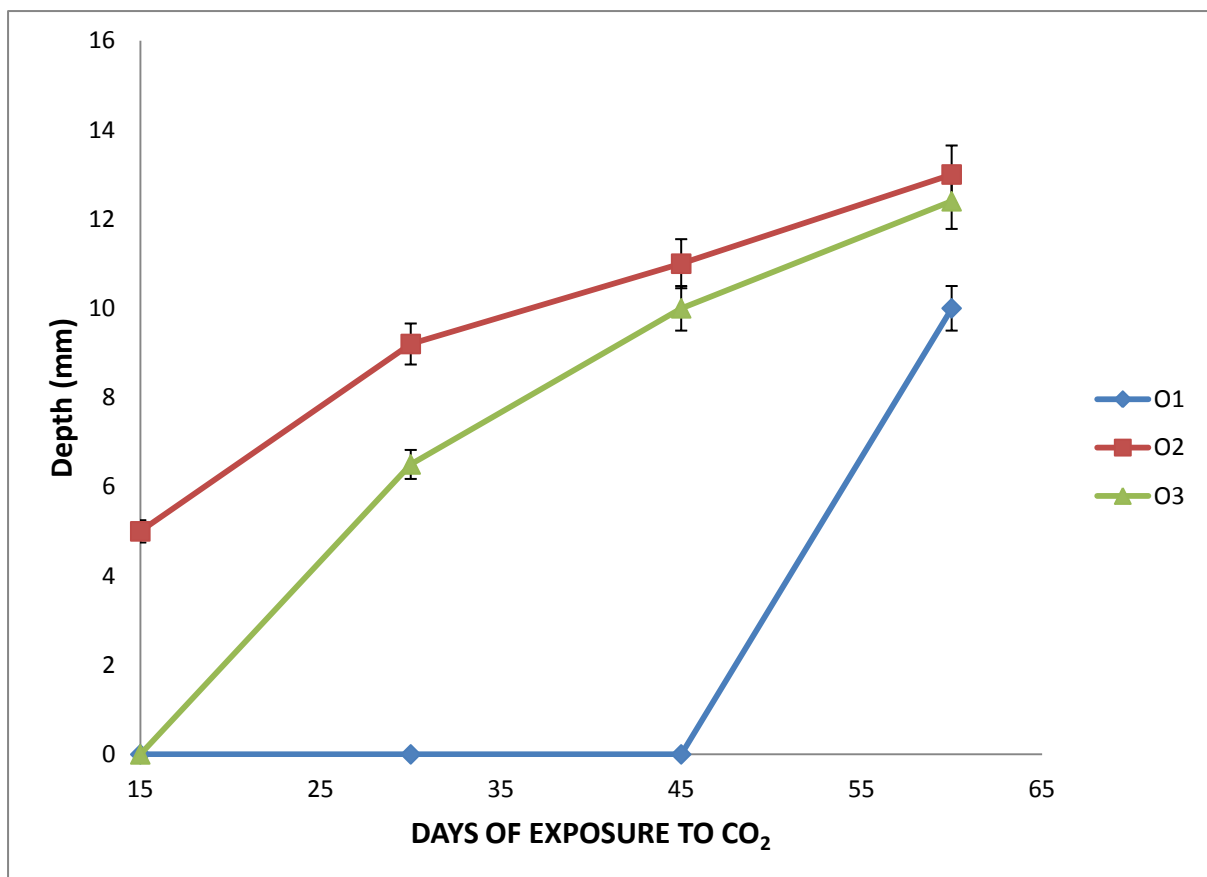
DAYS OF EXPOSURE To CO <sub>2</sub>	Carbonation Depth (mm)					
	O1	O2	O3	P1	P2	P3
15	0	5	0	0	5.2	0
30	0	9.2	6.5	0	10	5.9
45	0	11	10	0	11.4	10.2
60	10	13	12.4	9.2	13.5	12.3

Fig. 5.6 shows the variation of carbonation depth with time for cubes made with OPC. O1 cube was made without any admixture, while O2 was admixed with 3.5% NaCl and O3 containing 3.5% NaCl and 1% 2-aminopyridine as corrosion inhibitor. There was no carbonation depth in O1 cubes upto 45 days. The whole surface of cube showed purple red colour when phenolphthalein solution was applied, indicating zero carbonation front. This must be due to the slower penetration of carbonation in O3 specimens as compared to specimens with chlorides in concrete specimens (O2). Similar results were obtained by Wang *et al.* (2017).

While the O2 cubes admixed with chloride, showed high values of carbonation depth values from the starting i.e. 15 days and reached a value of 13mm after 60 days. This shows that the presence of chlorides increase the carbonation depth in the concrete specimens. Similar observations were made by Zhang *et al.* (2016). Carbonation of chloride contaminated

concretes results in the release of bound chlorides, which pushes chlorides inwards and, hence, could be detrimental to the corrosion of steel reinforcement, (Wang *et al.*, 2017)

The O3 cube with inhibitor and chlorides showed lesser values than the cube with chlorides (O2). It indicates the amine group inhibitors helps in pore refinement, thus decreasing the carbonation front in these specimens. So the initiation of carbonation depth is delayed in O3 specimens but once the carbonation starts taking place it reaches almost similar value as those O2 cube after 60 days. The inhibitor helps in delaying the onset of carbonation in concrete till the testing period.



**Fig. 5.6: Carbonation depth with time for various OPC cubes**

The same pattern was observed in the PPC specimens as that of OPC specimens. The variation for PPC specimens can be seen in Fig. 5.7. The P1 specimen showed no carbonation depth up to 45 days as there was no chloride and inhibitor in the specimen. The P2 specimen showed high carbonation depth from the starting testing time due to the presence of chlorides

in these specimens. The inhibitor helped in delaying the carbonation effect in the PPC specimens as can be seen in P3 specimen.

The cubes made with PPC cement showed almost same Carbonation depth values than the cubes made with OPC cement. The testing period was not sufficient to comment on which cement showed better resistance to carbonation. Both OPC and PPC specimens with corrosion inhibitor admixed (O3 and P3) showed better resistance to carbonation as compared to specimens with chloride (O2 and P2). This must be due to the pore blocking affect of amine-group corrosion inhibitors, (Soylev *et al.*, 2008).

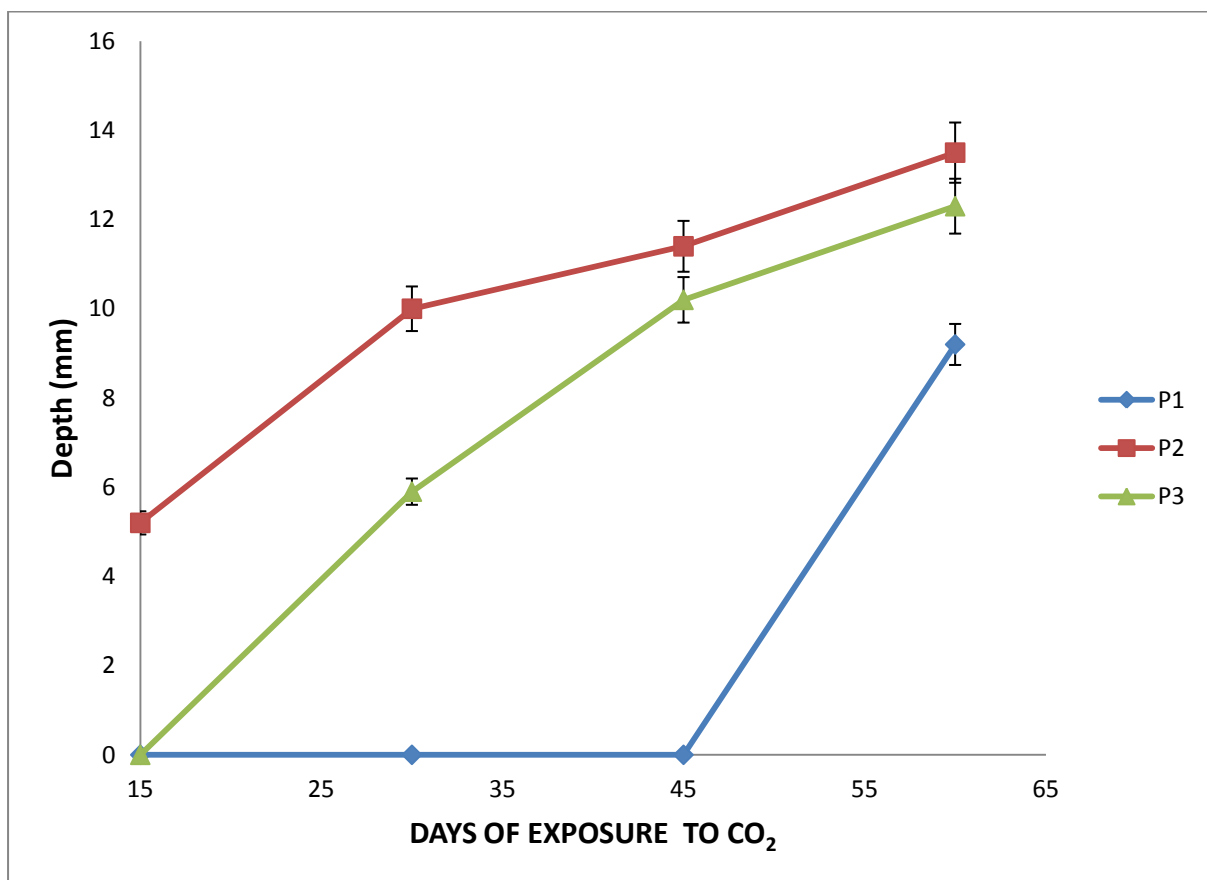


**Fig. 5.7: Carbonation depth with time for various PPC cubes**

## 5.5 CONCRETE PRISMS TEST RESULTS

The chloride was admixed in the concrete prism during casting by 3.5% wt. of cement. The amount of corrosion inhibitor (2-Aminopyridine) was taken as 1.5% by wt. of cement. The prisms were kept in carbonation chamber and CO<sub>2</sub> was passed at a rate of 5% throughout the testing period. The description of samples is given in Table 5.3.

The effect of addition of 2-Aminopyridine on the protection against rebar corrosion was monitored by using electrochemical tests in the concrete prisms is discussed. Half cell potential readings were taken on prism specimens with plan size of 300 x 300 mm<sup>2</sup>, depth 150mm and with 5 mm cover to rebar. The Half-cell potential measurements, Linear Polarization Resistance and Galvanic Potential readings were taken after every 15 days for samples with different cement types with chloride and corrosion inhibitors. The results of half cell potential measurements, galvanic potential and linear polarization resistance are discussed in the following section.

### 5.5.1 Half Cell Potential Test

The Half cell potential readings just indicate the depassivation of steel and hence the possibility of corrosion. This gives a rough idea of whether the corrosion in the rebar has started or not. The values of Half-cell potential at different exposure duration are presented in Table 5.5. The corrosion condition corresponding to Half- Cell potential values are compared with the values provided by ASTM C876 and is presented Table 5.6.

**Table 5.5: Values of Half-cell potential in mV for different prisms**

DAYS OF EXPOSURE TO CO <sub>2</sub>	Half Cell Potential (mV)					
	O1	O2	O3	P1	P2	P3
0	-166	-472	-441	-115	-470	-405
15	-110	-607	-476	-156	-528	-464
30	-110	-520	-510	-176	-470	-454
45	-47	-528	-472	-94	-487	-427
60	-89	-549	-441	-101	-510	-443

**Table 5.6: Corrosion condition corresponding to Half-Cell Potential Readings  
(ASTM C876)**

<b>Half-Cell Potential Readings</b>	<b>Corrosion condition</b>
< -426 mV	Severe corrosion, corrosion induced cracking may occur
< -276 mV	High risk, 90% probability of corrosion
-126 to -275 mV	Intermediate risk, corrosion activity in reduction
0 to -125 mV	Low risk, 10% probability of corrosion

The effect of type of cement in use of 2-Aminopyridine on Half-Cell Potential are discussed in following section.

### **1. OPC concrete**

Fig. 5.8 shows the variation of Half-Cell potential for with time for various OPC prisms. The half cell potential of O1 prism is below -275 mV which shows that the corrosion has not yet started or there is only 10% of probability of corrosion. The O1 prisms were cast using ordinary Portland cement without any contamination of chlorides. The O1 prisms were exposed to only carbonated environment, no chloride or corrosion inhibitor was added to the concrete mix. According to the results obtained from the Half-Cell potential readings it can be observed that O1 prisms have very low probability of corrosion till 60 days of CO<sub>2</sub> of exposure.

The O2 prisms containing 3.5% NaCl by weight of cement, admixed at the time of mixing of concrete, showed more than -426 mV Half-Cell Potential readings which confirm probability of severe corrosion in these specimens. The values of Half-Cell Potential remained in the range of severe corrosion throughout the testing period of 60 days. This shows the adverse affect of chlorides on the reinforcement. Similar observations were made by *Malik et al. (2004)*, when concrete specimens were immersed in 5% NaCl solution.

Whereas in prisms O3, the NaCl content was same while additional 1.5% of 2-aminopyridine by weight of cement was added during the casting of concrete. These prism specimens showed slightly lower half cell potential readings but were still in the range of high probability of corrosion or severe corrosion in most cases. It shows that 2-Aminopyridine has not shown much effect in terms of lowering the corrosion potential till the testing period.

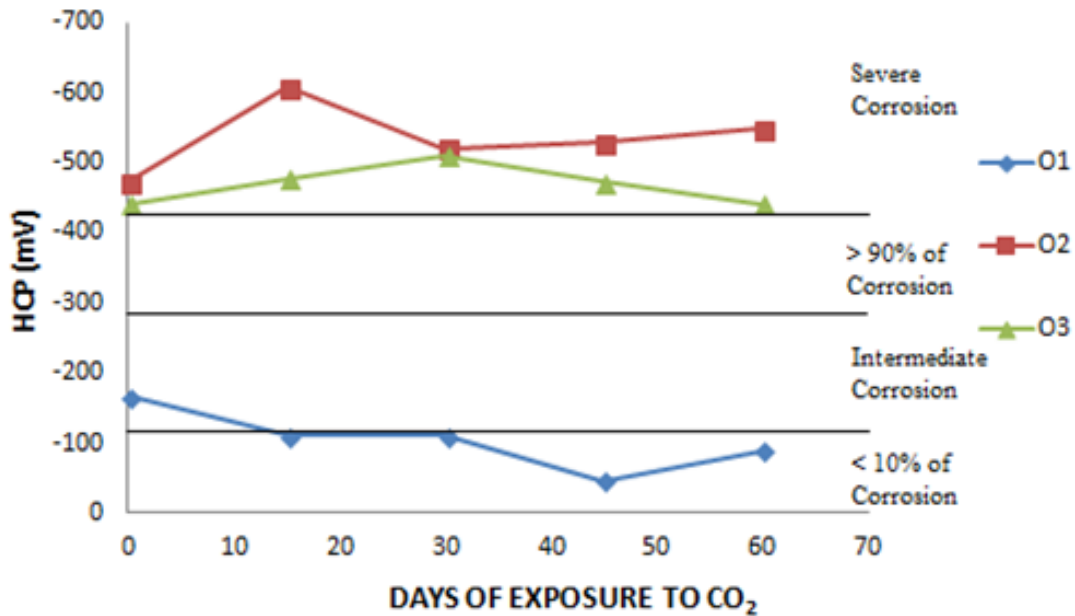


**Fig 5.8: Variation of Half Cell potential with time for OPC prisms**

## 2. PPC concrete

Similar to variation of Half-Cell Potential on prisms made with OPC, the effect of PPC on Half-Cell Potential is diagrammatically represented in Fig. 5.9. In order to compare the corrosion potential in terms of cement type, the PPC prisms were cast.

The PPC prisms showed almost a similar trend as that of OPC prisms. The P1 specimens having no chloride or inhibitor showed low Half-Cell Potential readings. It lies in the range of low risk corrosion as per ASTM C876 standards. These specimens showed no signs of carbonation induced corrosion till 60 days of testing period. The Half-Cell Potential readings of prisms containing 3.5% NaCl i.e. P2, is in range of Severe corrosion throughout the testing period. While, the P3 prisms containing chlorides as well as inhibitor showed slightly lower corrosion potential but was still in the range of probability of high corrosion.

The PPC prisms, whether it is with NaCl or with NaCl and 2-aminopyridine, showed slightly lower values of Half-Cell Potential than the prisms made with OPC. But, no conclusion can be drawn from the Half-Cell Potential readings, as these provide only the probability of corrosion. After Half-Cell Potential test, Linear Polarisation Resistance test is performed in order to get a better idea of rate of corrosion in the rebar.

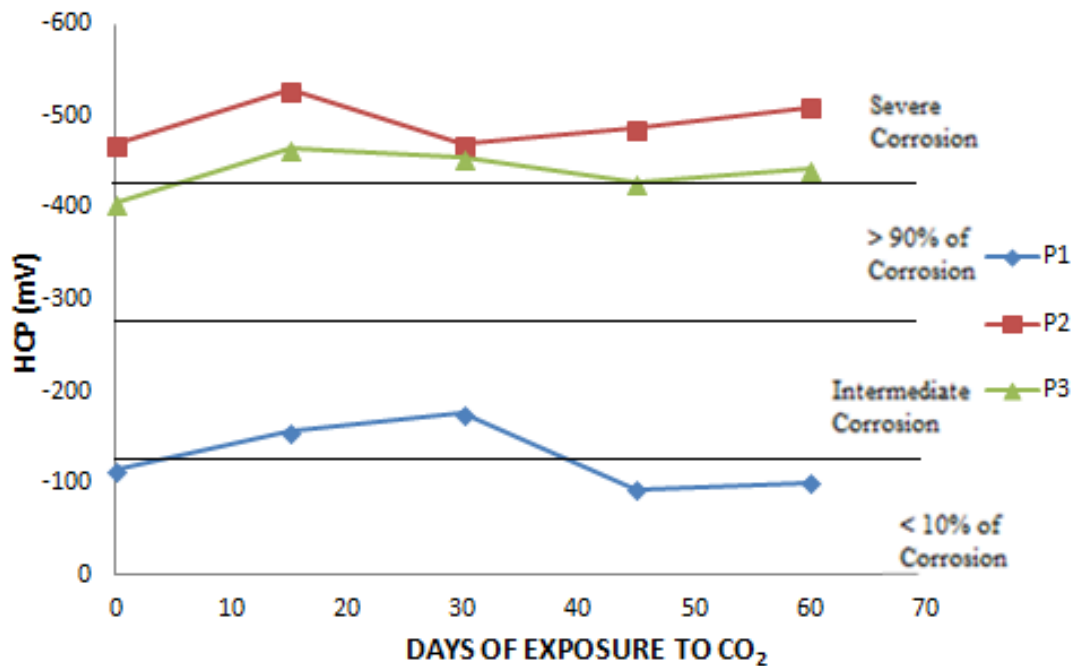


**Fig 5.9: Variation of Half Cell potential with time for PPC prisms**

### 5.5.2 Linear Polarisation Resistance Test (LPR)

On the basis of the measured values of corrosion current density, the given criteria for corrosion activity is taken. Corrosion current density values less than  $0.0001\text{mA}/\text{cm}^2$  correspond to passive condition or low corrosion rate and corrosion current density values ranging between  $0.0001\text{mA}/\text{cm}^2$  and  $0.001\text{mA}/\text{cm}^2$  correspond to moderate corrosion rate. Similarly corrosion current density values ranging between  $0.001\text{mA}/\text{cm}^2$  and  $0.01\text{mA}/\text{cm}^2$  and between  $0.01\text{mA}/\text{cm}^2$  and  $0.1\text{mA}/\text{cm}^2$  correspond to high and very high corrosion rate respectively for concrete, (Stewart and Vu, 2002).

The values of  $I_{\text{corr}}$  for the concrete prisms were measured till 60 days of CO<sub>2</sub> exposure periodically after every 15 days and results are shown in Table 5.7. The LPR test was conducted after every 15 days. As the Half-Cell Potential test only gives the probability of corrosion. The LPR test is an important parameter which gives an actual idea about the corrosion of steel bar inside the concrete specimen. The prisms were kept under controlled environment throughout the testing period.

For the comparison of cement type, specimens using OPC and PPC were cast. The values for OPC and PPC concrete are discussed in the following section.

**Table 5.7: Values of Icorr for different type of prisms**

DAYS OF EXPOSURE TO CO <sub>2</sub>	Icorr (mA/cm <sup>2</sup> )					
	O1	O2	O3	P1	P2	P3
0	0.000114	0.000868	0.00053	0.000076	0.000712	0.0003
15	0.00007	0.00181	0.00175	0.000053	0.00177	0.00169
30	0.000062	0.0014	0.001354	0.00003	0.00162	0.00148
45	0.000045	0.00131	0.000613	0.0000225	0.00151	0.000959
60	0.000051	0.00135	0.00042	0.00002	0.00154	0.00042

### 1. OPC Concrete

Fig 5.10 shows the variation in Icorr for prisms made with OPC. The O1 prisms lie in the passive state, as no chloride was admixed in these specimens and there was no sign of carbonation induced corrosion in these specimens during the exposure days. The rebars in O1 specimen were in the passive zone throughout the testing period.

While the prisms with 3.5% chloride admixed into them, i.e. O2, showed higher corrosion current from the start of testing. The O2 specimens retained the high values throughout the exposure period and were in the range of high corrosion rate.

The prisms containing 3.5 % chloride and 1.5% 2-aminopyridine, i.e. O3, showed lower corrosion current in the starting and end of exposure period. The corrosion current of O3 specimen remained lesser than O2 at all stages of testing. The corrosion current indicates the shift of rebars from active side to passive side at the end of testing period. The values of corrosion current shifted from the range of high corrosion rate to moderate corrosion rate. This means that the amine group in 2-Aminopyridine has adsorbed on the rebar. Thus forming a passive layer around the rebar covering all cathodic and anodic sites. (Soylev *et al.*, 2008). Similar results were found in pore solution tests. The amine group in the corrosion inhibitor takes time for bonding to the steel bar.

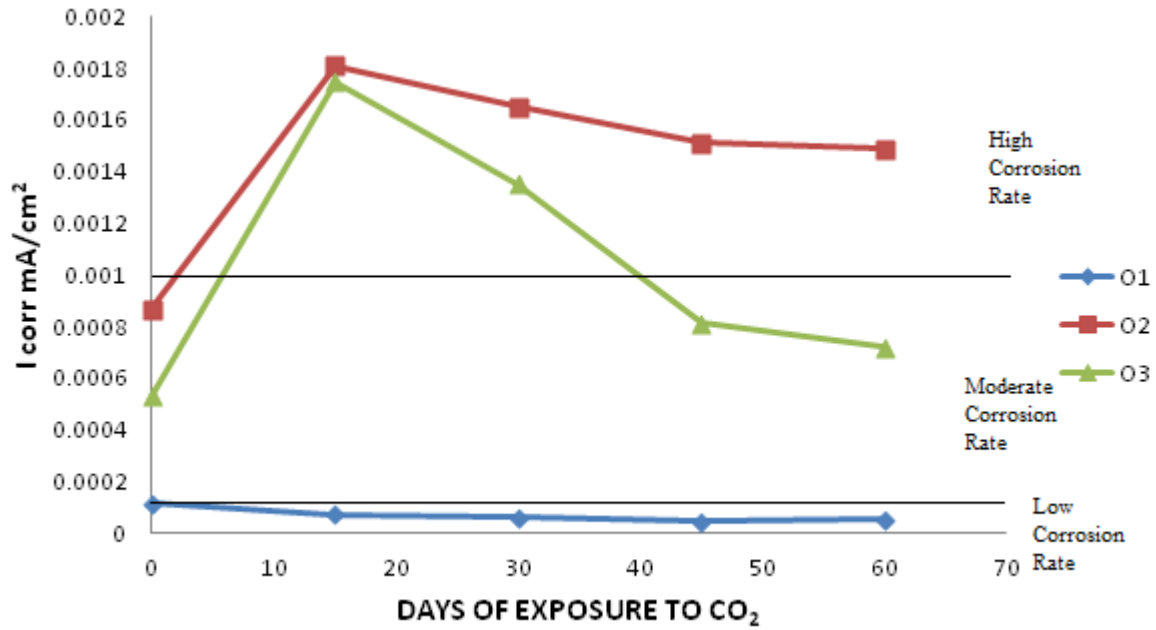


**Fig 5.10: Variation of corrosion current with time for different OPC prisms**

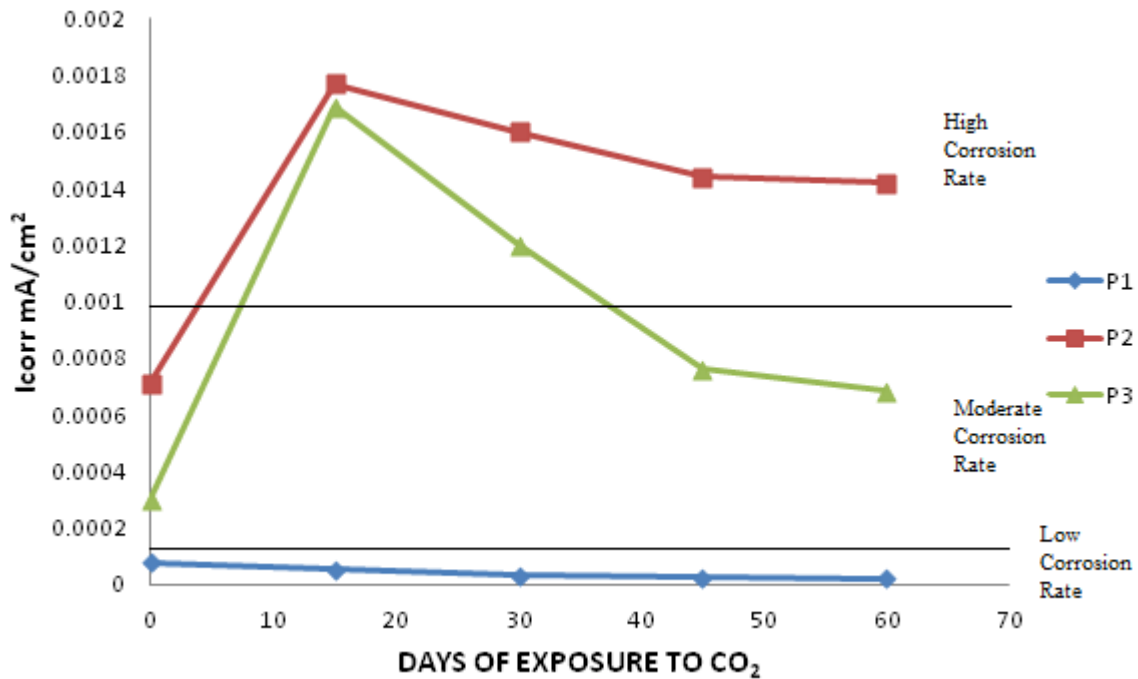


**Fig 5.11: Variation of corrosion current with time for different PPC prisms**

## 2. PPC Concrete

The similar pattern was found in PPC prisms as in the case of OPC prisms. The variation of  $I_{corr}$  with exposure days for PPC specimens can be seen in Fig. 5.11. The P1 specimens were found to be in the passive zone i.e. the corrosion has not yet started in these specimens. While

in P2 specimens with chloride admixed, the corrosion current lies in the High corrosion rate zone. The presence of chlorides highly affects the corrosion rate of the specimens. This can be seen with comparison of P1 and P2 prisms on basis of  $I_{corr}$ . The P3 specimens show slightly lower values throughout the testing period and after 30 days there is considerable reduction in corrosion current. This must be due to the formation of passive layer around the rebar as discussed earlier.

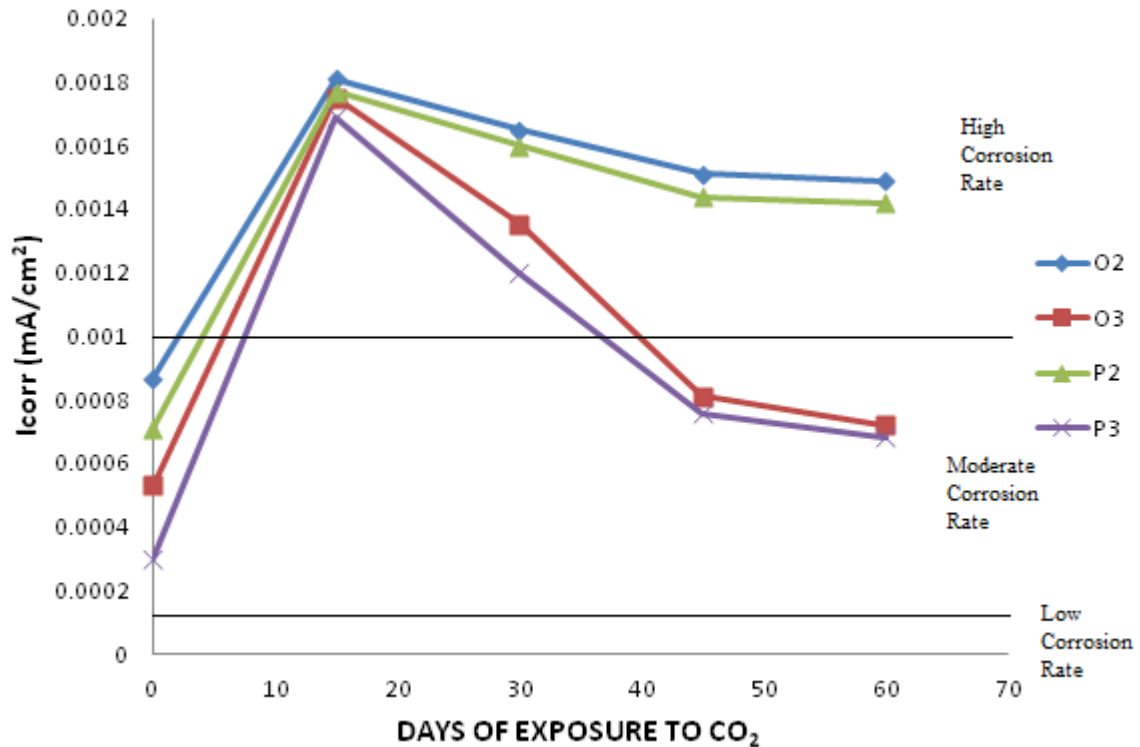


**Fig 5.12: Comparison of corrosion current with time for OPC and PPC prisms**

### 3. Comparison between OPC and PPC concrete

In Figure 5.12, the comparison was made with chloride and carbonated contaminated prisms only. The control prisms i.e. O1 and P1 showed no affect of carbonation induced corrosion and no chloride was admixed in these specimens.

Comparison was made with respect to the cement type on  $I_{corr}$  in Chloride and Carbonated environment i.e. for O2 and P2 prisms. The values of O2 were slightly higher than P2 specimens throughout the testing period. It must be due to the PPC cement containing fly ash. The fly ash contains  $Al_2O_3$  which reacts with Chloride ions and form more chloroaluminates thus, decreasing free chloride content in the concrete, (Saraswathy, 2007). Similar

observations were made by *Pradhan (2009)* on comparing Icorr of OPC and PPC specimens under chloride induced rebar corrosion in concrete.

Then the preparation of prisms O3 and P3 is to study the effectiveness of 2-Aminopyridine in the contaminated environment. In this study the difference between the values of Icorr for OPC and PPC specimens was very low till the exposure days. However, in both cement types, 2-Aminopyridine was found to be effective in reducing the rebar corrosion.

### 5.5.3 Galvanic Potential

The galvanic potential was calculated for all prism specimens. Galvanic potential tells about the macrocell corrosion in the concrete. A 100 ohm resistor was connected between the top steel bar and a common terminal of bottom steel bars. The different in potential of top and bottom steel bars is explained by galvanic potential. When top bar exhibited positive potential with respect to the bottom common terminal. This indicates that there is a reversal in direction of the current between the top steel bar and bottom steel bars. It further confirms the top steel bar has become anodic, (*Pradhan et al., 2009*).

**Table 5.8: Values of Galvanic potential in mV for different prisms**

<b>DAYS OF EXPOSURE TO CO<sub>2</sub></b>	<b>O1</b>	<b>O2</b>	<b>O3</b>	<b>P1</b>	<b>P2</b>	<b>P3</b>
0	-142	-410	-406	-180	-415	-391
15	-152	-464	-414	-214	-434	-410
30	-133	-475	-440	-204	-462	-408
45	-145	-465	-439	-165	-472	-452
60	-172	-430	-422	-192	-451	-410

The values of galvanic potential for all the prisms were measured till 60 days of exposure OPC and PPC prisms are tabulated in Table 5.8. The O1 prism values lies in the range of -140 to -170 throughout the testing period as there was no chloride admixed in these samples. The variation of Galvanic Potential with time for OPC specimens can be seen in Fig. 5.13. The value of O2 specimens lies in the higher range due to presence of chloride in these specimens. The values were above -400mV at all stages of testing. While, in O3 specimens

the values of galvanic potential were also higher, almost comparable to O2 specimens. No change in sign was observed in OPC prisms showing anodic formation on top steel bar.

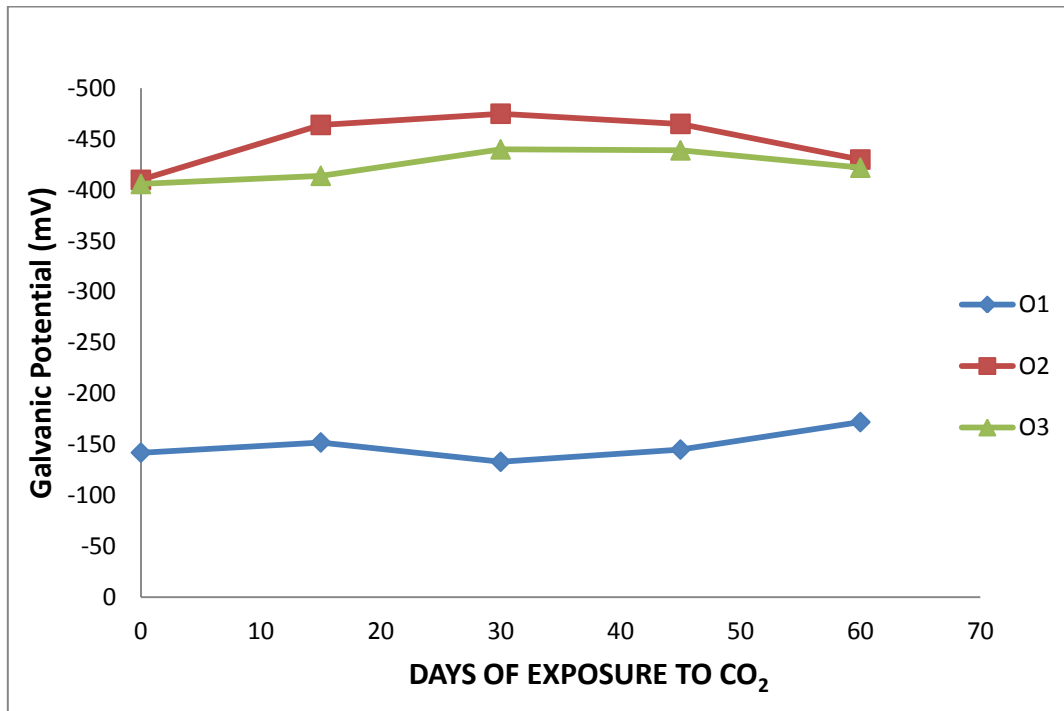


**Fig. 5.13: Variation of Galvanic Potential with time for different OPC prisms**

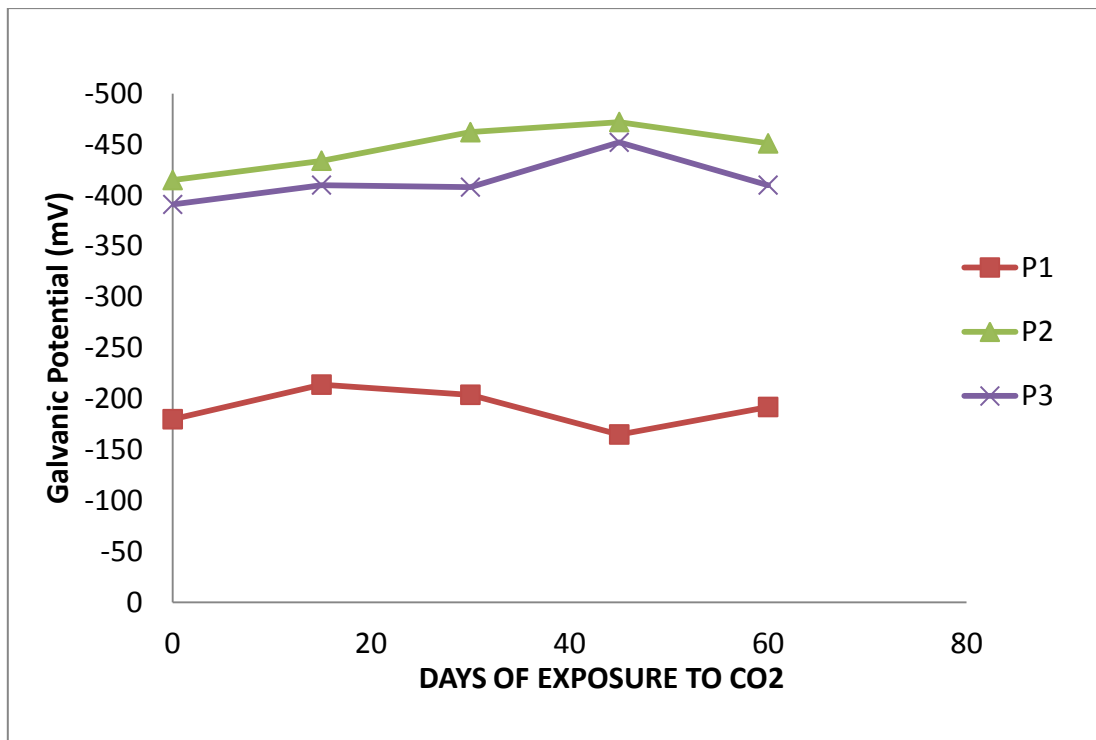


**Fig. 5.14: Variation of Galvanic Potential with time for different PPC prisms**

A similar pattern was observed in PPC prisms. The variation of Galvanic potential with time for PPC specimens can be seen in Fig. 5.14. The galvanic potential of P1 prisms was lower than -214mV in all cases. While the P2 specimens showed higher galvanic potential, all values were above -400mV. The P3 specimens showed slightly lower galvanic potential than P2 specimens. But, there is no change in sign of galvanic potential neither a sudden drop was observed in the PPC prisms as well.

In this study chloride was admixed into the concrete, so there is no difference in potential for top and bottom steel bars. The microcell corrosion must be taking place in these samples, forming anodic and cathodic points on individual rebar. Microcell corrosion results from a uniform electrochemical environment of the steel. In this case, anodic and cathodic areas appear as corrosion microcells, immediately adjacent on the steel surface. Therefore, each electron produced by an anodic reaction is locally consumed by a cathodic reaction. Ohmic drop between anodic and cathodic microcells due to electrolytic resistivity is negligible, the potential field appears to be uniform at macroscopic scale and no net current flows in the concrete volume, (*Sohail et al., 2013*).

## **CHAPTER 6 – CONCLUSIONS**

The effectiveness of 2-Aminopyridine was checked on two levels. Firstly, on pore solutions and secondly, on concrete specimens. From the experimental work performed in this thesis on the effectiveness of 2-Aminopyridine as corrosion inhibitor in chloride and carbonated induced corrosive environment, the following conclusions can be made on the efficiency of 2-Aminopyridine.

1. The Icorr and Half-Cell Potential values of solution containing 2-Aminopyridine decreased the rate of corrosion very effectively after 120 hours of testing as compared to the reference sample under carbonation and chloride induced corrosion. It indicated that 2-Aminopyridine was effective in forming a passive layer around the steel bar.
2. The onset of carbonation depth in cubes with inhibitor was reduced as compared to the specimens without inhibitor. The corrosion inhibitor showed lower carbonation depth irrespective of the cement type used till the testing period. This is due to the pore blocking effect of 2-Aminopyridine.
3. The Half-Cell Potential values were slightly reduced in concrete prisms with inhibitor, while the corrosion rate (Icorr) decreased significantly after 30 days of testing in both OPC and PPC concrete. This is due to the layer formation around the rebar and pore blocking effect of amine group corrosion inhibitor.
4. There was small difference in Icorr and HCP values of OPC and PPC prisms. Till the testing duration no conclusion could be made on which cement type performed better under contaminated environment.
5. The corrosion inhibitor (2-Aminopyridine) effect was considerable after some time. The inhibitor takes time in forming the layer around the rebar and reducing the corrosion rate in concrete as well as pore solution. The amine group in the 2-Aminopyridine forms a chelate ring around the steel bar. This makes a passive layer around the steel bar, hence providing resistance to corrosion.

## REFERENCES

**ASTM C 876 -91, (reapproved 1999).** “Standard test method for half-cell potentials of uncoated reinforcing steel in concrete”. West Conshohocken, PA.

**ASTM G 109 - 99a, (Reapproved 2005).** “Standard test method for determining the effects of chemical admixtures on the corrosion of embedded steel reinforcement in concrete exposed to chloride environments”. West Conshohocken, PA.

**Bastidas D.M., Criado M., La Iglesia V.M., Fajardo S., La Iglesia A. and Bastidas J.M. (2013).** “Comparative study of three sodium phosphates as corrosion inhibitors for steel reinforcements”. *Cement & Concrete Composites*, Vol.43 pp.31–38

**Benzina Mechmeche L., Dhouibi L., Ben Ouezdou M., Triki E., and Zucchi F. (2008).** “Investigation of the early effectiveness of an amino-alcohol based corrosion inhibitor using simulated pore solutions and mortar specimens”. *Cement & Concrete Composites*, Vol.30 pp.167–173

**Bhaskar Sangoju, Ravindra Gettu, Bharatkumar B.H. and Neelamegam M. (2011).** “Chloride-Induced Corrosion of Steel in Cracked OPC and PPC Concretes: Experimental Study” *Journal of materials in civil engineering*, Vol.23, pp.1057-1066

**Broomfield J. P. (2006).** “Corrosion of Steel in Concrete, understanding, investigation and repair”. 2nd ed.UK: Taylor & Francis.

**Bulu Pradhan and Bhattacharjee B. (2011).** “Rebar corrosion in chloride environment”. *Construction and Building Materials*, Vol.25, pp.2565–2575

**Bulu Pradhan and Bhattacharjee B. (2009).** “Half-Cell Potential as an Indicator of Chloride-Induced Rebar Corrosion Initiation in RC.” *Journal of Materials in Civil Eng.*, Vol.21, pp. 543-552

**Ceukelaire L.D and Nieuwenburg D.V, (1993).** “Accelerated carbonation of a blast-furnace cement concrete”. *Cement Concrete Research*, Vol.23, pp. 442–452

**Chaussadent T., Pujol V., Farcas F., Mabilie I. And Fiaud C. (2006)**, “Effectiveness conditions of sodium monofluorophosphate as a corrosion inhibitor for concrete reinforcements”. Cement and Concrete Research, Vol.36, pp. 556-561

**Duo Zhang and Yixin Shao (2016)**. “Effect of early carbonation curing on chloride penetration and weathering carbonation in concrete”. Construction and Building Materials, Vol.123, pp. 516–526

**Fedrizzi L., Azzolini F. and Bonora P.L (2005)**, “The use of migrating corrosion inhibitor to repair motorways concrete structures contaminated by chlorides”. Cement and Concrete Research, Vol.35, pp. 551-561

**Fukushima T., Yoshizaki Y., Tomosawa F. And Takahashi K. (1998)**. “Relationship between neutralization depth and concentration distribution of  $\text{CaCO}_3\text{-Ca(OH)}_2$  in carbonated concrete.” Advance in Concrete Technology, ACI SP-179, pp. 347-363

**Gonzalez J.A., Alonso C. and Andrade C. (1983)**. “Corrosion of Reinforcement in Concrete Construction”. Ber: Pub. Ellis Horwood Ltd, pp. 159.

**Haibing Zheng, Weihua Li, Fubin Mab and Qinglin Kong (2012)**. “The effect of a surface-applied corrosion inhibitor on the durability of concrete”. Construction and Building Materials, Vol. 37, pp.36–40

**Heiyantuduwa R., Alexander M.G. and Mackechnie J.R. (2006)**, “Performance of a Penetrating Corrosion Inhibitor in Concrete Affected by Carbonation-Induced Corrosion”. Journal of Materials in Civil Engineering, Vol.18, pp. 842-850

**Hwa-Sung Ryu, Jitendra Kumar Singh, Han-Seung Lee, Mohamed A. Ismail and Won-Jun Park (2017)**. “Effect of  $\text{LiNO}_2$  inhibitor on corrosion characteristics of steel rebar in saturated  $\text{Ca(OH)}_2$  solution containing NaCl: An electrochemical study”. Construction and Building Materials, Vol.133, pp.387–396

**Hwa-Sung Ryu, Jitendra Kumar Singh, Hyun-Min Yang, Han-Seung Lee and Mohamed A. Ismail (2016).** “Evaluation of corrosion resistance properties of N, N0-Dimethyl ethanolamine corrosion inhibitor in saturated Ca(OH)<sub>2</sub> solution with different concentrations of chloride ions by electrochemical experiments”. Construction and Building Materials, Vol.114 pp.223–231

**IS: 2386 (Part I and III) (1963).** “Methods of Test for Aggregates for Concrete”. Bureau of Indian Standard, New Delhi

**IS: 456-2000 (1989).** “Code of Practice for Plain and Reinforced Concrete”. Bureau of Indian Standard, New Delhi

**IS 8112 – 1989 (Reaffirmed 2005).** “Specification for 43 grade ordinary Portland cement”. Bureau of Indian Standards, New Delhi.

**IS 1489-1991.** “Specification for Portland pozzolana cement, Part 1: Flyash based”. Bureau of Indian Standards, New Delhi.

**IS 1786-2008.** “High strength deformed steel bars and wires for concrete reinforcement”. Bureau of Indian Standards, New Delhi.

**IS 383-1870 (Reaffirmed 1997).** “Specification for Coarse and Fine Aggregates from Natural Sources for Concrete”. Bureau of Indian Standards, New Delhi.

**Jamil H.E., Shriri A., Boulif R., Montemor M.F., and Ferreira M.G.S. (2005).** “Corrosion behaviour of reinforcing steel exposed to an amino alcohol based corrosion inhibitor”. Cement & Concrete Composites, Vol.27, pp. 671- 678

**Kulwinder Kaur, Shweta Goyal, Bishwajit Bhattacharjee and Maneek Kumar (2016).** “Efficiency of Migratory-Type Organic Corrosion inhibitors in Carbonated Environment.” Journal of Advanced Concrete Technology, Vol. 14, pp. 548-558

**Laurens S., Henocqb P., Rouleau N., Deby F., Samsonb E., Marchand J., Bissonnette B. (2016).** “Steady-state polarization response of chloride-induced macrocell corrosion systems in steel reinforced concrete — numerical and experimental investigations.” *Cement and Concrete Research*, Vol. 79, pp. 272–290

**Malik U., Andijani I., Al-Moaili F., and Ozair G. (2004),** “Studies on the performance of migratory corrosion inhibitor in protection of rebar concrete in Gulf seawater environment”. *Cement and Concrete Composites*, Vol.26, pp. 235-242

**Monticelli C., A. Frignani, A. Balbo and F. Zucchi (2011).** “Influence of two specific inhibitors on steel corrosion in a synthetic solution simulating a carbonated concrete with chlorides” *Materials and Corrosion*, vol.62, pp.526-535

**Moreno M., Morris W., Alvarez M.G. and Duff G.S. (2004).** “Corrosion of reinforcing steel in simulated concrete pore solutions Effect of carbonation and chloride content”. *Corrosion Science*, Vol.46 , pp.2681–2699

**Morris W., and Vazquez M. (2002),** “A migrating corrosion inhibitor evaluated in concrete containing various contents of admixed chlorides”. *Cement and Concrete Research*, Vol 32, pp. 259-267

**Nmai C.K.,(2004).** “Multi-functional organic corrosion inhibitor”. *Cement and Concrete Composites*. Vol.26, pp.199–207

**Ormellese M., Berra M., Bolzoni F., and Pastore T. (2006).** “Corrosion inhibitors for chlorides induced corrosion in reinforced concrete structures”. *Cement and Concrete Research*, Vol.36, pp.536 – 547

**Rakanta E., Zafeiropoulou Th., Batis G. (2013).** “Corrosion protection of steel with DMEA-based organic inhibitor.” *Construction and Building Materials* Vol.44 pp. 507–513

**Rong Liu, Linhua Jiang, Jinxia Xu, Chuansheng Xiong and Zijian Song (2014).** “Influence of carbonation on chloride-induced reinforcement corrosion in simulated concrete pore solutions”. *Construction and Building Materials*, Vol.56, pp.16–20

**Saricimen H., Mohammad M., Quddus A., Shameem M. and Barry M.S. (2002).** “Effectiveness of concrete inhibitors in retarding rebar corrosion”. *Cement & Concrete Composites*, Vol.24, pp.89–100

**Stewart M.G. and Vu Kat (2002).** “Service life prediction of reinforced concrete structures exposed to aggressive environments”.

**Sohail M. G.,Laurens S., Deby F., Balayssac J.P. (2013).** “Significance of macrocell corrosion of reinforcing steel in partially carbonated concrete: numerical and experimental investigation.” *Materials and Structures*.

**Soylev T.A., and McNally C. (2007).** “The effect of a new generation surface applied organic inhibitors on concrete properties”. *Cement and Concrete Composites*, Vol.29, pp.357-364

**Soylev T.A., McNally C., and Richardson M.G. (2007).** “Effectiveness of amino alcoholbased surface-applied corrosion inhibitors in chloride-contaminated concrete”; *Cement and Concrete Research*. Vol. 37, pp. 972-977

**Soylev T.A., Richardson M.G. (2008).** “Corrosion inhibitors for steel in concrete: State-of-the-art report.” *Construction and Building Materials*. Vol.22 pp. 609–622

**Tommaselli M.A.G., Mariano N.A., Kuri S.E. (2009).** “Effectiveness of corrosion inhibitors in saturated calcium hydroxide solutions acidified by acid rain components”. *Construction and Building Materials* Vol.23, pp. 328–333

**Velu Saraswathy, Ha-Won Song. (2007).** “Evaluation of corrosion resistance of Portland pozzolana cement and fly ash blended cements in pre-cracked reinforced concrete slabs under accelerated testing conditions.” *Materials Chemistry and Physics* Vol.104 pp. 356–361

**Wang Y., Nanukuttan S., Bai Y., Basheer P.A.M. (2017).** “Influence of combined carbonation and chloride ingress regimes on rate of ingress and redistribution of chlorides in concretes.” *Construction and Building Materials* Vol.140 pp. 173–183

**Welle A., Liao JD., Kaiser K., Grunze M., Mader U and Blank N (1997)**, “Interactions of N, N0-dimethylaminoethanol with steel surfaces in alkaline and chlorine containing solution”. Appl Surf Sci, Vol.119, pp.185-190

**Yuming Tang, Guodong Zhang and Yu Zuo (2012)**. “The inhibition effects of several inhibitors on rebar in acidified concrete pore solution”. Construction and Building Materials, Vol.28, pp.327–332